

# TRIUMF



## ANNUAL REPORT 1976

MESON FACILITY OF:

UNIVERSITY OF ALBERTA  
SIMON FRASER UNIVERSITY  
UNIVERSITY OF VICTORIA  
UNIVERSITY OF BRITISH COLUMBIA

OCTOBER 1977





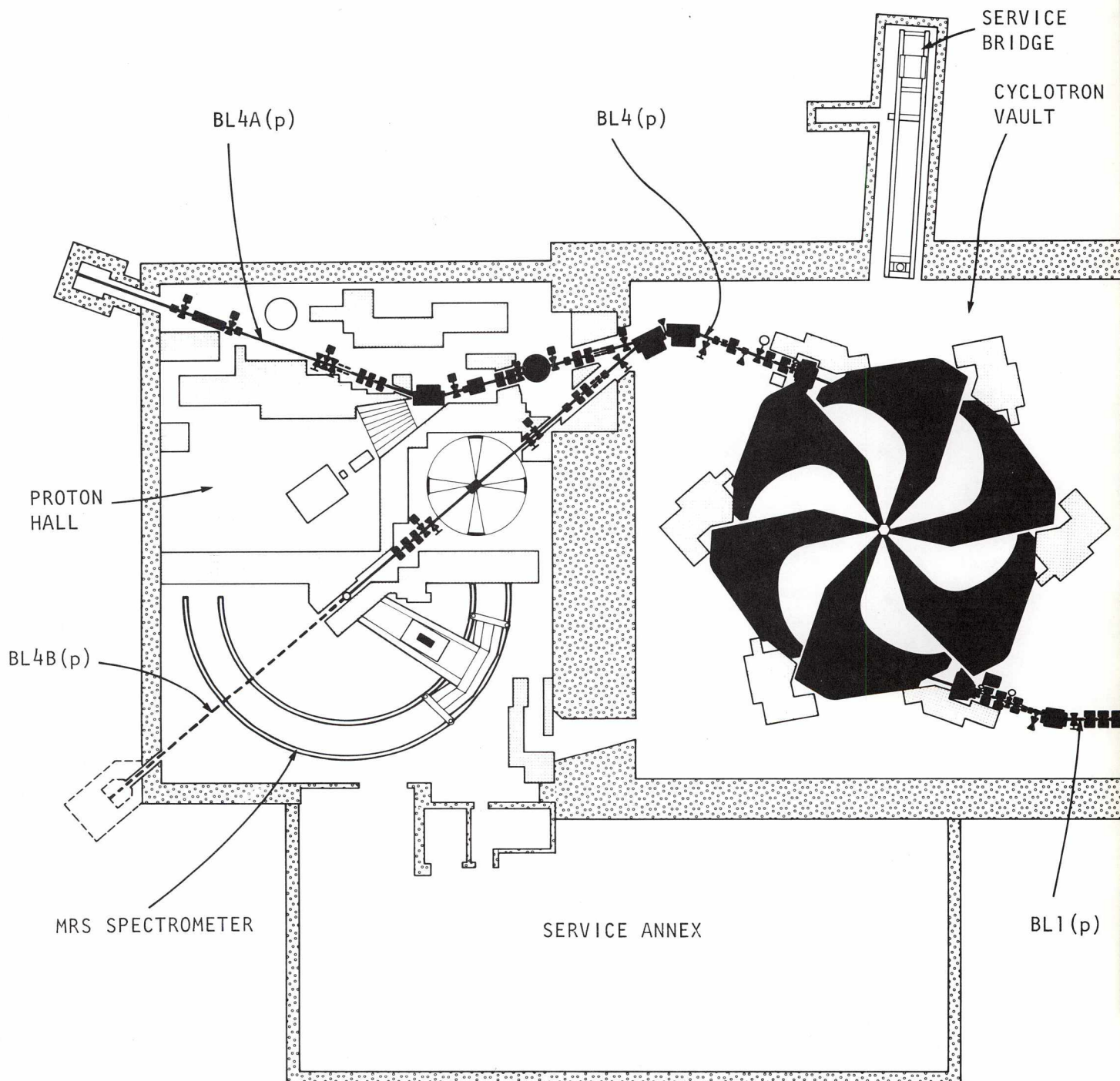


# TRIUMF

## ANNUAL REPORT 1976

TRIUMF  
UNIVERSITY OF BRITISH COLUMBIA  
VANCOUVER, B.C.  
CANADA V6T 1W5

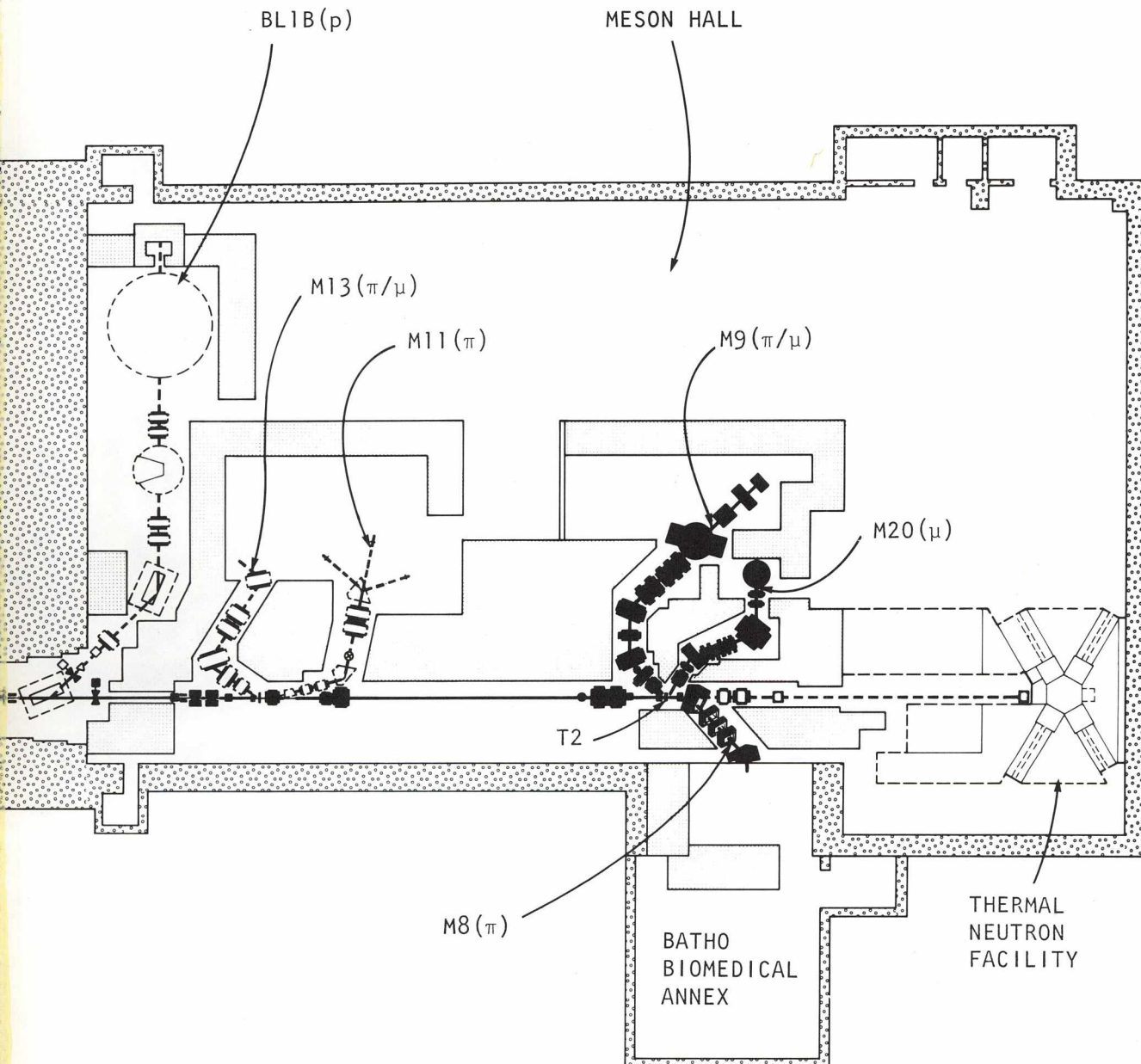






———— EXISTING

----- PROPOSED







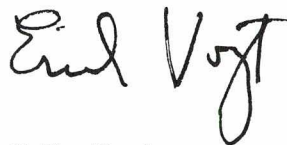
## FOREWORD

*This annual report chronicles a number of impressive achievements at TRIUMF toward operation at full design intensity and toward full development of the experimental program. The record of beam available to experimentalists stands for itself. Also, the high spirits and high momentum of the people associated with TRIUMF continue.*

*The year began with an important occasion—the formal opening of the TRIUMF laboratory by the Prime Minister of Canada, the Right Honourable Pierre Elliott Trudeau, on February 9. On hand for this occasion were many of TRIUMF's long-time friends and well-wishers, including the Honourable C.M. Drury, colleagues from laboratories around the world and across Canada, and many of the scientists and engineers who built TRIUMF and are now using it. It was a most happy occasion, and the Prime Minister brought the welcome news of full funding for full beam intensity.*

*Another important occasion was the change in directorship in mid-year. Completing his five-year term and returning to the scientific program of TRIUMF was Dr. J.R. Richardson. He conceived the idea of the TRIUMF cyclotron on Galiano Island in 1962. His constant advice was essential to the early development of TRIUMF. His firm hand led the achievement of the assembly and commissioning of TRIUMF's cyclotron and beam lines during his term as director. The Board of Management of TRIUMF join his many colleagues in congratulating him on his achievements as director and in wishing him well in his full-time return to TRIUMF's science.*

*Assuming the TRIUMF directorship was Dr. J.T. Sample from the University of Alberta. His association with TRIUMF goes back to the beginning of the project, and he now has the opportunity of leading TRIUMF during its important early years of full operation.*



E.W. Vogt  
Chairman of the Board of Management



TRIUMF was established in 1968 as a laboratory operated and to be used jointly by the University of Alberta, Simon Fraser University, the University of Victoria and the University of British Columbia. The facility is also open to other Canadian as well as foreign users.

The experimental program is based on a cyclotron capable of accelerating two simultaneous beams of protons, individually variable in energy, from 180-520 MeV. The potential for high beam currents—100  $\mu$ A at 500 MeV to 300  $\mu$ A at 400 MeV—qualified this machine as a 'meson factory'.

Fields of research include basic science, such as medium-energy nuclear physics and chemistry, as well as applied research, such as nuclear fuel research and isotope research and production. There is also a biomedical research facility which will use mesons in cancer research and treatment.

The ground for the main facility, located on the UBC campus, was broken in 1970. Assembly of the cyclotron started in 1971. The machine produced its first full-energy beam in 1974.

The laboratory employs approximately 165 staff at the main site. The number of university scientists associated with the initial scientific program is about 120.

# CONTENTS

	Page
INTRODUCTION	1
OPERATION AND DEVELOPMENT OF FACILITIES	4
Cyclotron	4
Beam Line Development	11
RESEARCH PROGRAM	13
Introduction	13
Beam Research and Development	15
Particle Physics	24
BASQUE	24
Gamma-ray studies	27
Measurement of the $\pi \rightarrow e\nu$ branching ratio	30
Pion production	31
A survey of proton-proton bremsstrahlung	34
Muonium in powdered insulators	35
Nuclear Physics and Chemistry	37
Pi scattering and total cross-section measurements	37
High-energy fission from pion absorption (HEFPA)	39
Measurement of pionic X-ray energies, widths and shifts	39
Elastic scattering of protons from $^4\text{He}$	40
Nucleon-Nuclear quasi-free scattering	42
Proton-deuteron quasi-elastic scattering	44
Polarization effects of the spin-orbit coupling of nuclear protons	44
The study of fragments emitted in nuclear reactions	46
Intermediate-energy fission	48
Gas jet	50
Research in Chemistry and Solid-State Physics	51
$\mu\text{SR}$ -New aspects of solids revealed by muons at TRIUMF	51
Muonium chemistry	55
Artificial negative muon polarization	58
Applied Research	60
Biomedical experimental program	60
Proton radiography	63
Isotope production	65
Fertile-to-fissile conversion (FERFICON)	67
Theoretical Program	69



	Page
THE STATUS OF EXISTING FACILITIES	76
Ion Source and Injection System	76
Safety	78
Remote Handling	82
RF System	84
Vacuum System	86
M9 Channel	87
M8 Channel and Biomedical Facility	90
M20 Channel	91
Control System	92
Instrumentation	94
PROGRESS TOWARDS ULTIMATE PERFORMANCE	96
100 $\mu$ A Task Force	96
Separated Turns Task Force	101
FACILITIES UNDER DESIGN AND CONSTRUCTION	104
M11 Channel	104
Proton Spectrometer	105
Beam Line 1B	106
Thermal Neutron Facility	107
Shielding and Activation	110
Data Interface Task Force	112
New Facilities	114
ORGANIZATION	115
APPENDICES	
A. Publications	117
B. Staff	119
C. Users Group	122
D. Experiment Proposals	124
E. Scientific Inauguration	130

# INTRODUCTION

1976 was the year when the major emphasis at TRIUMF turned from the development of the facility to the starting of important research projects which make use of the many unique capabilities of the facility. This change in emphasis is reflected in the organization of this Annual Report, where the research program comes to the forefront. This is not to say, however, that further development of the facility was neglected—in fact a number of important milestones were passed. Among these can be listed:

- 1) Operating currents were increased to 10  $\mu$ A for extended periods in the meson hall while the beam in the proton hall was increased to 1  $\mu$ A.
- 2) 75% polarized proton beams of 20-30 nA and 200-520 MeV energy were routinely sent down both beam lines.
- 3) A stable split ratio as high as 5000:1 between the beams in the meson hall and the proton hall was achieved.
- 4) 50  $\mu$ A was sent down beam line 1 for a short period limited by the thermal protection on the temporary beam dump.
- 5) Major reductions were made in the beam loss both in the cyclotron and in the beam lines. As a result it appears that residual radioactivity, although serious in some locations, will not make repairs as difficult as previously believed.
- 6) Reliability of the operating components continued to improve during the year, with facility availability approaching 80%.

As we have said, the research program has really blossomed during 1976, primarily due to the availability of the polarized proton beam and the gradual but large increase in beam current in the meson hall. The polarized beam allowed the BASQUE group to remove a long-standing ambiguity in the phase-shift analysis of p-p scattering by measuring the Wolfenstein parameters in the energy range 200-500 MeV. This group also developed a quite monoenergetic polarized neutron beam from the  $d(p,n)2p$  reaction and used it to measure the parameters for n-p scattering at 325 MeV. This is the beginning of an extensive program.

Experiments in particle physics include the work of the groups making use of the two very large NaI scintillators. They have observed the reaction  $\pi^-d \rightarrow \pi^0nn$  at rest for the first time and have obtained a greatly improved value for the Panofsky ratio in hydrogen. Another group has been studying pion production from the reaction  $p + p \rightarrow \pi^+ + d$  as a function of energy and angle. Particularly exciting results have been obtained from an investigation of the asymmetry dependence on the spin of the incident proton.



In nuclear physics some important results have been obtained in the low-energy scattering of pions by carbon (not dominated by the  $3/2, 3/2$  resonance). This area of research has received major contributions both from an experimental group making use of extra time on the M8 biomedical channel and by TRIUMF's new theoretical group. It appears that nuclear absorption must be included to obtain a satisfactory description of the process. The (p,2p) reaction in oxygen was studied by a group in the proton hall to test a disputed theoretical prediction that the cross-section would be j-dependent. The results indicate, at least for the conditions of this experiment, that the effect of spin-orbit distortion is small and that the cross-section *does* depend on the j-value of the struck proton. Another nuclear program is concerned with p- $^4\text{He}$  elastic scattering—during 1976 data have been obtained on the asymmetry in this process at both low- and high-momentum transfer using the polarized proton beam.

Research in chemistry and solid-state physics is being prosecuted by a group using the  $\mu\text{SR}$  facility and the M20 meson channel. This group is large and very active, and has produced results, for example on  $\mu^+$  spin relaxation in iron, which have attracted much attention. Research in gas, liquid and solid-state chemistry is also under way with the facility.

It is expected that applied research will eventually consume a large proportion of the research effort at TRIUMF. The biomedical program is proceeding apace and received a welcome boost with the 10  $\mu\text{A}$  beam available at the end of the year. Extensive work has been done on dosimetry and proving out the properties of the M8 pion channel. Also two biological irradiations using Chinese hamster cells ( $\text{CH}_2\text{B}_2$ ) have been completed. A research program in proton radiography, using the excellent properties of the TRIUMF proton beam, is under way and the medical applications of this technique appear very promising. Another program with important applications in medicine is radioisotope production. So far, test amounts of  $^{123}\text{I}$  have been made available to our medical colleagues, who have demonstrated its marked superiority over  $^{131}\text{I}$  for diagnostic purposes. An experimental program is being conducted to measure the neutron leakage and fertile-to-fissile conversion reaction rates in a variety of heavy-element targets. This program is performed under contract with Atomic Energy of Canada, Ltd.

Research and development have continued in accelerator and beam physics. In particular, new ways of measuring isochronism in the cyclotron have been found, and measurements of the effect of gas and electric stripping of the  $\text{H}^-$  ions have been made.

A major change occurred in TRIUMF's financial support during 1976—the source, awarding procedure and amount of funds all changed. The Atomic Energy Control Board of Canada, which had provided funds for the construction and operation of TRIUMF since the initiation of design studies in 1965, decided to discontinue its Grants in Aid of Research Program in order to concentrate upon its regulatory function. Support of TRIUMF (and several other projects) became the responsibility of

the National Research Council of Canada, which has been for many years the principal source of support for University research in the physical and biological sciences.

NRC completed the change in TRIUMF funding procedures begun by AECS in 1974, with operation of the facility and capital for development being provided by a contribution rather than a grant, requiring more detailed planning and reporting together with closer auditing. The experimental program is no longer supported as a TRIUMF operating expense but through grants awarded to the spokesmen of approved experiments (held in trust by TRIUMF). These changes reflect the progression from a construction phase to an operating phase.

The amount awarded to TRIUMF and the experimental program at TRIUMF totalled \$7,763,800 in fiscal 1976-77, with \$4,650,000 assigned to operating, \$2,130,000 to capital and \$983,800 to grants for experiments. A program forecast has been submitted which shows annual increases to enable the commissioning and operation of experimental facilities as their construction is completed.

In addition to the formal opening of TRIUMF in February by the Prime Minister of Canada (described in the Foreword), a Scientific Inauguration of the facility was held in June, with a group of distinguished scientists giving presentations on fields of research appropriate to TRIUMF. The program of the ceremony is reproduced in the appendices to this report.

We should like to express the thanks of TRIUMF to several members of the TRIUMF Board of Management who left the Board during 1976 after a number of years of valuable service. They are Dean G.M. Volkoff and Dr. R.R. Haering of the University of British Columbia and Dean S. Aronoff and Mr. G. Suart of Simon Fraser University.

J.R. Richardson  
J.T. Sample (since July 1)  
Director



# OPERATION AND DEVELOPMENT OF FACILITIES

## CYCLOTRON

A good indication of cyclotron performance during 1976 can be seen in Fig. 1 which shows the total number of microampere-hours of beam delivered in the years 1975 and 1976. During 1975 a large part of the available beam time was used in commissioning the major facilities of the project—the cyclotron and its systems, the external proton beam lines, the meson production target, and the secondary meson channels. A number of experiments were started but the experimental program, in particular in the area of meson physics, was limited by the low operating currents: 300 nA in beam line 1 and 50 nA in beam line 4A. This limitation was dictated primarily by the lack of shielding along the external beam lines. During 1976 the addition of further shielding, together with improvements in the tune of the cyclotron and the external beam lines, has allowed operation at currents sufficiently high that TRIUMF can truly be called a 'meson facility'. The operating currents have been increased to 10  $\mu$ A for extended periods in beam line 1 and 1  $\mu$ A in beam line 4A. Late in November 50  $\mu$ A was achieved for several minutes during a test, the current being limited by heating of the temporary beam stop.

Another major improvement in the TRIUMF facility has been the addition of a polarized ion source which is capable of delivering currents of

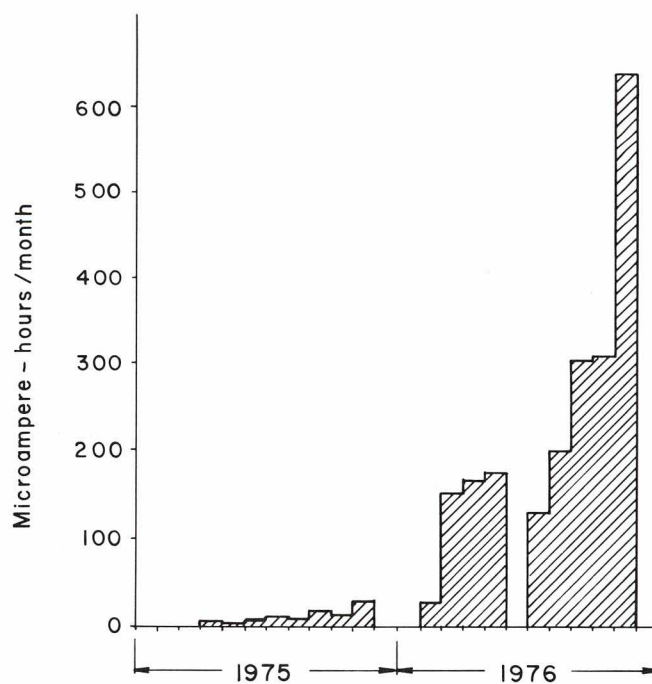


Fig. 1. Cyclotron beam current.

250 nA with 75% polarization. This source together with the variable-energy feature of the cyclotron—proton beams can be extracted with energies from 180 to 520 MeV—makes TRIUMF a unique facility for nuclear physics. Since coming on line in February the polarized source has been run about 40% of the time, indicating its popularity amongst the experimentalists.

Highlights of the year's operation are shown in Fig. 2.

### *Operation*

This year has seen cyclotron operation gradually switch from the hands of the beam physicists to the operations staff. Five crews, three men per crew, operated the cyclotron on a 24-hour/day, 7-day/week basis. However, a beam physicist is still on duty during the day and evening shifts on week-days, and on call at week-ends, to provide assistance in cyclotron or beam line tuning. The machine is operated on a 14-day cycle with 12 days of beam operation followed by two days of machine maintenance. Some of the routine tasks during the maintenance periods are the defrosting of the cryogenic panels in the vacuum system; the switchover from the normal ion source to the polarized source when it is scheduled, or a filament change in the operating ion source. At present the polarized source has a maximum running time of 7-8 days, limited by cesium contamination and filament lifetime, and therefore polarized beam is usually scheduled for about this duration. Both sources can be operated independently and a switchover can be completed in two or three hours.

The polarized source and the higher current levels during normal running have increased the complexity of cyclotron operation. The higher circulating currents necessary to allow extraction of microamperes of beam down beam line 1 for meson production have made it more difficult to operate simultaneously beam line 4 at the nanoampere level for some nuclear physics experiments. Special shapes of stripping foils and improved tuning of the cyclotron have helped to ease the problem for the operator. A stable split ratio between the beams on beam line 1 and beam line 4 of 5000:1 has been achieved using a 0.001 in. diam carbon stripping wire on the extraction probe for beam line 4. Another factor affecting the quality of the low-intensity beam is the presence of decelerated beam which can exist if the circulating beam is not completely stripped by the outer stripping foil. This effect is described in more detail in the Beam Development report (p.20).

The most significant improvement in the beam operation during the year has been in the tuning of the external beam lines. This has resulted in lower spills and therefore less activation of beam components, reduced beam halo and smaller beam spots on target for the experimenters. In fact, the beam spill along beam line 1 for 10  $\mu$ A operation at present is not too different from the spill levels at 1  $\mu$ A earlier in the year. These improvements have come about by the elimination of windows in the beam pipe which were causing multiple scattering, the

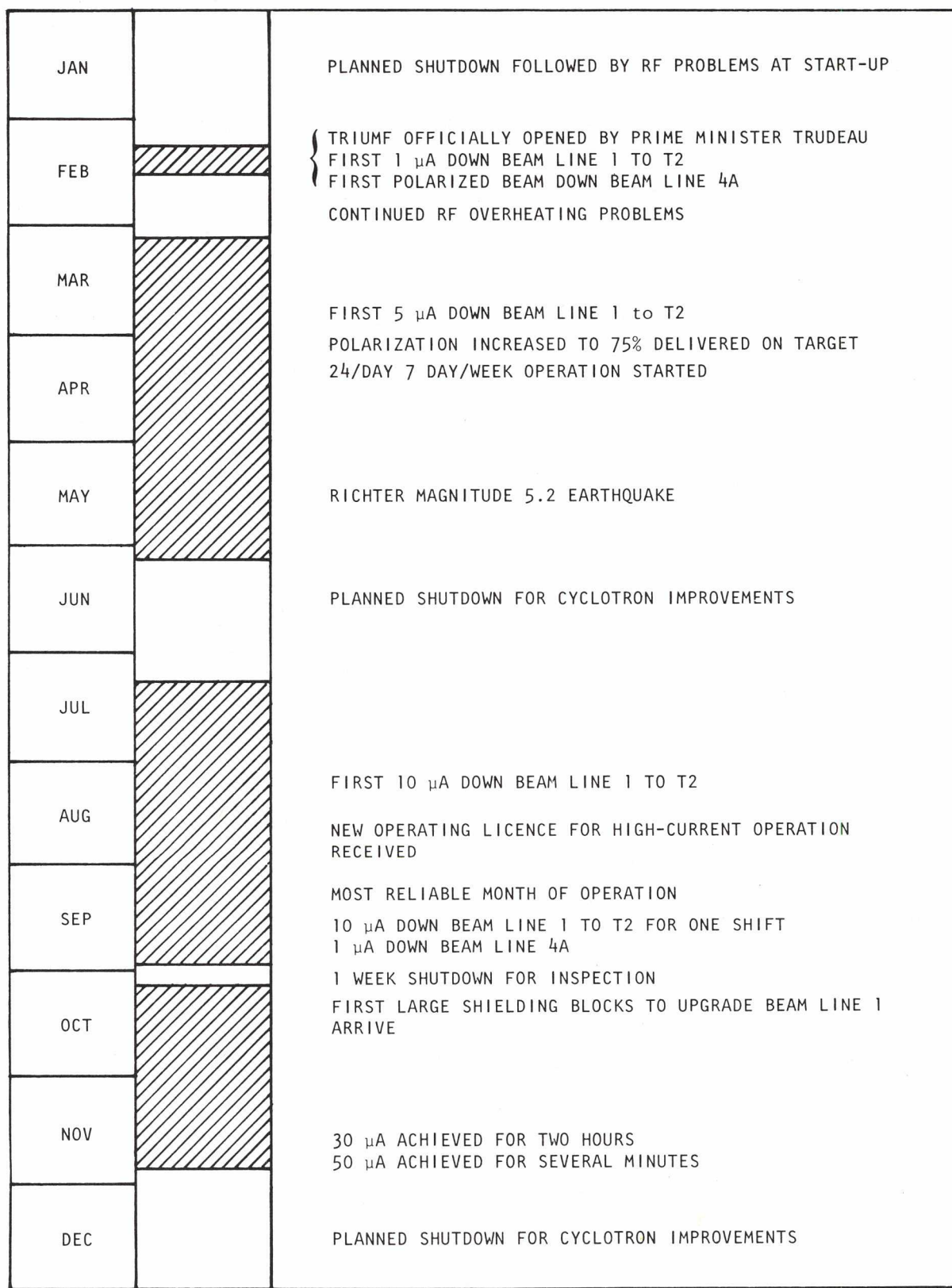


Fig. 2. Cyclotron performance 1976.



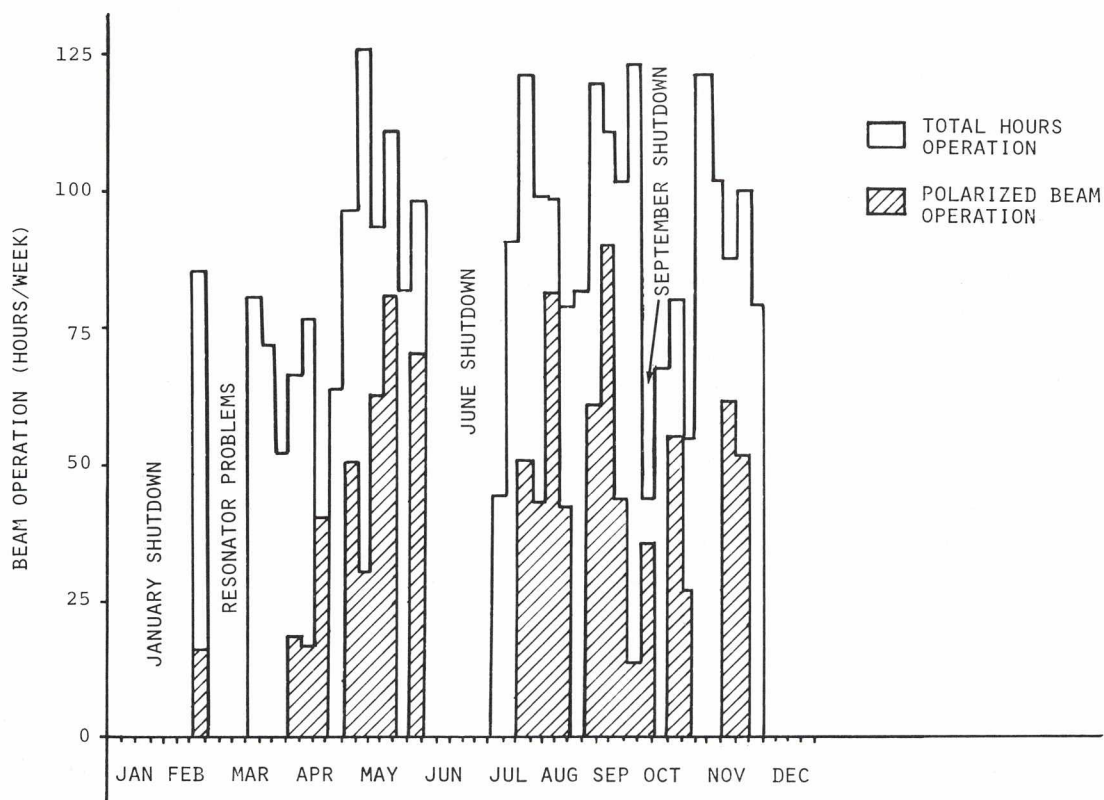


Fig. 3. Beam operation 1976.

use of carbon stripping foils instead of aluminum, and a better understanding of the beam behaviour both inside the cyclotron and along the beam lines.

With operation at higher currents it has been necessary to provide a number of machine protection interlocks and warning devices to help the operator in his task. This is an ongoing effort and many of the improvements came about as a result of operating experience. The flexibility of the control system has allowed implementation of these systems with little difficulty.

Improvements have also been made in the storage and retrieval of the operating parameters for the cyclotron and the settings of the beam lines for the many different energies.

### Performance

The performance of the cyclotron is summarized in Table I and Fig. 3. Machine availability, as defined by the ratio of hours of cyclotron operation to scheduled operating time, increased by about 25% over the corresponding figure in 1975 and is close to the 80% level which is considered acceptable for a facility of TRIUMF's complexity.

Through the year there has been a gradual decrease in the length of time spent in going from cyclotron start-up after a maintenance shutdown

to simultaneous extraction with beam delivered to experimenters' targets on both external beam lines. The cyclotron itself is very reproducible and a 500 MeV beam is obtained usually within only minutes of first injection, even after a week's shutdown. There has been considerable effort and success in improving the reproducibility of the ion source and injection line at the higher current levels.

Usually the beam line extracting the higher-energy beam is set up first. This typically means 500 MeV extraction along beam line 1 for meson production. A 1  $\mu$ A beam can be tuned along beam line 1 and the beam spills reduced to an acceptable level in about one-half hour. The stripper foil for extraction along beam line 4 is then inserted and adjusted vertically to give the desired split ratio. This line usually takes more time to set up as there is less control of the critical beam conditions once beam line 1 is operating. The experimenters' requirements of beam size on target, target location and operating currents also vary considerably, and in some cases where polarimeters

Table I. Summary of Machine Performance 1976

Scheduled operating time (hours)		4248
Injected beam	Unpolarized	1888
	Polarized	1095
Cyclotron	Tune-up and development	483
	$\mu$ A hours	2070
Beam line 1	Tune-up and development	290
	Experiment	2381
Beam line 4	Tune-up and development	485
	Experiment	2045
Downtime - System failures (hours)		965
RF system		344
ISIS and POLISIS		336
Vacuum		40
Magnet		22
Diagnostics		37
Beam lines		72
Controls		42
Safety system		15
Services		57
Machine availability (average)		77.3%

are used the requirements are more stringent. In spite of this the ease of simultaneous extraction allows an experimenter to vary the beam energy a number of times during a beam shift without seriously disrupting operation of the other line.

#### *Downtime and cyclotron improvements*

The most serious problem affecting operations this year has again been with the RF system. Overheating of the centre quadrants of the resonators, first observed in November 1975, appeared again early in the year. The accepted theory is that the heating is caused by electron bombardment from electrons trapped in the crossed electric and magnetic fields in the central region. The solution has been to replace two of the aluminum centre quadrants with copper ones shaped so as to reduce the volume where the electric potentials are parallel to the magnetic field lines. Also thermocouples to monitor the quadrant temperatures were installed. This heating has been kept under control since March, and further tests are being carried out to try to understand the source of the electrons. Other problems causing downtime in the RF system, mainly water leaks, are described in the RF system report (pp. 84-85).

With the addition of the polarized ion source and the operation of the normal ion source at higher current levels, there has been an increase in downtime in this area. Most of the lost time has been due to power supply failures, and it is hoped that as the faulty supplies are weeded out this downtime will be reduced.

There were three scheduled shutdowns during the year, one lasting five weeks in June, a second for one week at the end of September, and a third starting in late November and continuing into 1977. In each case the cyclotron lid was raised for inspection, maintenance and improvements. The activities during these shutdowns are described in detail in the various group reports. Inside the cyclotron a number of improvements were made to the resonators and diagnostic probes. Graphite shielding cans were installed around the outside of the vacuum tank to absorb the beam lost due to electromagnetic and gas stripping. This has resulted in a substantial reduction of the radiation levels inside the tank, and it is expected that the levels will allow hands-on maintenance of most cyclotron components to at least the 10  $\mu$ A operating level. Lead shielding susceptible to remote installation and removal will also be used to reduce the radiation from the inside of the tank wall during periods when work is required inside the vacuum chamber.

The Remote Handling group has expanded activities substantially during the year. There have been a number of changes to the service bridge and its related hardware, with the first fully remote operation being the radiation survey of the cyclotron tank.



# *Beam time to experiments*

Table II indicates the number of shifts scheduled and the number of hours of beam delivered to experiments for the period March-December. For each shift the users have been assumed to be those indicated on the beam time schedules. It is difficult to determine the number of hours for those groups sharing beam line 1 T2. Frequently the M9 user is the only one shown in the beam time schedule as there are more users on this channel. Therefore, the groups using the other secondary channels received considerably more beam time than is indicated.

Table II. Beam Time to Experiments 1976

Experiment	Short title	Spokesman	Number of 12 h shifts scheduled	Hours of beam delivered	
				Jul-Dec	Mar-Jun
BEAM LINE 1					
1, 54	$\pi$ scattering	R.R. Johnson	29	209.3	-
9	$\pi^- + p \rightarrow \gamma + n$	D.F. Measday	16	-	101.3
10	$pp \rightarrow \pi^+ + d$	G. Jones	94	597.5	272.8
23b	$\pi^+ \rightarrow e\nu_e\gamma$	P. Depommier	27	254.8	-
35, 71	$\mu$ SR	D.G. Fleming T. Yamazaki	23	145.8	50.3
41a,b	$\pi$ capture	M. Salomon M. Hasinoff	28	79.8	98.0
42a, 80	$\pi$ -mesic X-rays	G.R. Mason A. Olin	31	216.3	55.5
46	Polarized muonic $^{209}\text{Bi}$	G.T. Ewan R.M. Pearce	2	16.0	-
52	$\pi \rightarrow e\nu$	D.A. Bryman	38	145.2	187.4
53	HEFPA	P.W. Martin	2	-	19.3
60	$\mu$ capture in MgO	J.B. Warren	10	56.7	8.0
61	Biomedical	L.D. Skarsgard	30	232.7	33.5
BEAM LINE 4A					
3	Heavy fragments	R.G. Korteling	21	65.6	83.5
6	Fission	B.D. Pate	6	38.0	5.3
11	Gas-jet	J.M. D'Auria	24	89.1	145.9
26	$D(n,p)2n$	L.P. Robertson	12	107.0	-
27,40	BASQUE	D.A. Axen	83	459.5	262.0
48	FERFICON	B.D. Pate	15	85.3	25.5
75	$d(p,\pi^+)t$	W.C. Olsen	4	30.0	-
77	$^{123}\text{I}$ production	J.S. Vincent	6	33.5	15.5
87	Proton radiography	E.W. Blackmore	7	41.3	28.8
BEAM LINE 4B					
14	Proton elastic scattering	J.M. Cameron	40	145.8	92.2
15	Quasi-elastic scattering	W.J. McDonald	15	31.0	63.8
58	Polarized (p,2p)	P. Kitching	11	46.0	54.5
66	pp bremsstrahlung	J.G. Rogers	11	34.0	27.0

## BEAM LINE DEVELOPMENT

The past year has seen:

- a) an increase in beam line 1 current from 0.3 to 30  $\mu\text{A}$ , with routine operation at 10  $\mu\text{A}$ ;
- b) an increase in beam line 4A current from 0.1  $\mu\text{A}$  to a routine 1  $\mu\text{A}$ ; and
- c) a halving of the beam line 4B spot size to 0.5 cm and operation with steady currents of a few nanoamperes, while 10  $\mu\text{A}$  were being delivered to beam line 1.

This has been achieved, in so far as the beam lines are concerned, by improvements to the vacuum (which permitted the removal of windows), the installation of additional shielding, improved tuning, and the use of low mass carbon stripping foils. A carbon filament, 0.001 in. diam, is used for the 1/5000 split ratio. The beam current limitations at present are set by the temporary dumps in beam line 1 and beam line 4A; these will be replaced in 1977.

The beam line layout is shown in the frontispiece. New equipment installed during the year includes cryogenic hydrogen, deuterium and helium targets, polarimeters in all beam lines, and devices giving beam pulse timing information from either the scattered protons from polarimeter targets or a non-intercepting capacitive pick-up monitor. The magnet for the medium resolution spectrometer, resolving power 350 keV at 500 MeV, has been installed and magnetic field surveys started. A multi-sample irradiation station for the production of isotopes from solid targets has been installed near the beam line 4A dump, and a separate cesium heat pipe device has produced medically useful quantities of  $^{123}\text{I}$ . Several ex-cyclotron magnets have been transferred to TRIUMF and are enjoying a useful retirement as magnets in the secondary channels.

The T2 production target package has been commissioned ready for 100  $\mu\text{A}$ , and individual targets have been replaced remotely. The concrete shielding around beam line 1 and 4A dumps has been increased twofold, and additional special blocks of concrete and iron have been installed to reduce experimental background or to shield accessible areas of the beam line from the dumps. The radiation levels for routine maintenance in these areas are all less, usually much less, than 40 mrem/h. Beam line components close to the cyclotron and production targets are being made remotely handleable and radiation hard to be compatible with the highest beam currents contemplated for the future. This program is about 30% complete and should be completed in 1977. During the coming year it is planned to upgrade all beam dumps; to move beam line 4B dump outside the building to permit forward angle data-taking with the MRS; to remove the temporary dump in beam line 1 and extend the line to a combined high-current dump and thermal neutron facility well away from the meson production targets; and to insert a carbon plug in beam

beam line 4A dump to absorb a high beam power yet give low residual activity. During normal operation the radiation environment along the beam lines is about  $10^5$  rad/ $\mu$ A year, except in regions close to the cyclotron or beam dumps. Many items need not then be made radiation hard, and it is expected that access to such areas for short periods of maintenance will continue. This will not be true for the beam lines being constructed downstream of the meson production targets. The vacuum valve controllers have been modified and an interlock system designed and installed. This system allows the status of all valves and pressure interlocks to be monitored via CAMAC and to be conveniently displayed on a Telterm screen, as is the status of the monitors.

Routine maintenance and improvements to existing primary beam lines are now carried out by the site engineering staff (with some assistance from interested experimental groups), and routine beam delivery is now the responsibility of operations staff. Downtime due to beam line hardware was 5% of total downtime, and a 500 MeV beam of several microamperes can be restored in beam line 1 in about half an hour without reference to position or profile monitors except at the target. Minor tuning is carried out to reduce spills as measured by the safety monitors. New energies or modes of operation are set up initially by a beam physicist and the magnet settings and stripping foil parameters stored in the control computer as a master tune. Control computer software now compares the magnet element settings with those stored in a master file for that energy and gives an audible warning if a deviation occurs.

Setting up a beam in beam lines 4A or 4B, usually at a lower energy to beam line 1, takes about 2 h, unless a master solution exists, since the split ratio and steering need to be carefully adjusted. It should be possible to reduce this to about 1 h with the assembly of an extended range of master tunes, further shielding of the cyclotron fringe field, and development of software steering algorithms. There is no evidence for any beam-constricting apertures in the beam line; quadrupole settings and profile measurements give values close to the expected settings, and all magnetic elements are able to be tuned significantly either side of their optimum values before the spill monitor readings begin to increase.



# RESEARCH PROGRAM

## INTRODUCTION

This has been a year of many milestones in the experimental program. It was the first full year of operation and saw the fruition of several experiments. The accelerator was far more reliable than in 1975, and this was of great importance for experimenters who were battling with new and untried equipment. The polarized ion source came into preliminary operation in February and regular operation in April. It immediately transformed the experiments using the proton beam directly. Several reactions were studied and exhibited strong polarization effects. In the meson hall, the inexorable increase in the intensity of the primary beam allowed the meson experiments to develop rapidly from tests into true measurements.

A feature of TRIUMF which is unique in the world is the variable energy proton beam that can be easily extracted from 180 to 520 MeV. This feature was used to full advantage by the BASQUE group in their study of the triple scattering parameters in nucleon-nucleon scattering. The proton-proton data have been completed and the neutron-proton measurements are well under way. The (p,2p) reaction was studied by another group, and very strong asymmetry effects were observed along the lines suggested by theorists. Measurements on proton-helium elastic scattering by a third group have been expanded to include the asymmetry effects. In the meson hall a group has been studying the  $p + p \rightarrow \pi^+ + d$  reaction and has obtained spectacularly good data on the asymmetry of the pion when the polarized beam is used.

On the meson channels activity has been hectic and many successes have been recorded. With borrowed time on the biomedical channel a group has been measuring pion-carbon elastic scattering of several low energies and found unusual features in the angular distribution. The large NaI crystals have been working hard, and the reaction  $\pi^- d \rightarrow \pi^0 nn$  has been observed at rest for the first time. An improved value of the Panofsky ratio in hydrogen has also been obtained.

In addition to research in particle and nuclear physics, research and development have continued in accelerator and beam physics, with more precise measurements on the properties of the beam and the development of more new techniques for the determination of deviations from isochronism in the cyclotron.

A large and lively group has already completed some experiments on the  $\mu$ SR facility and dedicated M20 channel. In particular, a study of  $\mu^+$  spin relaxation in iron has attracted much attention.

Applied research in the biomedical program has benefited by the increase in current to 10  $\mu$ A, and two irradiations of CH<sub>2</sub>B<sub>2</sub> have been

completed. Programs are under way on proton radiography at 200 MeV and the production of  $^{123}\text{I}$ , both primarily for medical applications.

The morale of all the experimenters at TRIUMF has soared to great heights. Enormous progress has been made and already several publications have been completed. We look forward to a long and successful career for the TRIUMF accelerator.

Further details of the progress during the year will now be given. A full list of experiment proposals is covered in Appendix D.

## BEAM RESEARCH AND DEVELOPMENT

In line with the project's main thrusts—towards increased intensity and reliability—the main achievements in beam development this year have been

- (i) better beam quality and steering, allowing acceleration of beams of up to 50  $\mu\text{A}$  without excessive spill, and
- (ii) better isochronism, giving a less critical tune, and improving the prospects for separated turn operation.

Also of note was

- (iii) acceleration of polarized ions without depolarization.

In addition individual members of the group have co-ordinated Beam Line Development and chaired the 100  $\mu\text{A}$ , ISIS Commissioning, and Separated Turns Task Forces; full accounts of this work will be found under those headings. The beam performance at the end of 1976 is summarized in the following table:

Table III. Beam Performance

Property	Aim	Achieved
Energy range	165-500 MeV	183-520 MeV
Current (unpolarized)	100 $\mu\text{A}$ (500 MeV) 300 $\mu\text{A}$ (450 MeV)	1 $\mu\text{A}$ (regular) 10 $\mu\text{A}$ (12 h/week) 50 $\mu\text{A}$ (test run)
Current (polarized)	60 nA	50 nA
Polarization (reversible)	80%	78%
Split ratio (Line 4/Line 1)	1/1 to 1/2000	1/1 to 1/5000 ( $\pm 25\%$ )
Duty factor - maximum	{ 11% 20% (3rd harmonic)	11% (5/43 nsec)
minimum		4% (chopped)
Transmission (5-500 MeV)	86%	80%
Fraction of dc beam to 500 MeV	10%	8% 30% (buncher on)
Vertical centring	$\pm 6$ mm	$\pm 6$ mm
Isochronism ( $\sin \phi$ )	$\pm 0.02$	$\pm 0.1 \rightarrow \pm 0.4$
Energy spread (10% peak)	1.8 MeV 0.5 MeV (slits) 0.1 MeV (3rd harmonic)	2.0 MeV 1.5 MeV (chopped)
Radial emittance (90% beam)	$3\pi$ mm-mrad	$3\pi$ mm-mrad
Vertical emittance - internal	$1.2\pi$ mm-mrad	$1\pi$ mm-mrad
(90% beam)                      external	$2.4\pi$ mm-mrad	$3\pi$ mm-mrad
Spot size at T2	$2 \times 10$ mm <sup>2</sup>	$3 \times 14$ mm <sup>2</sup>



### *Towards higher intensities*

The rise in beam current, from 0.3  $\mu\text{A}$  at the beginning of the year to 10  $\mu\text{A}$  or more at the end, has required considerable improvements in beam quality and steering everywhere between ion source and targets in order to keep the beam spill at an acceptable level. In ISIS the 12 keV region has proved to be particularly sensitive; optics studies plus the installation of new collimators there have permitted passage of more intense beams with better quality and stability.

Inside the cyclotron about 80% of the beam accepted by the central region is transmitted to full energy. The loss in beam is attributable partly to gas stripping of the  $\text{H}^-$  ions (4 to 8% depending on the residual vacuum), partly to electromagnetic stripping (10% between 400 and 500 MeV) and partly to local beam dynamics effects (a few per cent due to excessive vertical motions—the phase excursions are too small to cause loss of beam). To avoid these localized vertical losses good beam quality and centring must be maintained in the cyclotron. Two technical improvements this year have contributed greatly in this regard.

Firstly, digitized data from the probes can now be transmitted directly to the UBC Computing Centre, allowing any trim coil current adjustments needed to centre the beam vertically to be computed and implemented within minutes rather than hours (the vertical centring is often

changed to adjust the relative intensities in the two beam lines, and small changes also sometimes occur through magnet hysteresis effects). The beam centroid is normally kept within  $\pm 0.25$  in. of the desired plane between 70 and 500 MeV.

Secondly, beam scrapers and spill monitors have been installed. The scrapers consist of extended aluminum foils mounted 1.4 in. above and below the median plane so as to strip excessively high or low ions which might otherwise be dumped on the resonators. The foils are so positioned in azimuth that all the scraped protons land close together on the tank wall (Fig. 4). This not

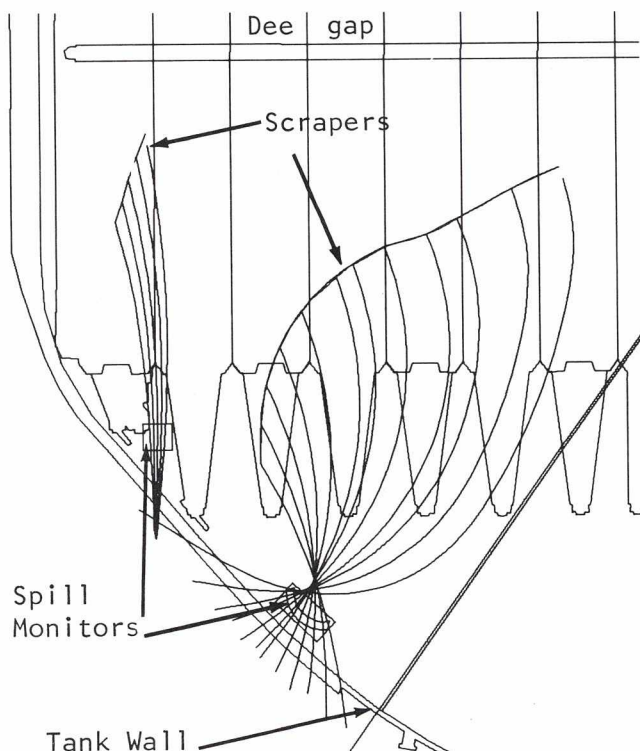


Fig. 4. Scraped beam orbits (50-500 MeV).

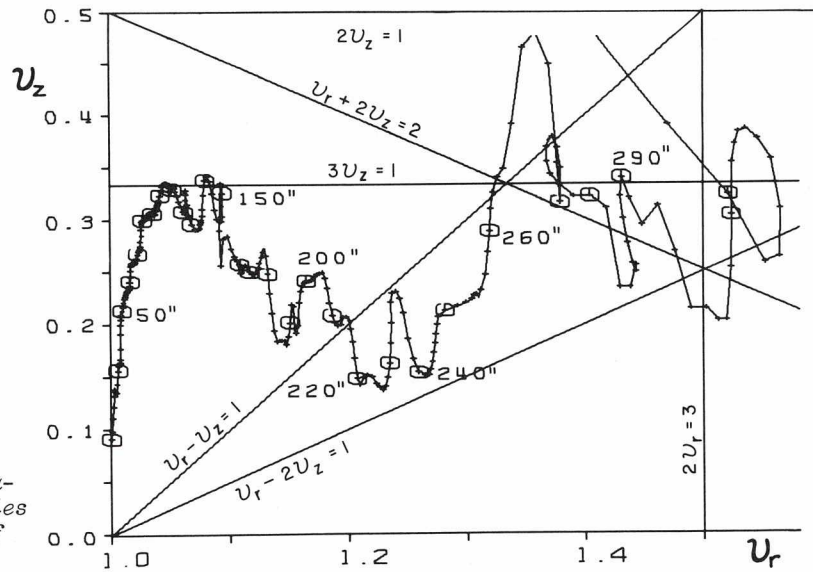


Fig. 5. Variation of beta-tron oscillation frequencies  $\nu_r$  and  $\nu_z$  as a function of radius.

only localizes the activation but makes it possible to monitor the spill from all radii simultaneously with secondary emission detectors placed just inside the wall. Direct monitoring in this way has provided a much more sensitive indication of spill than looking for losses in the transmitted beam.

The radii at which the spills occur have been determined by driving one of the HE probes in to limit the beam energy; most of the signal from the spill monitors disappears as the probe passes radii of 235 in. and 213 in. These radii coincide with the operating point crossing or coming close to the  $\nu_r - \nu_z = 1$  resonance; also  $\nu_z^2$  is low (Fig. 5). There is a smaller loss at 260-270 in. where we are again close to  $\nu_r - \nu_z = 1$  but  $\nu_z^2$  is high. Investigation with a chopped beam,  $10^\circ$  FWHM, showed that the losses were associated with the extreme positive phases (a  $15^\circ$  interval out of a total phase acceptance of  $45^\circ$ ). Furthermore, shadow measurements made at 80 MeV indicated that the extreme positive phases are less well centred radially, having a combined coherent and incoherent amplitude of about 0.6 in. It therefore seems likely that the loss is caused by the resonance converting some large radial amplitudes into large vertical motions. Further evidence of coupling resonance effects comes from a comparison of the extracted beam intensities arising from accelerating and decelerating components of the internal beam; these indicate increases in the vertical emittance of the beam as it passes certain radii, in either direction. The spill detected under normal operating conditions is 3% of the circulating beam; however, the scrapers are known to be only partially effective at some radii, so the total spill may be higher. The loss could be reduced by eliminating the positive phases with either the chopper/buncher or a radial flag, or by improving the centring for all phases.

Since the beam losses due to gas and electromagnetic stripping are not localized in azimuth, it is not possible to dump and monitor them all together. The activity induced by the split protons is distributed around the tank wall in a pattern characteristic of the loss process. Electromagnetic stripping occurs only at large radii and only on the hills, irradiating the neighbouring tank wall in six  $40^\circ$  wide bands. Gas-stripped atoms hit the tank wall at all azimuths, but the distribution is peaked because of orbit scalloping. These theoretical distributions of proton flux are illustrated in Fig. 6 for a residual vacuum of  $1 \times 10^{-7}$  Torr air. To determine the actual distribution of activity, aluminum activation foils were hung around the interior of the vacuum tank during one shutdown and retrieved the next. The activity associated with  $^{22}\text{Na}$  was measured and the activity density per unit angular interval is also plotted in Fig. 6. During the period of exposure the residual gas pressure fell from  $3.5 \times 10^{-7}$  to  $1.6 \times 10^{-7}$  Torr air equivalent. Allowing for one or two hot spots attributable to spill from probes the measurements and calculations appear to be in fairly good agreement.

In the external lines beam spill has been reduced in a number of ways. Firstly, aluminum stripping foils are being replaced by carbon, reducing the multiple-scattering halo. Secondly, magnetic shielding of sections of beam line in the vault has led to much better centred beams, in agreement with calculations. Thirdly, several foil windows were removed or reduced in thickness. Fourthly, the beam line tunes were refined and restricted to a fairly smooth variation with energy; in beam line 4A it is now possible to find an acceptable tune at a new energy by interpolation.

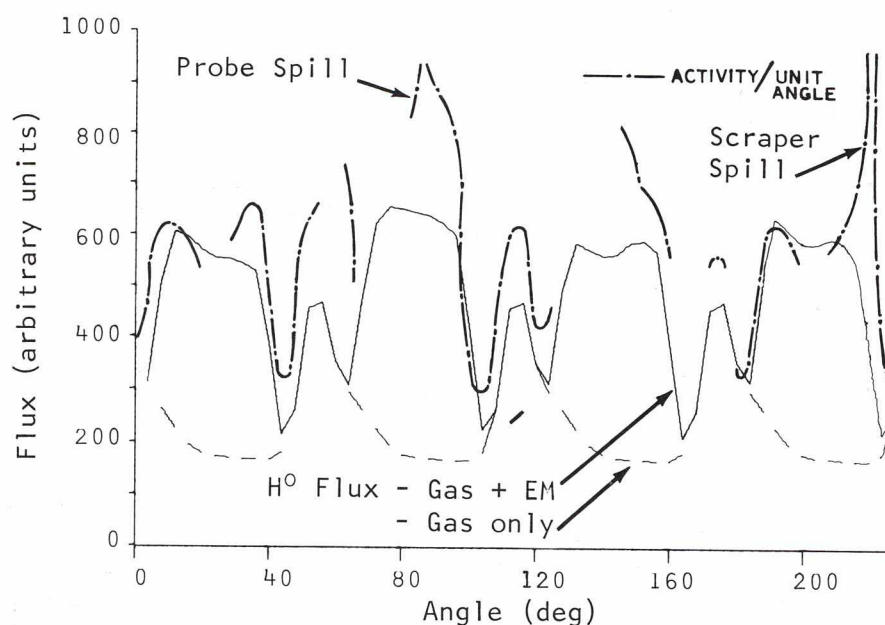


Fig. 6. Distributions around the tank wall of measured activity and calculated neutral atom flux due to stripping processes.



## Isochronism

At the beginning of the year the major outstanding tuning problem for the cyclotron was its isochronism. The first measurements of the phase history inside 220 in. radius had just been made and had revealed several excursions of  $\pm 0.7$  in  $\sin \phi$ . As a consequence the cyclotron resonance was rather narrow, the main coil and trim coil tunes being sometimes difficult to maintain and often difficult to recover after a magnet shutdown. There were thus immediate operational reasons for wanting to improve the phase history; in addition, plans for the eventual acceleration of separated turns require good isochronism.

During 1976 several iterations of measuring and improving the phase history were carried out. As a result the phase excursions were reduced from  $\pm 0.7$  to  $\pm 0.1$  from 90 to 220 in. radius; outside this the residual excursions grow from  $\pm 0.2$  to  $\pm 0.4$ , their wavelength being too short for effective treatment with the trim coils. Figure 7 shows some recent measurements taken by both trim coil detuning and 4VM2 timing techniques. In the latter method (crosses) beams are extracted at a series of energies, and protons scattered from the 4VM2 beam line profile monitor are timed relative to the RF. The trim coil detuning technique is a development of the traditional techniques based on observing beam loss as the RF or magnet is detuned. To obtain greater radial sensitivity neighbouring trim coils are ganged together to provide local phase bumps. Trim coil doublets are powered nearly equal and opposite, rather like quadrupole doublets; a similar analogy holds for triplets (with which bumps as narrow as 30 in. FWHM can be produced). The procedure is to measure the beam current at full energy as the trim coil currents are varied, the appropriate proportions being maintained by computer control. The phase bumps at various radii which induced a 50% loss in beam current are plotted as dashed lines in Fig. 7. Since the median phase history must touch each of these curves it is defined by

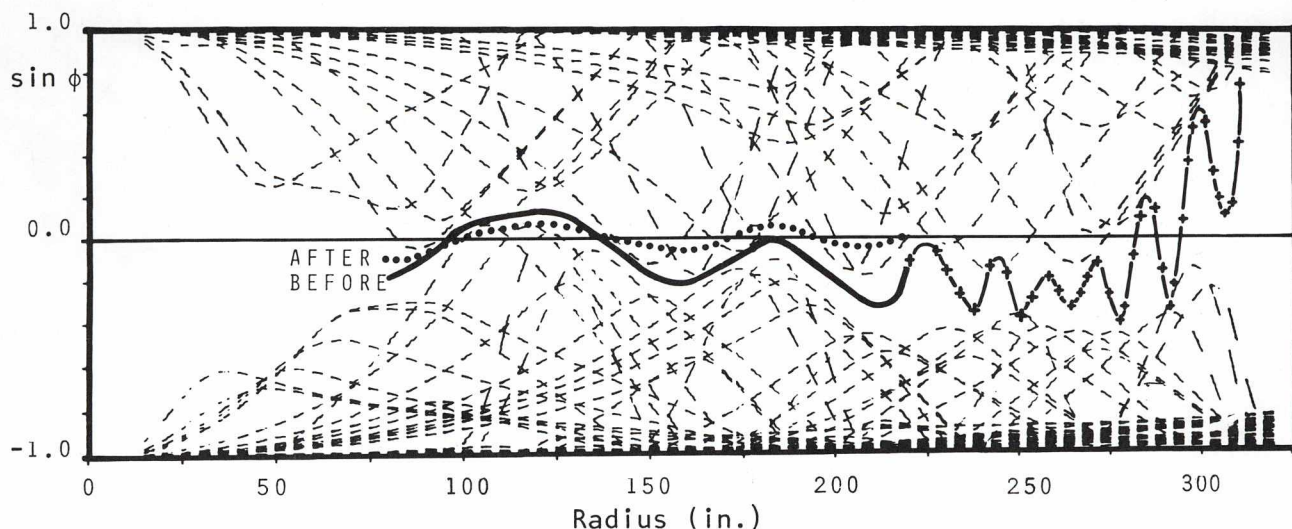


Fig. 7. Phase history determined by trim coil detuning (dashed curves) and timing the extracted beam (crosses).

the narrow passage between them (solid curve); the wider passage outside 200 in. is consistent with the phase oscillations determined by timing. The dotted curve shows the estimated result of computer-generated corrections to the 36 trim coil currents. Although tedious to perform and less precise than timing, this method has been effective in reducing the errors in  $\sin \phi$  from  $\pm 0.7$  to  $\pm 0.1$  at intermediate radii.

It should not be thought, however, that the process of tuning for isochronism is now complete. Experience has shown that the phase history can change significantly after a magnet shutdown, presumably through hysteresis effects, requiring changes in some of the trim coil settings. On the other hand, these settings are normally quite stable between shutdowns. In fact timing tests have shown that the phase stability over periods of an hour is better than  $\pm 0.04$  in  $\sin \phi$ .

The recent observation of a decelerating beam component in the cyclotron under certain conditions, in addition to the normal accelerating component, is not only of intrinsic interest [Richardson, Nucl. Instr. & Meth. 24, 493 (1963)], but could be of practical use in improving the 4VM2 timing technique for phase measurement. The decelerating component arises when the beam runs  $\pm 90^\circ$  out of phase, an event that normally only occurs when beam is allowed to reach maximum energy without being stripped. Theoretically the beam then returns on the decelerating half of the RF wave with a mirror image phase history relative to  $90^\circ$ . A measurement of the time difference between the two components would therefore immediately give the absolute value of the phase. The present 4VM2 timing technique has no absolute reference, and depends on a calculated time-of-flight correction which is strongly energy dependent.

A more fundamental drawback of the 4VM2 timing technique is that it requires extracting a beam at a series of energies, for each of which the stripping foil, combination magnet and beam line elements must be reset; moreover, it cannot be applied at energies below the extraction threshold. Timing techniques independent of the external beam lines have therefore received some consideration. One technique, on which preliminary tests have been successful, involves timing protons stripped from an HE probe as they pass outside the tank wall. For fast timing a scintillation counter is used, with a 10 ft long internally-blackened air-filled tube as a light pipe to keep the photomultiplier away from strong magnetic fields. Clean fast-rising signals were detected from protons stripped near 100 MeV and 500 MeV. Methods of extending the counter to detect protons of other energies, which arrive at different azimuths, are under study. Optical fibres with stepped refractive index, which have low loss and good timing properties, are also being tested for use as long flexible light pipes.

Time-of-flight measurements between ISIS and an HE probe, using a beam pulsed on for 10  $\mu$ sec every millisecond, also give data sensitive to the phase history. Flight times  $\tau$  vary from 70 to over 300  $\mu$ sec, depending on radius, and can be measured with a resolution  $< 0.3 \mu$ sec. The rate of change of energy with time  $dE/d\tau$  is of course proportional to  $V_d \cos \phi$ ,  $V_d$  being the local dee voltage. Unfortunately the accuracy to



which this slope can be determined from the data diminishes rapidly as the energy interval is decreased. Over the whole energy range the average value  $\overline{V_d \cos \phi}$  rose from 61.8 kV in June to 74.8 kV in September, with an estimated error of  $\pm 0.1$  kV. Locally, however, the accuracy is more like a few kilovolts; in addition to measurement errors there is the basic quantization of time in units of the orbit period  $0.216 \mu\text{sec}$ . There is also the problem of determining  $\sin \phi$  from  $\cos \phi$ ; not only is there a basic ambiguity in sign, but the sensitivity falls off rapidly as  $\phi$  approaches  $0^\circ$ . The presence of a phase spread, even for a chopped beam, also tends to wash out details in the data. In practice then, even applying data-smoothing techniques, it has not been possible to distinguish values of  $\sin \phi$  lying between  $-0.4$  and  $+0.4$ . The existence of this insensitive region together with the sign ambiguity have so far made it impossible to extract  $\sin \phi(r)$  unequivocally from the time-of-flight data. On the other hand, the data is consistent with the phase variations determined by other techniques. What also appears from the data is that  $\overline{V_d \cos \phi}$  is somewhat further below values of  $V_d$  determined in the central region by threshold measurements, etc. then can reasonably be accounted for by phase excursions. The radial variation of  $V_d \cos \phi$  would also be consistent with a drop-off in  $V_d$  by about 10 kV between half- and full-radius.

#### *Polarized beam*

A polarized  $H^-$  ion beam was first accelerated in the cyclotron in February. Out of a 200 nA beam leaving the polarized ion source 70% can be transmitted through ISIS, with an emittance of  $10\pi$  mm-mrad at 306 keV. With the use of the buncher 30 nA polarized protons can normally be extracted from the cyclotron; a maximum of 50 nA has been recorded.

As expected theoretically, no evidence has been found for significant depolarization in the cyclotron. The BASQUE group has measured the polarization of the extracted beam at five energies between 210 and 516 MeV. The results were within  $\pm 2\%$  of 78% at all energies (Fig. 8); this variation is consistent with the accuracy to which the analyzing power of the polarimeter is known at one energy relative to another. The polarization has not been measured at any lower energy; however, 78% would be a good typical polarization from a source of the POLISIS type. The Wien filter settings giving maximum polarization agreed with those calculated; the filter corrects for a  $63^\circ$  spin precession in the horizontal section of ISIS.

Efforts were made to see if the polarization could be affected by changing the machine parameters. Variations of up to  $\pm 6\%$  were obtained when the changes also resulted in loss of part of the beam, suggesting that the polarization varies across the beam. Although these measurements do not determine where the variation arises, such a variation is to be expected from polarized sources using the Sona zero field-crossing technique to enhance the polarization, since it is hard, if



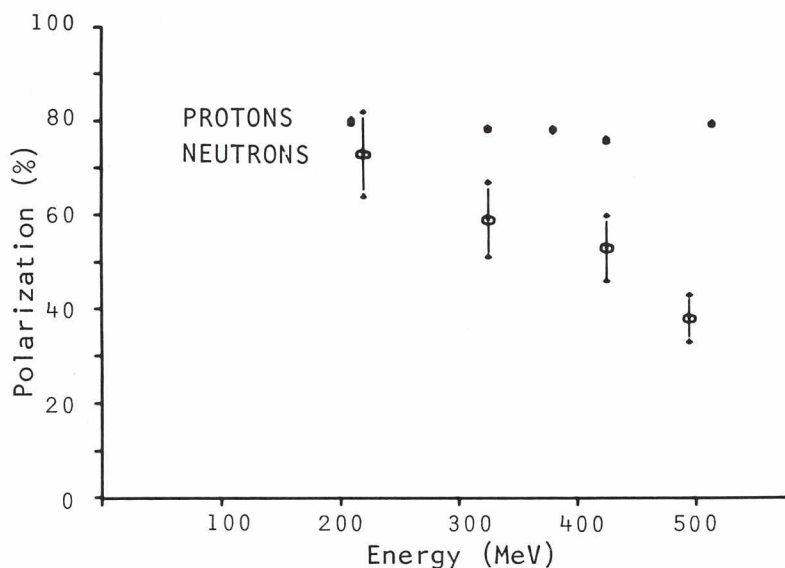


Fig. 8. The polarization of the extracted proton beam and of the secondary beam of neutrons produced from a liquid deuterium target (see p.24) as a function of energy.

not impossible, to maintain the field conditions required across the whole beam.

#### Miscellany

During October the beam physicists were surprised to find a beam in the vault section of line 4 even when the stripping foil had been withdrawn. Various tests showed that they were observing TRIUMF's first extracted beam of neutral hydrogen atoms, produced at about 410 MeV by gas stripping. The relatively high intensity was a consequence of a local gas leak—the neutral beam proving to be an effective leak detector! A beam of 100 MeV neutrals had previously been produced by stripping with a gas jet, but had only been taken as far as the tank wall.

In April the use of a 0.001 in. diam carbon stripping wire for beam line 4 enabled the 'split ratio' between the two beams (with acceptable stability in the weaker beam) to be raised to a record 5000:1. This is a factor 2.5 better than the design aim.

On the theoretical side, the possibility of extracting 70-200 MeV protons through exit port 2 has been investigated, and a proposal to extract 70-80 MeV protons for  $^{123}\text{I}$  production is being actively pursued. Orbits and matrix elements have been calculated for ions stripped by a foil mounted on the H4 slit shaft. Because of the relatively large multiple scattering (2 mrad for 0.001 in. C) and the relatively long flight paths in the hill fringe fields, the extracted beam quality is highly dependent on stripper azimuth. Studies are continuing to determine the best azimuth as a function of energy.

The problem of electrons becoming trapped in the central electric and magnetic fields and then drifting to a common escape point where they hit the RF resonators—one possible cause for the overheating of

quadrant 2 last winter—has also been studied. Electric fields were calculated in detail for various electrode geometries using the three-dimensional relaxation code. When electrons were tracked numerically through the fields present last winter they were found to hit the resonator surface close to where a hot spot was observed experimentally.

In programming, the relaxation code for determining electric potentials in three dimensions has been rewritten in FORTRAN and debugged and tested. This is nearly as fast and as accurate as the old assembler language version and is a lot easier to use. On an analytically soluble problem with Cartesian boundaries the average error was reduced to  $1/32000$  and the maximum error to  $4/32000$ . On a problem with spherical symmetry the average error was  $1/4000$ , consistent with the accuracy expected for the grid spacing.

A major effort has also gone into improving the Monte Carlo ray-tracing program REVMOC for primary and secondary beam lines. New features include format-free input, a plotting option, alternative beam pipe shapes, collimators, a Y-bend option, and relativistic multiple-scattering corrections. In addition several bugs have been removed, error checks and error messages have been added, and the speed of the program has been doubled.

The melting of aluminum stripping foils at currents of  $10\text{--}20\text{ }\mu\text{A}$  has confirmed computer predictions of their operating temperature. The Monte Carlo code PECS tracks stripped electrons through multiple foil traversals, including scattering effects, and calculates the power distribution over the foil. Another code then computes the temperature from thermal conductivity and emissivity data.

A new method is being developed to measure emittance in terms of the population density of cells in phase space; i.e., the shape is not assumed to be elliptical and the density is not assumed to vary in any particular way. The method works well for test data incorporating moderate amounts (10%) of noise and, when used on real experimental data from, say, a wire stripper, gives the gross features expected. The analysis code was a constrained least squares method; its reliability in the halo region is still being explored.

The last few years have seen the initiation of interactive programming at TRIUMF and a considerable growth in its popularity. To meet the demand the number of interactive CRT terminals has been increased to six in under three years; in this development the UBC Computing Centre has been most co-operative in providing additional ports to their IBM 370/168 and in making available the basic interactive software support. At the same time the TRIUMF computing group has built up a library of routines supporting interactive FORTRAN programs. In particular a very versatile plotting package has been developed, which this year has been upgraded to support graphics as well as alphanumeric terminals. Of the programs, INTRAN, an interactive version of TRANSPORT, has been the most widely used and has been the object of continuing improvements.

## PARTICLE PHYSICS

*Experiments 40, 74*

**BASQUE**

During the past year the BASQUE group has completed the calibration of the carbon polarimeter, the measurements of  $D$ ,  $R$  and  $R'$  at four energies for elastic proton-proton scattering, measured the polarization transfer to neutrons in liquid deuterium, measured the analyzing power of carbon in neutron charge exchange scattering, measured the precession of the neutron spin in the fringing field of the bending magnet 4AB2, and measured the depolarization parameter  $D$  in neutron-proton scattering at 325 MeV incident energy.

The carbon polarimeter described briefly in the 1975 annual report consists of an array of 12 multiwire proportional chambers, six on each side of a 6 cm thick carbon plate. Polarized protons were obtained by elastic scattering from liquid hydrogen in the nominal liquid deuterium target. Experimental asymmetries were removed by reversing the polarization direction with the superconducting solenoid in the scattered proton beam. Calibrations were made at 518, 482, 435, 387, 343, 307, 271, 327 and 209 MeV.

Upon completion of this work the superconducting solenoid was moved into a position upstream of the liquid deuterium target in beam line 4A. The depolarization  $D$  and the polarization transfer parameter  $R$  in the reaction plane for elastic proton-proton scattering were measured at  $9^\circ$ ,  $15^\circ$  and  $24^\circ$  at 210, 380, 425 and 516 MeV. In this measurement polarized protons were incident on liquid hydrogen, again in the liquid deuterium target, and the carbon polarimeter was moved to each of the three angular positions.  $R'$  was measured at  $15^\circ$  for each of the above four energies in the same series of measurements.

In order to determine the optimum production angle for the polarized neutron beam the following measurements were made for the reaction  $D(\bar{p}, \bar{n})pp$ :

$D_t$  and  $R_t$  at  $0^\circ$ ,  $6^\circ$ ,  $9^\circ$ ,  $12^\circ$ ,  $15^\circ$ ,  $18^\circ$  at 345 and 516 MeV

$R_t$  at  $6^\circ$ ,  $9^\circ$ ,  $12^\circ$  at 210 MeV.

As a result of these measurements  $9^\circ$  was chosen as the production angle and  $R_t$  and  $R'_t$ , as well as the neutron spin precession in the fringing field of the bending magnet, were measured at 237, 343, 445 and 516 MeV.

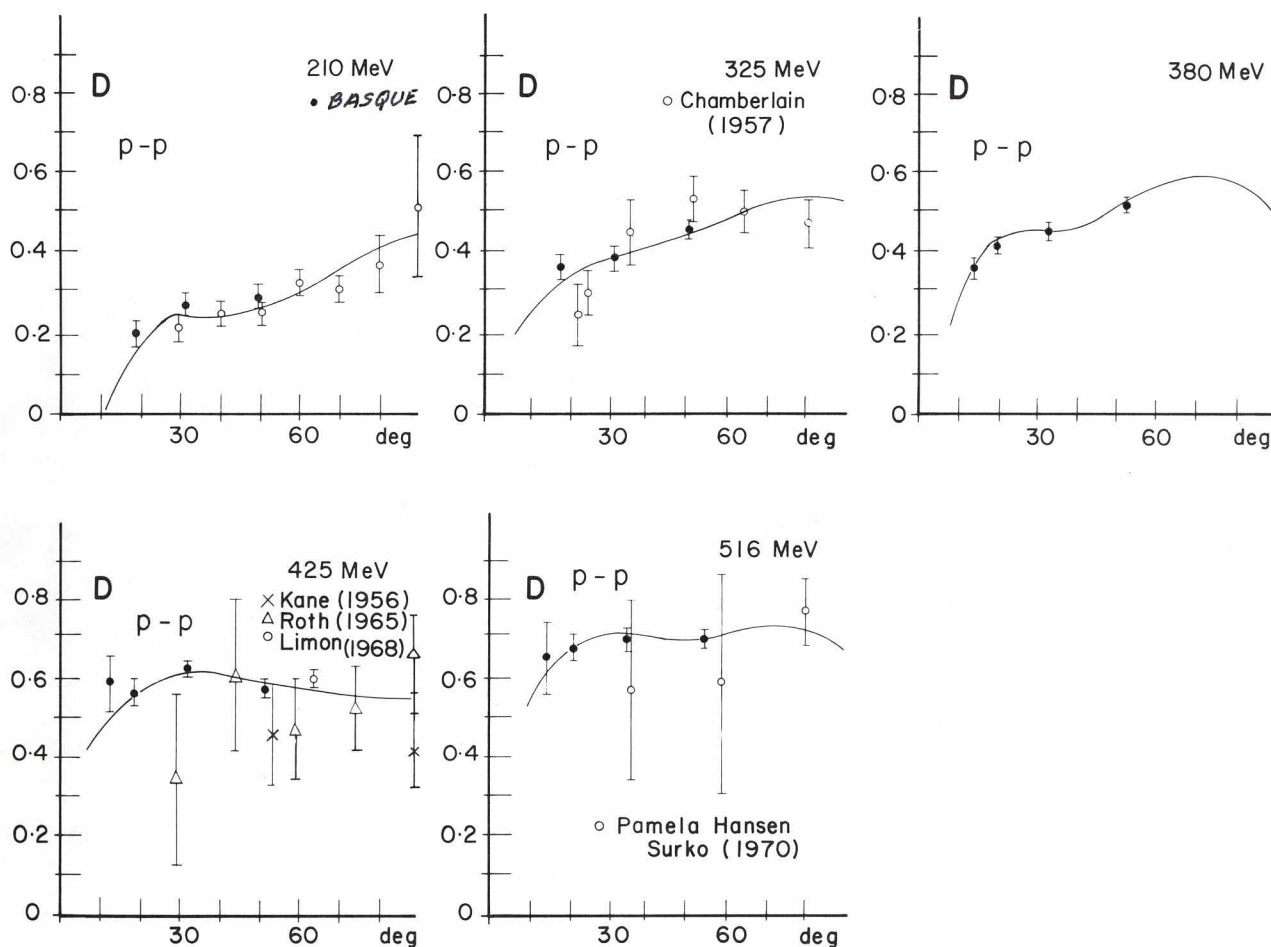
The analyzing power of carbon for neutrons was measured by bombarding a carbon target at the nominal liquid deuterium target position and observing the asymmetry of the protons produced in the charge exchange reaction.

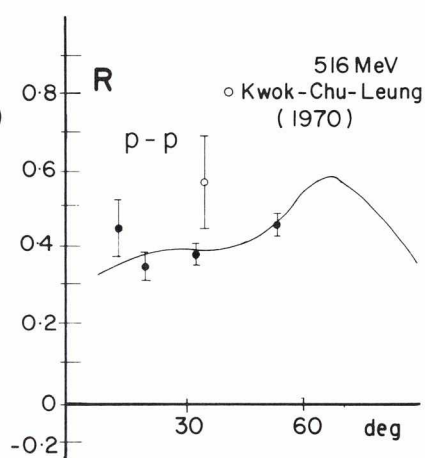
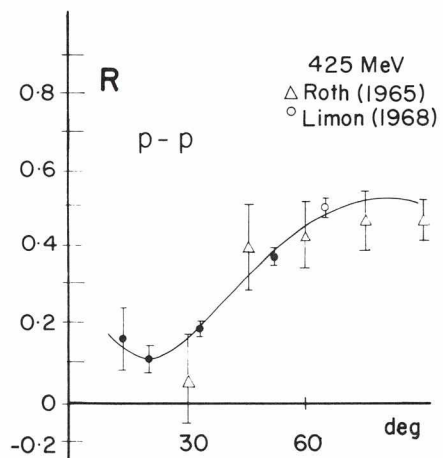
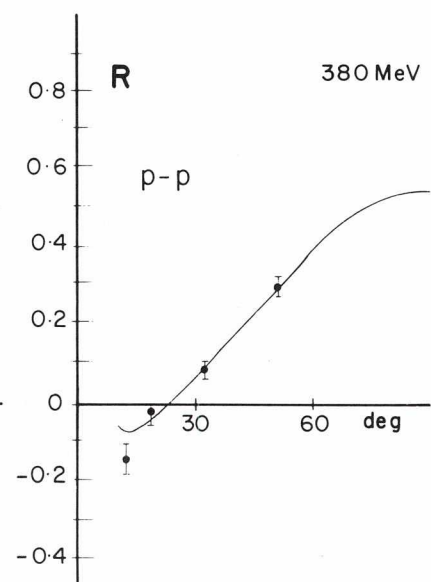
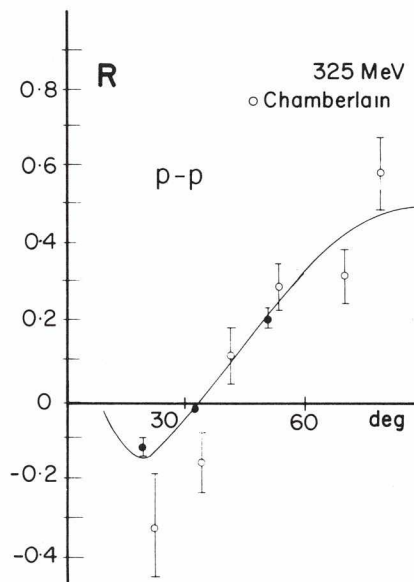
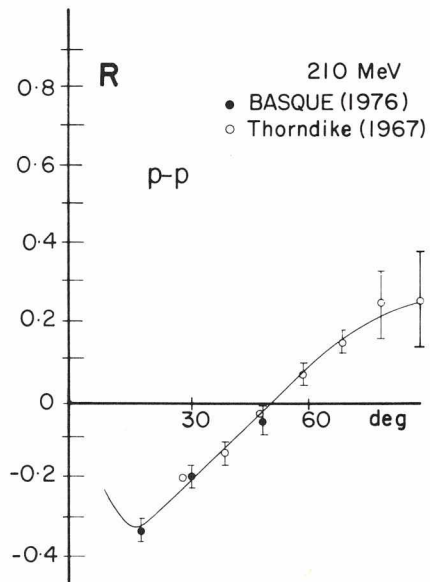
Upon completion of the preliminary calibration the UCLA magnet and the PLA magnet were installed in the  $9^\circ$  neutron line to act as neutron spin



precession magnets, and the 50 cm long liquid hydrogen target was installed. The polarimeter and neutron detector were arranged in the originally conceived configuration, and the depolarization parameter  $D$  in free neutron-proton scattering was measured at 325 MeV.

Final determination of the scattering parameters will only be available when a double scattering experiment has been done to measure the polarization parameter in  $pp$  scattering to give an absolute calibration of the carbon polarimeter. Preliminary results of the  $pp$  scattering experiment are shown in the following graphs.





Experiments 9, 41a, 41b, 23b  
Gamma-ray studies

This year has seen the first experimental results from the two large NaI crystals, TINA (46 cm  $\phi$   $\times$  51 cm) and MINA (36 cm  $\phi$   $\times$  36 cm).

Because of a change in the priorities of the BASQUE group the liquid hydrogen target, which was designed for the neutron-proton scattering experiments, became available for a few months. After some difficulties the target finally worked correctly, and pions from the M9 beam were first stopped on the liquid hydrogen flask in April. Initially both crystals gave an energy resolution of 7% for 129 MeV  $\gamma$ -rays, but with some minor improvements it is now possible to achieve 5% on a regular basis.

The first experiment to be completed was a remeasurement of the Panofsky ratio (P) in hydrogen, which is defined as

$$P = \frac{\omega(\pi^- + p \rightarrow \pi^0 + n)}{\omega(\pi^- + p \rightarrow \gamma + n)}.$$

The result was  $P = 1.546 \pm 0.009$ , which represents a factor of two improvement over the previous best value of  $P = 1.533 \pm 0.021$  obtained by Cocconi *et al.* [Nuovo Cimento 22, 494 (1961)].

The second experiment to be completed was the discovery of pion charge exchange at rest in deuterium. The allowed reactions are:

- (i)  $\pi^- + d \rightarrow \gamma + n + n$
- (ii)  $\pi^- + d \rightarrow n + n$
- (iii)  $\pi^- + d \rightarrow \pi^0 + n + n$  ( $Q = +1.09$  MeV)

The charge exchange reaction has never been observed before, and the only information was an upper limit on the branching ratio of about  $10^{-3}$  [Chinowski and Steinberger, Phys. Rev. 100, 1476 (1955)]. The technique in the present experiment was to use the two NaI crystals in coincidence. This eliminates background from the radiative capture and also minimizes the effect of the hydrogen contamination in the deuterium target. Figure 9 illustrates three spectra; the upper one is the singles spectrum for gamma-rays from deuterium, which is dominated by the radiative capture reaction (i). The centre spectrum shows the energy region where gamma-rays from  $\pi^0$  decay would be observed. A slight bump is seen but this is almost entirely from the hydrogen contamination. The lower spectrum shows the gamma-ray spectrum on TINA for a coincidence between TINA and MINA. The deuterium events are well separated from the hydrogen events because the  $\pi^0$  from deuterium has a lower energy, and the  $\gamma$ -rays therefore suffer much less of a Doppler shift. The coincidence technique has another advantage in that the geometrical efficiency is a factor of seven less for hydrogen, again because of the kinematic factors due to the  $\pi^0$  velocity. A preliminary



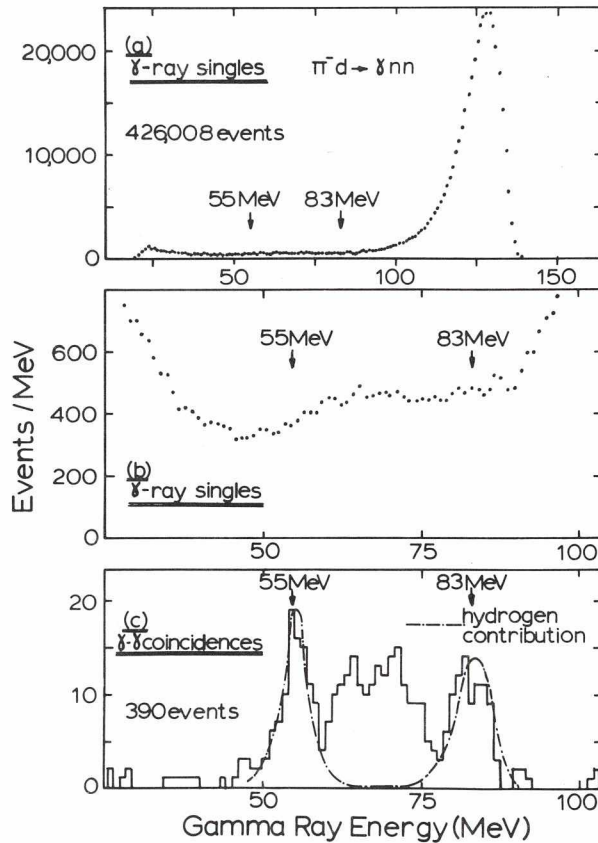


Fig. 9. (a) Singles spectrum from  $\pi^- + d \rightarrow \gamma + n + n$  with stopped pions. (b) The arrows show the region where the gamma-rays from the reaction  $\pi^- + d \rightarrow \pi^0 + n + n$  would be observed in the singles spectrum. (c) The  $180^\circ$  coincidence  $\gamma$ -ray spectrum. The dotted lines for the hydrogen contribution were obtained from a background run. The preliminary value for the branching ratio is  $(1.4 \pm 0.2) \times 10^{-4}$ .

value for the branching ratio is  $(1.4 \pm 0.2) \times 10^{-4}$ . A calculation by D. Beder is in excellent agreement with the experimental result.

Towards the end of the year some effort was expended on searches for pion charge exchange at rest in other nuclei, e.g.  ${}^6\text{Li}$ ,  ${}^{27}\text{Al}$  and  ${}^{63}\text{Cu}$ . No evidence was found and improved limits on the branching ratio of about  $10^{-6}$  were obtained.

A further experiment, performed mainly by the Université de Montréal group, is the measurement of the  $\pi^+ \rightarrow e^+ \nu_e \gamma$  decay branch (Experiment 23b). This decay proceeds via two interfering amplitudes:

- internal bremsstrahlung, which is well understood in terms of electrodynamics
- structure-dependent effects, where the photon is emitted from the weak interaction components of the  $\pi^+$  (V or A interactions are possible)

By looking at wide angles, for the  $e\text{-}\gamma$  pairs close to the maximum energy following a  $\pi^+$  stop, one preferentially selects  $\pi \rightarrow e\nu\gamma$  events which are dominated by the structure-dependent production mechanism.

A good event is then characterized by an  $e\text{-}\gamma$  pair with  $E_e$  and  $E_\gamma > 45$  MeV following a  $\pi^+$  stop. In the stopping counter one should see the

incoming and stopping  $\pi^+$  pulse ( $\sim 25$  MeV), the cluster pulse on its way out but no  $\mu^+$  pulse. The main source of background will come from the normal decay chain  $\pi^+ \rightarrow \mu^+ + \nu_\mu \rightarrow e^+ \nu_e \nu_\mu$  when the  $\mu^+$  pulse will be hidden under the huge  $\pi^+$  pulse --- in that part of the Dalitz plot where  $e, \gamma < 50$  MeV.

Because of the short lifetime of the pion one must be able to see a second pulse in the stopping counter in the shortest time possible to keep the efficiency high without affecting too much the energy resolution on that pulse, since the amount of energy lost by the electron in the stopping counter must be included in its total energy. The high-energy electrons and photons are detected through an array of plastic counters in front of two large sodium iodide crystals, TINA and MINA.

The performance of TINA has been discussed above. During the experiments on  $\pi^-$  absorption the resolution and response function at various energies for both NaI crystals was obtained. By raising the overall voltage on the MINA photomultipliers we have improved the resolution (FWHM) and measured 4.9% FWHM for 100 MeV electrons incident on a 6.75 in. diam collimator centred on the crystal axis. The resolution of MINA compares with the one of TINA but the rise time is poor (70 nsec for 10-90% rise time).

The stopping counter is the heart of the experiment. We want to be able to see a second pulse following the incident  $\pi^+$  pulse as soon as possible, determine the time at which this second pulse has occurred and the corresponding energy. Unfortunately the incident  $\pi$  pulse corresponds to 25 MeV deposited in the plastic scintillator whereas the second pulse corresponds to either a 4.1 MeV  $\mu^+$  or to 4-10 MeV left by the electron.

The counter is made of a  $6 \times 6 \times 8$  cm<sup>3</sup> Pilot U block viewed by a RCA C31024 5 stages tube. A special base has been designed to accommodate the high average current on the dynodes (for an incident  $\pi$  flux of  $5 \times 10^5$ /sec) without affecting the good timing characteristics of the fast tube. The last stage is separately powered. A passive filter is used to shorten the  $\pi$  pulses and a 15 nsec FWHM has been obtained with a 30% energy resolution on the  $\mu^+$  line. The energy is measured in a CAMAC EGG AD410 ADC with a 10-nsec-wide gate. The consecutive pulses are sorted out by a special module built at the Université de Montréal, which is capable of outputting the pulses on separate lines with a pulse pair resolution of 5 nsec.

At a stop rate of 500,000  $\pi^+$ /sec, which is a limit set by the stopping counter anode current, and the overall counting rates in the two sodium iodide crystals (70,000/sec), we expect to see close to 40 events per day.

During our last running period in November, we were able to acquire enough data to see good candidates for structure-dependent  $\pi$  evy events. In a one-day run we stopped  $10^{10}$   $\pi^+$  and 24 good events are presently being analysed for systematic effects. This experiment should be taking data during 1977.

## Experiment 52

### Measurement of the $\pi \rightarrow e\nu$ branching ratio

A measurement of the  $\pi \rightarrow e\nu$  branching ratio with a proposed accuracy of 0.5% is under way at TRIUMF. The method chosen makes use of the energy difference between the 70 MeV electrons,  $e_\pi$ , from  $\pi \rightarrow e\nu$  decay and the 0-53 MeV electrons,  $e_\mu$ , which arise in the  $\pi \rightarrow \mu\nu_\mu$  and  $\mu \rightarrow e\nu_e\nu_\mu$  chain. The energies are measured with a large NaI (Tl) spectrometer. The potential for high accuracy comes about because it is actually the ratio

$$R = \frac{\Gamma(\pi \rightarrow e\nu + \pi \rightarrow e\nu\gamma)}{\Gamma(\pi \rightarrow \mu\nu + \pi \rightarrow \mu\nu\gamma)}$$

being measured, and the ratio is independent of many experimental parameters such as the detection solid angle. An improvement in the measurement at TRIUMF is possible because of the high pion rates available, the good duty cycle, and the large high resolution TRIUMF NaI (Tl) detector (TINA).

Initial running of the experiment began in the spring. The work has concentrated on reducing backgrounds which would limit the sensitivity in determining the number of events from the  $\pi \rightarrow e\nu$  decay and at the same time maximizing this number. The electron spectrum from an October run is shown in Fig. 10. The  $e_\pi$  electrons from  $\pi \rightarrow e\nu$  decay and those from the  $\pi \rightarrow \mu \rightarrow e$  chain,  $e_\mu$ , are well separated, and pile-up background in the  $e_\pi$  region is small. However, in order to reach the proposed accuracy, one must carefully determine the fraction of  $e_\pi$ 's under the  $e_\mu$  spectrum due to the tail of the TINA resolution function. The resolution function measurement is under way using MWPC's with an

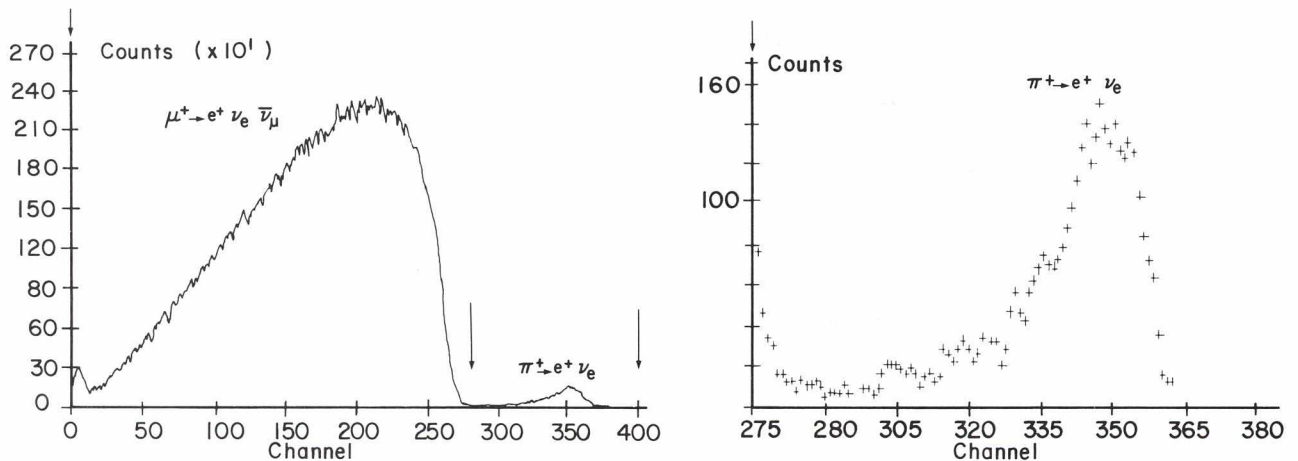


Fig. 10. The spectrum observed in the  $\pi \rightarrow e\nu$  measurements. The plot on the right shows the  $\pi \rightarrow e\nu$  region expanded.



inexpensive, fast and accurate delay line readout system developed for this purpose by the group.

A preliminary analysis of the  $\pi \rightarrow e\nu$  data taken during the year gives

$$R = 1.22 \pm 0.04 \times 10^{-4}.$$

This is comparable in accuracy to the previous best measurement [Bryman and Picciotto, Phys. Rev. D 11, 1337 (1975)], which gave  $R = 1.274 \pm 0.024 \times 10^{-4}$ , and consistent with the theoretical prediction  $R_{th} = 1.233 \times 10^{-4}$  [Marciano and Sirlin, Phys. Rev. Lett. 36, 1425 (1976)] assuming  $e-\mu$  universality.

### Experiment 10

#### Pion production

The instrumentation of the 50 cm Browne-Buechner pion spectrograph together with initial results for the differential cross-section for the  $p + p \rightarrow d + \pi^+$  reaction were summarized in the 1975 annual report. During 1976 extensive data (both differential cross-section and pion azimuthal asymmetry) were obtained for the  $p + p \rightarrow d + \pi^+$  reaction using a polarized proton beam at proton energies of 330, 350, 375, 400 and 422 MeV.  $CH_2-C$  differences were used to obtain information on a proton target. In addition, pion production cross-sections and asymmetries for the reaction  $p + {}^{12}C \rightarrow {}^{13}C^* + \pi^+$  were also measured using a polarized proton beam at 200 MeV.

Considering first the  $p + p \rightarrow d + \pi^+$  reaction, a typical pion spectrum obtained for protons of 422 MeV incident energy is shown in Fig. 11. The monoenergetic pions from this reaction stand out clearly from the pion continuum associated with the  $p + p \rightarrow p + n + \pi^+$  reaction. The unpolarized differential cross-section for 422 MeV incident energy, obtained by averaging the data obtained using polarized beam, is shown in Fig. 12. Fitting this data to a cross-section of the form  $d\sigma/d\Omega \propto A_0 + \cos^2\theta$  yields a value for  $A_0$  of  $0.23 \pm 0.01$ . Similar analyses for the data measured at 375 and 350 MeV yield the  $A_0$  values shown in Fig. 13. The previous values for  $A_0$  (reported in the 1975 annual report) as well as other recently reported results are also shown. The increase in  $A_0$  suggested by this data for values of  $\eta$  (c.m. pion momentum,  $k_\pi/\mu c$ ) below 0.7 is larger than that expected on the basis of most theories of the process. The 330 MeV data currently undergoing analysis will be used to check this dependence.

A large azimuthal asymmetry in the production of pions from the  $p + p \rightarrow d + \pi^+$  reaction using polarized protons is also observed. The analyzing power of the reactions,  $A_\pi$  (defined to be the left-right symmetry/proton beam polarization for proton spin-up), for the three proton energies discussed are shown in Fig. 14. The corresponding data measured by Dolnick [Nucl. Phys. B22, 461 (1970)] at 425 MeV are also included. The agreement between the two sets of data is excellent.

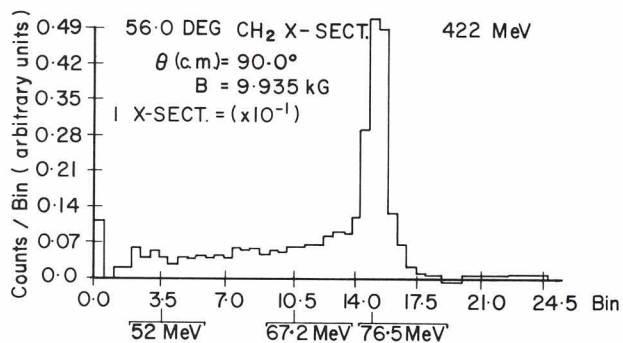


Fig. 11. A typical pion spectrum from the bombardment of a  $\text{CH}_2$  target by 422 MeV protons.

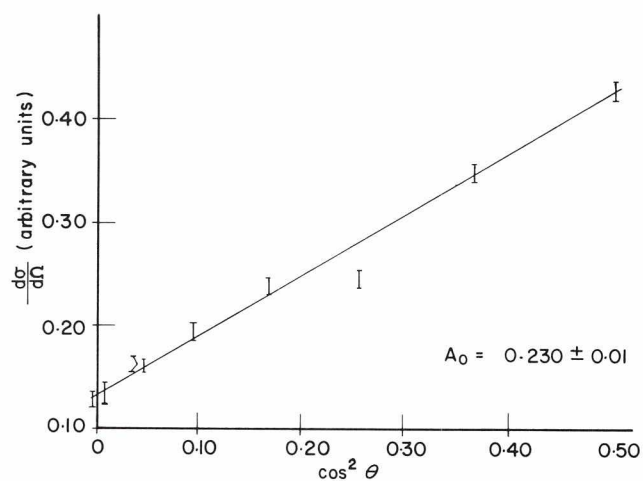


Fig. 12. The unpolarized  $p + p \rightarrow p + n + \pi^+$  differential cross-sections for 422 MeV protons.

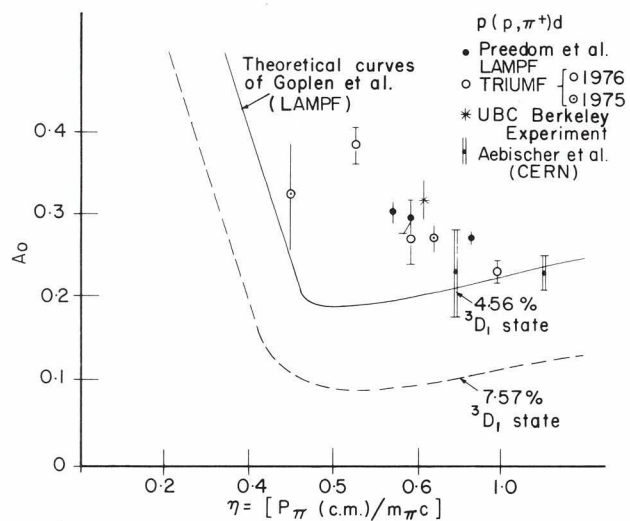


Fig. 13. The experimental values of the constant  $A_0$  in the expression  $d\sigma/d\Omega \sim A_0 + \cos^2\theta$  are shown as a function of the c.m. pion momentum. Theoretical predictions are included for comparison with experiment.

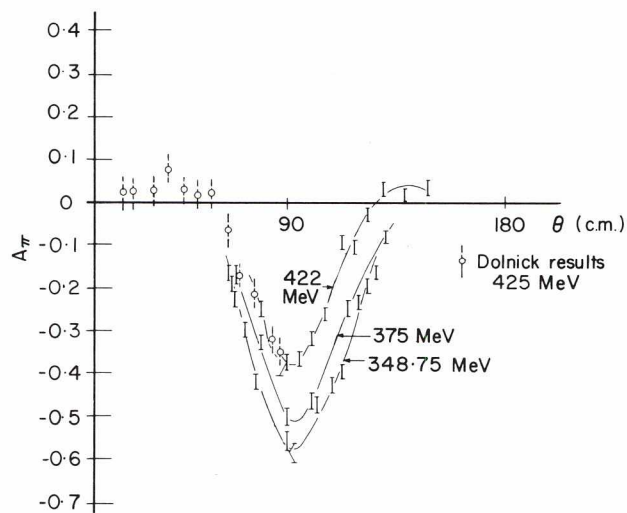


Fig. 14. Summary of analyzing power for  $pp \rightarrow d\pi^+$  reaction.

The current measurements are the first to provide  $A_\pi(\theta)$  for proton energies less than 425 MeV. The asymmetry in  $A_\pi$  about  $90^\circ$  evident in all the curves is indicative of the significance of d-wave amplitudes in this pion production reaction down to proton energies of 350 MeV.

Pion production from the bombardment of  $^{12}\text{C}$  at 200 MeV incident energy was studied at seven different laboratory angles between  $35^\circ$  and  $135^\circ$ . Pions leading to the ground state of  $^{13}\text{C}$  and the group leading to the three excited states of  $^{13}\text{C}$  at excitations between 3 and 4 MeV were clearly resolved from the rest. Cross-sections for these two groups are shown in Fig. 15 as a function of  $\theta$ . The Uppsala 185 MeV data are included for comparison. In Fig. 16 is shown the analyzing power  $A_\pi$  of this reaction for the production of these two groups of pions. Negative values for  $A_\pi$  indicate a preference for the production of pions in the direction  $\vec{k}_p \times \vec{P}$ , where  $\vec{k}_p$  is the beam momentum and  $\vec{P}$  is the beam polarization. These measurements are the first reported observations of such asymmetries in pion production leading to discrete nuclear states. The magnitude of the effect together with the interesting angular dependence should provide a useful test of models of pion production from nuclei.

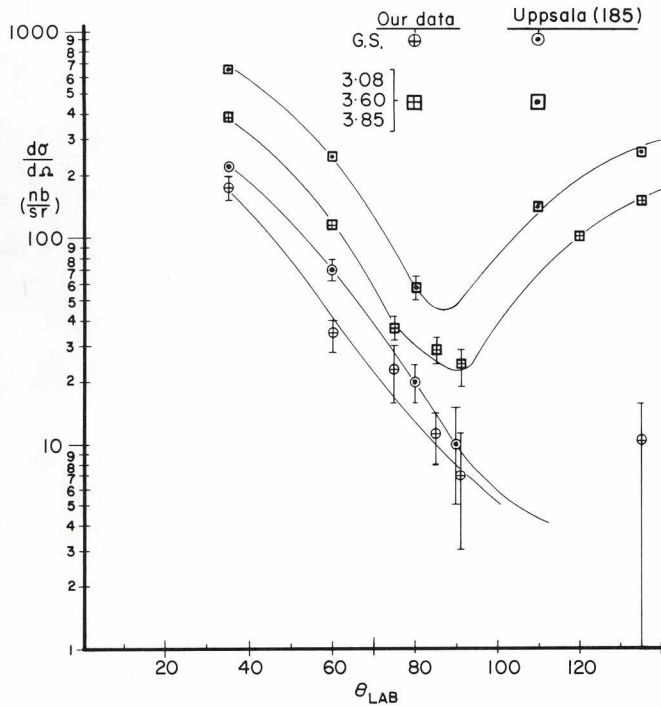


Fig. 15. Cross-sections for the reaction  $^{12}\text{C}(p,\pi)^{13}\text{C}$  leading to the ground state of  $^{13}\text{C}$  and to the sum of three excited states are shown at 200 MeV. The Uppsala data at 185 MeV are shown for comparison.

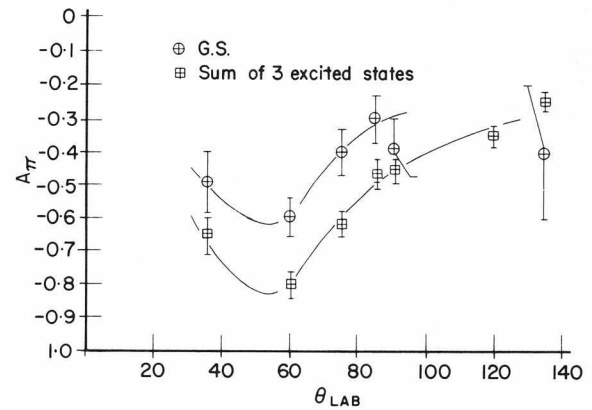


Fig. 16. Analyzing power of  $(p,\pi)$  transition to  $^{13}\text{C}$ .



**Experiment 66**  
**A survey of p-p bremsstrahlung**

The  $pp\gamma$  experiment had two runs on the cyclotron in 1976, one in April and one in September. The April run was used to measure the response of the total energy detectors to protons of energies 25-125 MeV. Figure 17 shows a cutaway drawing of one of the two identical detector telescopes. The detector is designed to have a usable detection area of 5 in.  $\times$  10 in. A tagged proton 'beam' of known energy was used to measure the response of the detectors as a function of the position that the proton entered the detector. [This technique is described in more detail in Cameron *et al.*, TRIUMF preprint TRI-PP-76-14 (1976).] Although the response of a particular photo-multiplier tube (PMT) varied greatly from side to side, by summing the signals from left and right PMT's on each detector most of this position sensitivity could be eliminated. This feature is especially important in the  $\Delta E$ -detectors because it allows rejection of events based on  $\Delta E$  pulse height as the data are being acquired.

In April the group also measured the efficiency of the veto detectors for rejection of elastic protons. The final detector on each telescope is used to veto the higher-energy, elastically scattered protons based on range. Some of the elastic protons undergo nuclear reactions in the

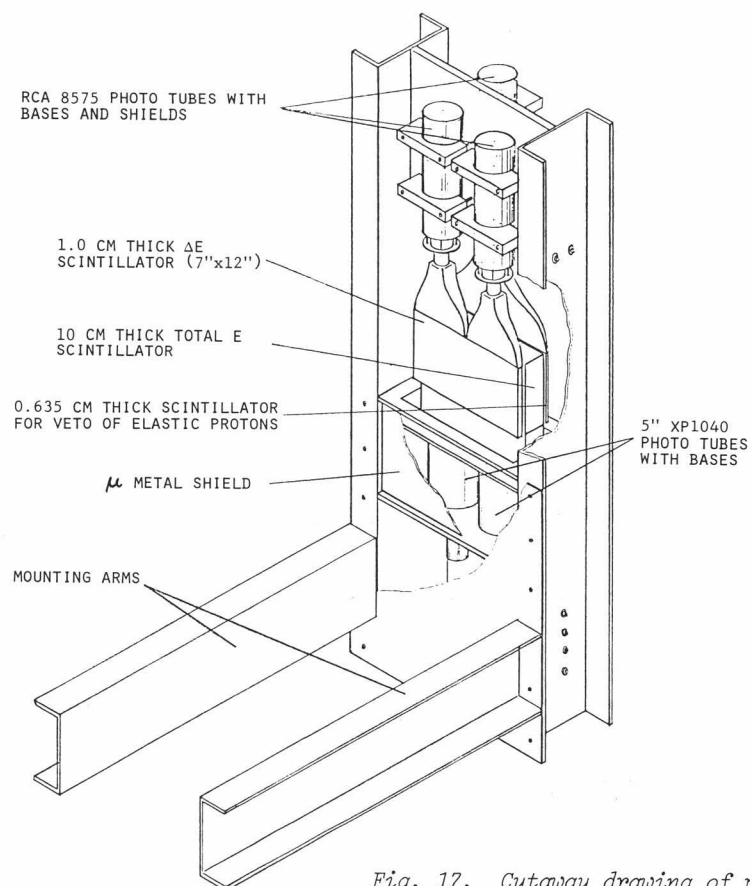


Fig. 17. Cutaway drawing of proton telescope.

$\Delta E$ - or E-detectors which prevent them from reaching the veto detector. The rejection factor of the veto detector was measured to be 10. Rejection of elastics based on  $\Delta E$  pulse height gave another factor of 10. This would give an overall rejection factor of 100 per telescope, or  $10^4$  for the coincidence events. The rejection factor is high enough that the accidental coincidences from elastic scattering will not limit the ppy counting rate.

In the September run the entire target and detector system was assembled to measure backgrounds and to attempt a preliminary ppy measurement. A design flaw in one of the MWC chambers limited the amount of beam current to a very low level, so it was not possible to actually acquire ppy data. However, the run was very useful for measuring the target-out, single-arm background as a function of angle. The background produced by the beam halo striking the edges of the entrance aperture of target chamber was found to be quite large. A system of three baffles has been designed to eliminate this background by shielding the entrance aperture from the halo produced at the upstream target entrance window.

The detector apparatus has been modified from that originally proposed. For 1977 runs the group will add a second MWC and  $\Delta E$ -detector to the detector assembly shown in Fig. 17. These modified telescopes will have better event vertex resolution and will make possible independent energy measurement by time of flight. However, the new telescopes are limited to angles larger than  $10^\circ$  because the detectors clash with the beam pipe at this angle. In 1977 the ppy cross-section will be measured at 200 MeV and at the smallest possible angles for proton emission.

#### *Experiment 60*

##### *Muonium in powdered insulators*

Muonium atoms have been shown to form in the grains of fine (70-140 Å)  $\text{SiO}_2$  (silica) powders and diffuse thermally out of the grains into vacuum. The time required for the Mu atoms to escape the grains was measured by observing the relaxation of the Mu precession signal due to depolarization by paramagnetic oxygen molecules; for the finest powder it was less than 100 nsec.

Highly polarized 'surface muons' from the M9 beam line were stopped in about 400 mg/cm<sup>2</sup> thick targets of powdered quartz at rates of typically  $2 \times 10^4 \text{ sec}^{-1}$  (using proton currents of 1  $\mu\text{A}$ ). The Mu atoms formed by these muons were precessed in an applied transverse magnetic field of about 2.5 G. Decay positrons were detected at  $90^\circ$  and  $270^\circ$  to the beam direction in the same apparatus used for gas-phase muonium chemistry.

The characteristic muonium precession frequency of 1.4 MHz/G was consistently observed in the powder targets at high vacuum, demonstrating that Mu is formed in the silica. This is expected from previous studies of solid quartz. When small amounts of oxygen were introduced into the vacuum chamber the Mu precession signal showed a relaxation rate proportional to the  $\text{O}_2$  pressure, indicating that the Mu atoms had

diffused to the surfaces of the grains and been ejected into vacuum. The hypothesis that they then remain in vacuum, bouncing between powder grains, is supported by the agreement between relaxation rates measured this way and those observed in an argon moderator with similar partial pressures of oxygen.

Four possible applications of this effect are envisioned. The original justification for the experiment was the production of muonium in high vacuum in order to search for the muonium-antimuonium conversion reaction, whose discovery would force a revision of lepton conservation schemes. Silica powders may also prove useful as moderators in muonium chemistry experiments, since the region of Mu formation is much smaller and better defined than for the usual gas moderators. It may be possible to study surface chemistry by adsorbing gases on the powder grains at low temperature; exfoliated graphite will also be studied with this possibility in mind. Finally, it is possible to accurately measure the diffusion constant for Mu in silica, for comparison with the known positronium diffusion rate.



## NUCLEAR PHYSICS AND CHEMISTRY

### *Experiments 1. 54*

#### *Pi scattering and total cross-section measurements*

The elastic scattering of pions by nuclei is dominated in the resonance region by the p-wave (3/2,3/2) interaction. However, at low energies the cross-section should be sensitive to other important effects. It was thought that the dip in the cross-section caused by the Coulomb-nuclear interference would be a particularly sensitive region.

The  $\pi^+$  flux at  $30 \pm 1$  MeV is about  $10^5/\text{sec}$  for the  $1 \mu\text{A}$  proton beam presently available. The beam is focused into a  $1.8 \times 1.2$  cm target spot and suffers a beam divergence of less than 3 msr. The small-angle data were taken with an angular resolution of about  $4^\circ$ . The most important aspect of the experimental procedure is pion identification on all stopping counters since the small-angle scattering cross-sections are measured within the  $\pi$ - $\mu$  decay cone. The electron contamination of the beam tends also to be bothersome. The pion identification efficiency was 53% with a FWHM resolution of 1.5 MeV. Pulse-height information from the two stopping counters is recorded on pulse-height analyzers. In addition, all linear signals are routed into CAMAC analogue-to-digital converters, and a third monitor arm has been installed in anticipation of higher incident fluxes.

Pi nuclear scattering has seemed well understood over a considerable pion incident energy region by using multiple scattering formalisms to obtain pion optical potentials used to calculate elastic scattering angular distributions. The pion optical potential  $v$  has been written as

$$\langle p' | v | p \rangle = \sum_i \langle p' | t_i | p \rangle \rho(p-p')$$

where the  $t_i$  are some form of the bound nucleon-pion amplitudes and  $\rho(p-p')$  is the nucleon density. The matrix elements of  $t_i$  have also been represented explicitly in terms of s- and p-wave amplitudes by writing

$$\langle p' | t_i | p \rangle = a_0 + a_1 p' \cdot p.$$

These forms of the pi nuclear optical model reproduced experimental data rather well down to 50 MeV incident pion energy.

One of the more important corrections to these scattering calculations is the consideration of the Fermi motion of the nucleons. This results in the inclusion of  $\pi$ -nucleon amplitudes over a wide range of effective energies. In fact, at 30 MeV the range of effective  $\pi$ -nucleon energies includes 0 MeV. Since nuclear absorption is the dominant effect at low energies (cf. mesic X-ray studies), it must be included in low-energy scattering calculations. These effects may be included by modifying

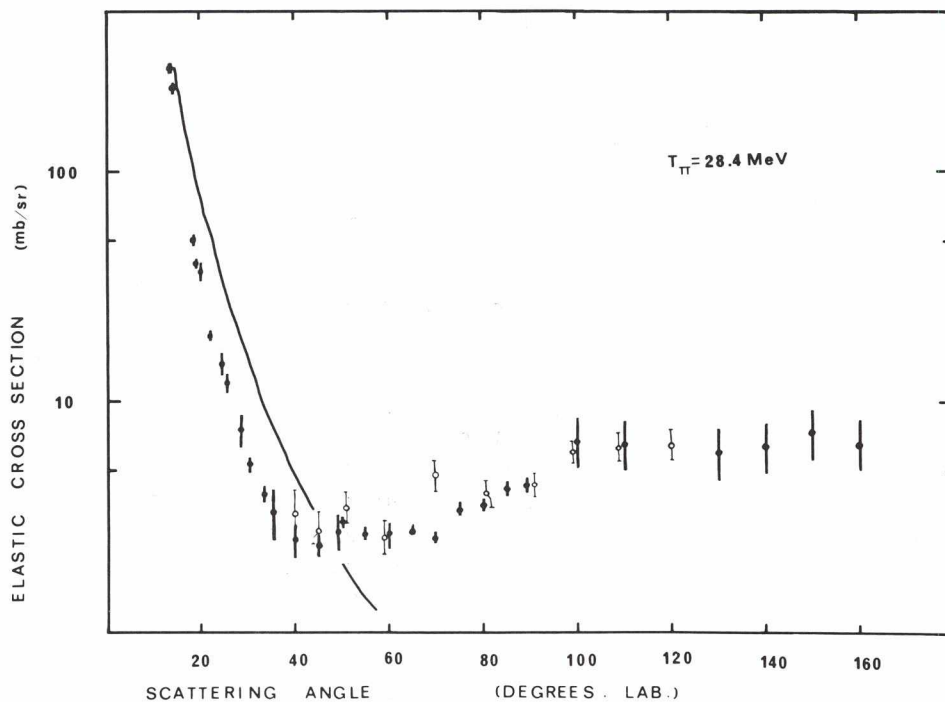


Fig. 18. The angular distribution of positive pions elastically scattered from  $^{12}\text{C}$  at  $28.4 \pm 1$  MeV. The solid points are this experiment while the open points are from Marshall et al. (Phys. Rev. C 1, 1685 (1970)). The solid line is the Rutherford cross-section for this energy.

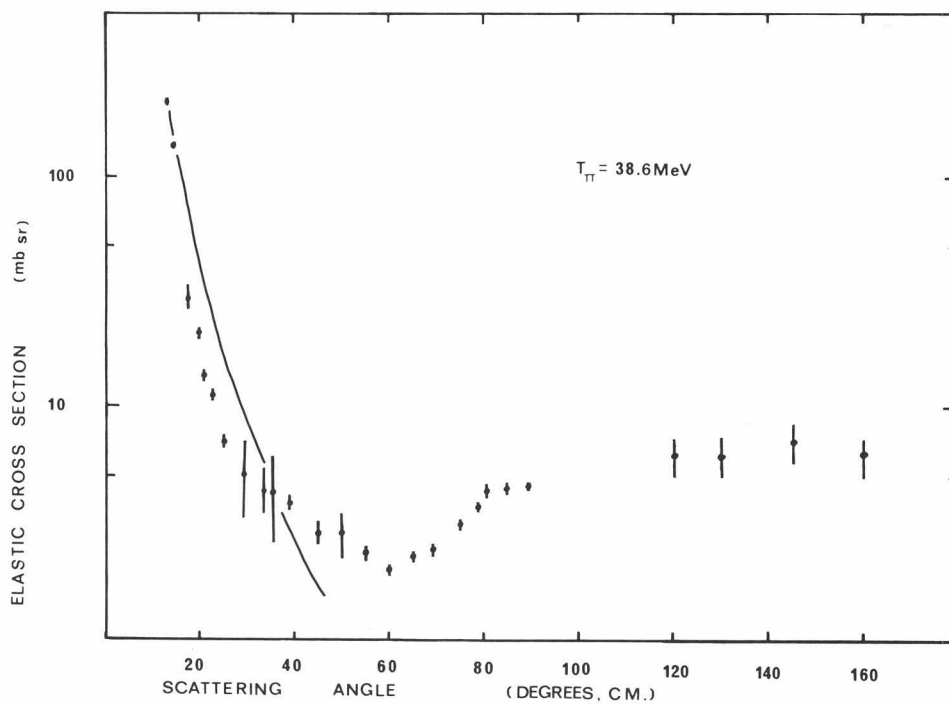


Fig. 19. The angular distribution of positive pions elastically scattered from  $^{12}\text{C}$  at  $38.6 \pm 1$  MeV. The solid line is the Rutherford cross-section for this energy. The dip at about  $60^\circ$  is largely due to the interference of nuclear p- and d-wave amplitudes.

the potentials. Since the absorptive process involves more than one nucleon, the potential must have a term proportional to  $\rho^2$ . The additional term can be estimated from a detailed analysis of the  $\pi + D \rightarrow p + p$  reaction over an energy region that includes low energies. Using this information, at least some nuclear absorption effects can be included. Figure 41 (p. 70) presents angular distributions for a selection of pion bombarding energies without these absorptive effects and then with these absorptive effects. These calculations are preliminary but certainly indicate a significant change in the angular distribution when absorption is included. The large changes in the angular distribution demonstrate that measurements are required to test any model used to calculate pion waves in this energy region (e.g. low-energy pion production calculations).

Figure 18 shows the angular distributions of  $\pi^+$  elastically scattered from  $^{12}\text{C}$  at  $28.4 \pm 1$  MeV. The solid points are the present results and replace the data shown in Fig. 2 of Dollard *et al.* [Phys. Letters 63B, 416 (1976)]. (The deep minimum shown there could not be reproduced.) The open points are from Marshall *et al.* [Phys. Rev. C 1, 1685 (1970)]. The solid line is the Rutherford cross-section for this energy. Preliminary results at 38.6 MeV are shown in Fig. 19.

The results of the theoretical analysis of these data are shown in the section on Theoretical Studies (pp. 69-75). The agreement with the calculations including nuclear absorption is impressive.

### Experiment 53

#### High-energy fission from pion absorption (HEFPA)

The target chamber, detectors and electronics set-up were tested in May. The beam current to T2 was  $\sim 700$  nA. It was found that at this level the count rate was low, one charged particle into a 100 msr solid angle counter telescope in three seconds. With appropriately placed shielding inside the target chamber the target-out count rate was one event/minute. This measured event rate and low background indicate that the first part of the HEFPA experimental program will be viable at  $\geq 3$   $\mu\text{A}$  proton currents on T2.

### Experiment 80

#### Measurement of pionic X-ray energies, widths and shifts

This experiment measures X-rays which are severely weakened and broadened by the  $\pi$ -nucleus interaction. These measurements probe the interaction at threshold and are particularly sensitive to the many-body aspects of the theory (e.g. Lorentz-Lorenz effect). The experiment has so far received twelve shifts of beam at M9, and the group's main effort has been to reduce the background by exploiting the optics of the channel.



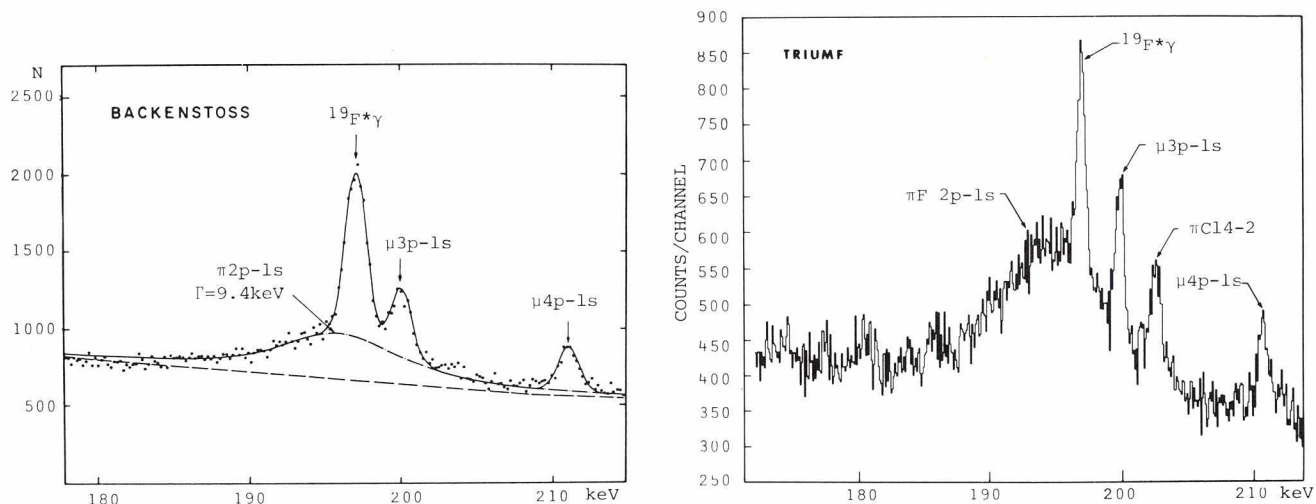


Fig. 20. Pionic 2p-1s X-ray spectrum in fluorine.

Figure 20 shows data on  $\pi$   $^{19}\text{F}$  compared with the best previous data taken at CERN some ten years ago. The energy of the 2p $\rightarrow$ 1s X-ray from a preliminary analysis is  $194.9 \pm 0.3$  keV, and the width is  $9.6 \pm 0.7$  keV. These values deviate somewhat from previous work [Backenstoss *et al.*, Phys. Letters 25B, 365 (1967)] and have errors approximately two times smaller.

Preliminary data have also been taken on Na and Mg.

#### Experiment 14

##### Elastic scattering of protons from $^4\text{He}$

##### 1. p- $^4\text{He}$ elastic scattering at small momentum transfer

Extensive measurements have recently been made of p- $^4\text{He}$  elastic scattering in the region of the first minimum at intermediate energies. It is now clear that there is no deep minimum below 1 GeV and that the ratio of height of the second peak to the depth of the dip reaches a maximum near 0.65 GeV. The behaviour of this ratio is still not understood but it seems clear that spin-orbit forces must play a crucial role in this region. Thus, it seems clear that to make further experimental contributions one should measure polarization effects. This is being undertaken at energies of 200, 350 and 500 MeV. Measurements have to date been concentrated in the region of very small momentum transfer using a gas target and detecting the recoil alpha particle and proton in coincidence. Differential cross-section data were shown in the 1975 annual report. During the past year polarization data have been added at 350 and 500 MeV in the angular range between  $4^\circ$  and  $14^\circ$  lab. Preliminary analysis of these data are shown in Fig. 21.

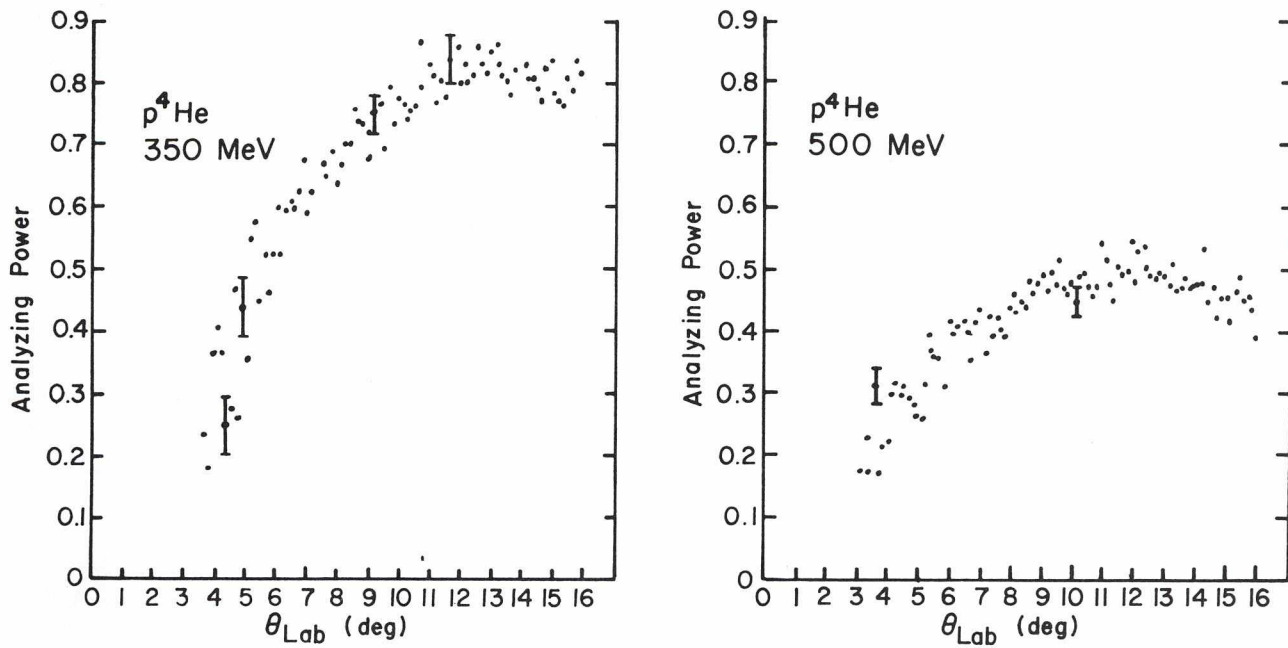


Fig. 21. Preliminary results on the angular distribution of  $p\text{-}^4\text{He}$  elastic scattering analyzing powers at 350 and 500 MeV. Typical statistical uncertainties are illustrated.

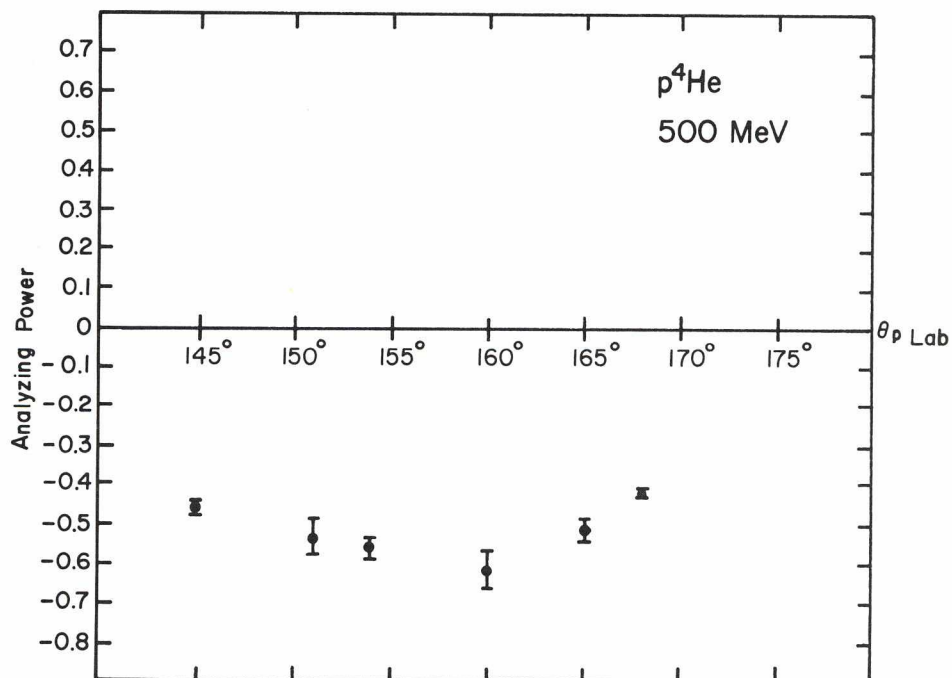


Fig. 22. Preliminary results on the analyzing powers for backward  $p\text{-}^4\text{He}$  elastic scattering as a function of proton scattering angle in the laboratory system at 500 MeV.

## 2. $p\text{-}^4\text{He}$ elastic scattering at large momentum transfer

Backward peaking of the differential cross-section for elastic scattering of protons from light nuclei in the intermediate-energy range is now well established. The reason for this peaking is still, however, not well understood, many alternative explanations being available. Possible explanations for backward peaking in scattering from  $^4\text{He}$  include nucleon isobar exchange of the type introduced to explain the  $p\text{-d}$  system, tri-nucleon exchange, or it may also be due to relativistic corrections to and high momentum components of the  $^4\text{He}$  wave function.

There were two runs this past year in which data have been accumulated. For this phase of the program a liquid  $^4\text{He}$  target and range counter telescopes were used. Measurements have been made over the laboratory angular range of  $140\text{-}168^\circ$  at incident energies of 500, 440, 350, 275 and 250 MeV. Additional measurements will be made in a forthcoming run at 225 and 200 MeV. Analysis of the data is currently in progress; a preliminary version for the analyzing power at 500 MeV is shown in Fig. 22. In addition to the statistical uncertainty shown, there is an additional uncertainty of about 15% due to the uncertainty of the  $p\text{-p}$  analyzing power used for the beam polarization polarimeter. Calibrations of this at a later date will remove this uncertainty. The large polarization effects seen clearly substantiate the importance of spin-orbit effects in this region.

### *Experiment 15*

#### *Nucleon-nuclear quasi-free scattering*

Preliminary experiments have been done at  $E_p = 200$  and 400 MeV in order to check the time resolution and counting rates for  $(p,pn)$  events. The results were encouraging and some useful data were obtained on the  $^{12}\text{C}(p,pn)^{11}\text{C}$  reaction. It was possible to observe the  $s$ - and  $p$ -hole states in  $^{11}\text{C}$  and compare them with the proton hole states from the  $^{12}\text{C}(p,2p)^{11}\text{B}$  reaction. The binding energies of the  $p$ - and  $s$ -neutron hole states in  $^{11}\text{C}$  were found to be 20 and 39 MeV, respectively, each with an uncertainty of 1 MeV.

Figure 23(b) shows a plot of the summed energies of the two outgoing nucleons vs. the energy difference for  $(p,2p)$  events which are collected simultaneously. The  $p$ -state ridge shows the expected minimum at  $q = 0$ . The sharp peak in the foreground is due to elastic scattering from hydrogen which was present in the target. Figure 23(a) shows the same plot for  $(p,pn)$  events.

The data are being analyzed to obtain momentum distributions for the hole states.



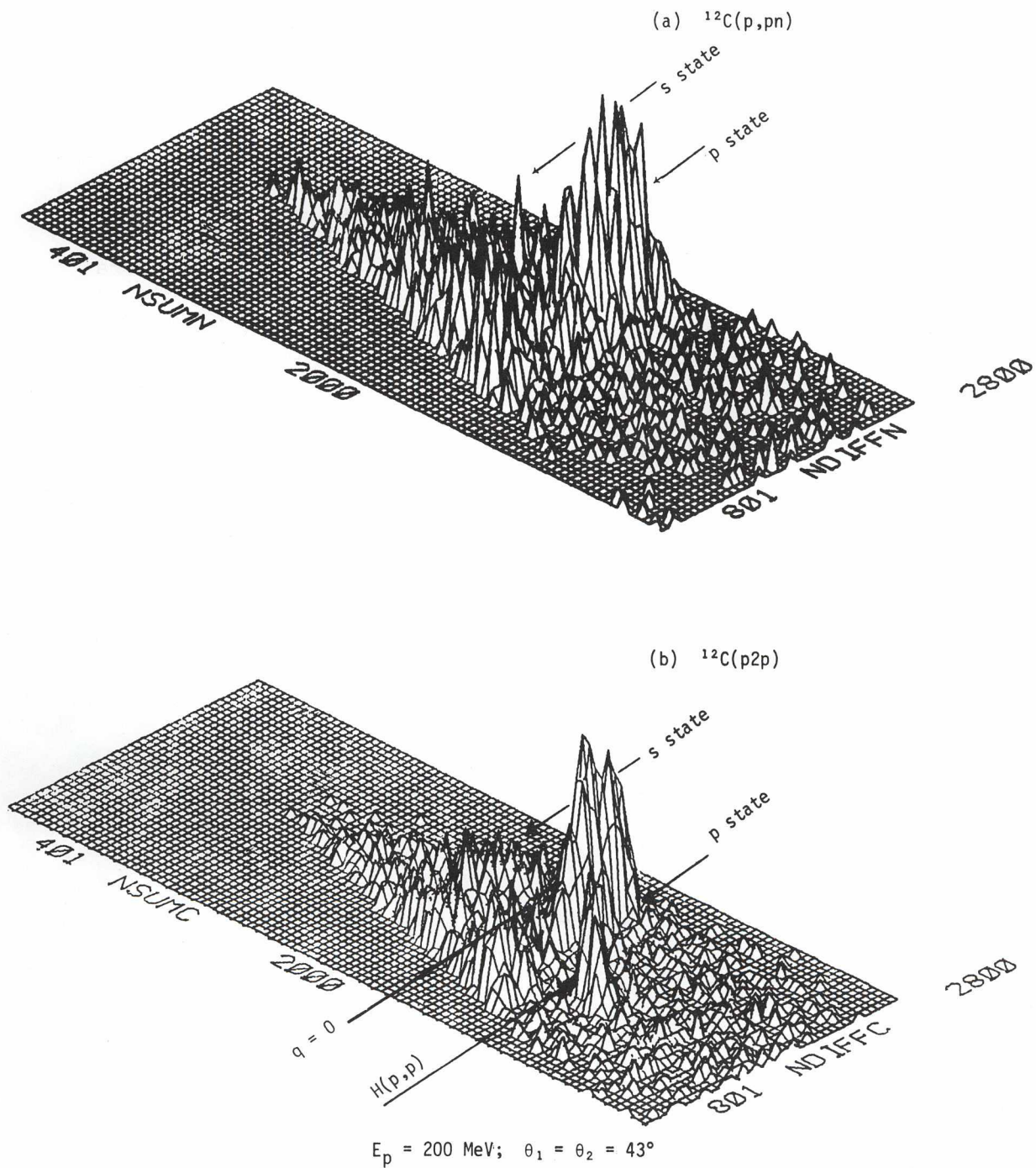


Fig. 23. The summed energies vs the energy difference for (a)  $p,pn$  and (b)  $p,2p$  events.

**Experiment 16**  
**Proton-deuteron quasi-elastic scattering**

This experiment has completed data-taking. The apparatus and some preliminary results were discussed in the 1975 annual report. Measurements of the  $^{12}\text{C}(p, pd)^{10}\text{B}$  reaction were taken for two different incident energies and five different angular settings. The main aim of the experiment is to investigate the reaction mechanism, the simplest model for which is the pole approximation. In this model the carbon nucleus is assumed to be able to dissociate into  $^{10}\text{B} + d$  and the incoming proton scatters from this deuteron. The Feynman diagram for this process is given in Fig. 24. The  $(p, pd)$  cross-section is

$$\frac{d\sigma}{d\Omega_p d\Omega_d dE_p} = K \left( \frac{d\sigma}{d\Omega} \right)_{pd} |\phi(q)|^2 g,$$

where  $K$  is a kinematic factor,  $(d\sigma/d\Omega)_{pd}$  is approximated by the free  $p$ - $d$  elastic cross-section,  $g$  is the coupling constant for  $^{12}\text{C} \rightarrow d + ^{10}\text{B}$ , and  $|\phi(q)|^2$  is the momentum distribution of  $d$ . Near the pole this momentum distribution is given by the propagator  $1/(m_d^2 - t)$ , where  $t = P_N - P_N'$ ;  $P_N$  = initial 4-momentum of  $^{12}\text{C}$ ,  $P_N'$  = final 4-momentum of  $^{10}\text{B}$ .

The data is currently being analyzed to see whether it can be understood in terms of this model. If it can, it should be possible to extract a value for  $g$ , the coupling constant.

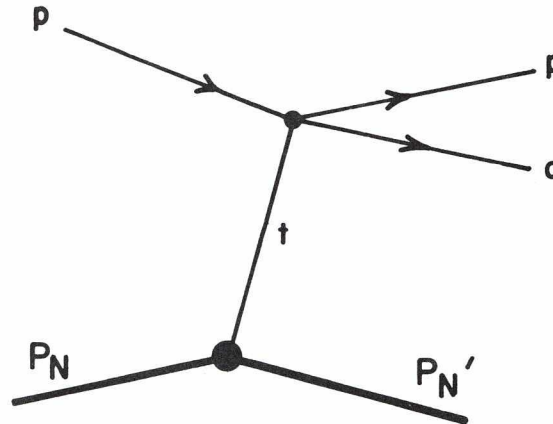


Fig. 24.

**Experiment 58**  
**Polarization effects of the spin-orbit coupling of nuclear protons**

A method of polarizing nuclear protons has been suggested by Jacob *et al.* [Phys. Letters 45B, 181 (1973)] which relies on the strong absorption of nucleons in quasi-free scattering and predicts pronounced asymmetries for the  $(\vec{p}, 2p)$  cross-section. The size and sign of the asymmetry depends on the  $j$ -value of the nuclear proton. D.F. Jackson has pointed out that the inclusion of spin-orbit distortion in the DWIA treatment of knock-out reactions makes it impossible to factorize the cross-section (as Jacob *et al.* have done) into the product of the free

p-p cross-section and the distorted momentum distribution of the nuclear proton. If the spin-orbit distortion is large, this could have a profound effect on the  $(\vec{p}, 2p)$  cross-section. In particular, spin-orbit distortion could change the asymmetries from those predicted by Jacob *et al.*, and might produce polarization of the nuclear protons in kinematics situations where the mechanism suggested by Jacob *et al.* would result in no polarization.

The main aim of this experiment was to measure the  $(\vec{p}, 2p)$  cross-section in  $^{16}\text{O}$  and, in particular, to investigate the mechanism suggested by Jacob *et al.* for selecting nuclear protons with a given polarization. Since this effect is predicted by DWIA calculations of knock-out reactions, the experiment can be looked upon as a sensitive test of DWIA, and may hopefully give information on the importance of spin-orbit distortions. So far as we are aware there has been no previous work on the  $(\vec{p}, 2p)$  reaction at medium energies.

To date energy-sharing coplanar measurements on  $^{16}\text{O}(\vec{p}, 2p)$  have been made and completely analyzed for two sets of equal angles ( $\theta_{\text{lab}} = 30^\circ$ - $30^\circ$  and  $58^\circ$ - $58^\circ$ ). The  $30^\circ$  angle pair was chosen to give a nuclear recoil direction almost normal to the direction of motion of the more strongly absorbed low-energy outgoing proton. This is the condition which will maximize the polarization of the nuclear protons arising from the mechanism suggested by Jacob *et al.* The other angle pair,  $58^\circ$ - $58^\circ$ , corresponds to a nuclear recoil direction almost parallel to the more strongly absorbed proton. In this situation the polarization of the nuclear proton could not result from the mechanism of Jacob *et al.*, and hence the data at these angles may be sensitive to the presence of spin-orbit distortion effects.

A 200 MeV polarized proton beam from the TRIUMF cyclotron was used to bombard a 1-mm-thick water target. Outgoing protons were detected by four similar detector telescopes, each consisting of a multiwire proportional chamber, a thin plastic scintillation counter, and a 5-in.-diam by 3-in.-thick NaI(Tl) scintillation detector. Two of the telescopes (FL and FR) were set at  $30^\circ$  on either side of the beam and two (BL and BR) were set at  $58^\circ$ . All coincidence events between a left and right telescope were recorded. For each event the NaI(Tl) detectors gave the energies of the particles, the plastic counters gave timing information, and the multiwire proportional chamber co-ordinates were used to reject events in which a particle was too close to the edge of a NaI(Tl) detector.

The results of these measurements were compared with partial wave DWIA calculations in which spin-orbit distortion effects are neglected. The observed asymmetry at both angle pairs and for knock-out of both  $p_{1/2}$  and  $p_{3/2}$  protons agreed well with the predicted asymmetry. A large discrepancy in normalization was observed between the measured cross-sections and the DWIA calculation at  $\theta_L = \theta_R = 58^\circ$  for  $p_{3/2}$  nuclear protons. These results have been published. During the summer a large amount of additional data were taken on  $^{16}\text{O}(\vec{p}, 2p)$  at 200 MeV. Coplanar energy-sharing measurements were made for  $\theta_1 = 30^\circ$  and  $\theta_2 = 26^\circ, 30^\circ$ ,



35°, 40°, 45°, 50°, 65°, 70°, and  $\theta_1 = \theta_2 = 30^\circ, 35^\circ, 40^\circ, 50^\circ, 55^\circ, 58^\circ, 65^\circ, 70^\circ$ , where  $\theta_1$  and  $\theta_2$  are the angles of the outgoing protons. (Measurements were also made on  $^{16}\text{C}(\vec{p}, 2p)$  at a few angles.) These data are currently being analyzed at the University of Alberta. Approximately fifteen 12-hour shifts have been used to date by this experiment. During the year 1977-78 the group hopes to make measurements on  $^{16}\text{O}(\vec{p}, 2p)$  at an incident energy of 300 MeV, and also to investigate the reaction  $^{40}\text{Ca}(\vec{p}, 2p)$  at 200 MeV. Both of these measurements change, in quite different ways, the absorption of the incoming and outgoing nucleons. It will also be of great interest to compare the results with DWIA calculations for the more complicated  $^{40}\text{Ca}$  nucleus.

### *Experiment 3*

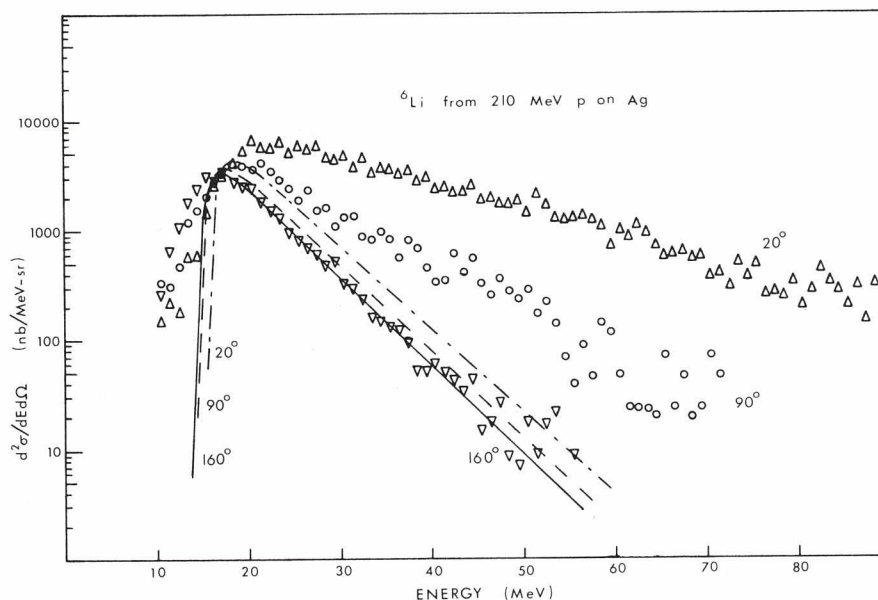
#### *The study of fragments emitted in nuclear reactions*

This experiment was designed to study the characteristics of fragment emission from Ag between 200 and 500 MeV and to compare the results with those available at 1 and 5 GeV. Both dE-E and TOF techniques using Si detectors are being used to obtain the angular distributions of particle energy spectra and total cross-sections for the emitted fragments. For scientific and practical reasons the study was divided into two parts. The first part involves the determination of the fragment excitation functions for fragments up to oxygen between 200 and 500 MeV. These measurements include only dE-E measurements for a limited number of angles and will give isotopic resolution to boron and elemental resolution to oxygen. This will give an overview of some of the main features.

The second part involves a detailed survey of fragment emissions at 500 MeV using both dE-E and TOF measurements at sufficient angles to accurately determine the angular distributions for resolved isotopes to beyond mass 20. It is necessary to decrease the target thickness (from  $\sim 2 \text{ mg/cm}^2$  to  $\sim 100 \text{ } \mu\text{g/cm}^2$ ) for these measurements since energy losses in the target for the heavy elements are substantial. This part of the study will be started shortly (about January 1977) when new TOF equipment is obtained and increased beam currents ( $>1 \text{ } \mu\text{A}$ ) are routinely available in beam line 4A where the experiment is being conducted.

Progress during the last year includes the collection of the data for the first part of this experiment and its partial analysis. Energy distributions for H to O were collected for 20°, 90° and 160° at energies of 210, 300 and 480 MeV. On the basis of this information it is already evident that whereas many of the results of the GeV studies are also observed at these lower energies there are substantial differences. The primary one is illustrated by Fig. 25 where the  $^6\text{Li}$  results at 210 MeV are presented, together with a calculation of what would be predicted for a purely evaporation process for the emissions of  $^6\text{Li}$ . This is the same calculation that was used at 5 GeV with suitable changes made for the difference in incident energy. At 5 GeV the calculation was in fair agreement for Li's up to fragment energies of  $\sim 150 \text{ MeV}$ . It is clear

Fig. 25. The double differential cross-section for  ${}^6\text{Li}$  from 210 MeV protons on Ag. The curves give the predicted distribution assuming  ${}^6\text{Li}$  was evaporated from an excited nucleus with  $E_{\text{mean}}^* = 50$  MeV and a level density parameter  $a = 5.4 \text{ MeV}^{-1}$ .



that at 200 MeV, except for extreme backward angles, the calculation is totally inadequate. For the first time then, one can say that without doubt processes other than pseudo-compound nucleus evaporation are involved in the emission of these fragments. It is now necessary to devise some direct type of process which will involve interaction with many nucleons resulting in the emission of these large fragments. Further comment must await the completion of the detailed analysis of this data.

During the initial data analysis a study was made to determine the optimum particle resolution by investigating the sources contributing to the widths of the  $\Delta E$  measurements. It was found that the major uncertainty in identifying a particle stems from energy straggling in the  $\Delta E$  detector followed by the nonuniformity of the detector. Inherent detector resolution and electronic noise generally contributed less than 1% to the FWHM's measured. At the same time a new improved algorithm based on the Bethe-Bloch equation, and including a universal effective charge curve, was developed. It is now possible to calculate the  $MZ^2$  value of any fragment without adjustable parameters and obtain improved resolution over the range of  $Z = 1$  to 10 and particle energies from 1 MeV energy deposited in the E detector to total energies in excess of 200 MeV. With these improvements it is now possible to determine the maximum resolution fundamentally possible and approach these limits with an algorithm which has only  $\Delta E$ , E and detector thickness as inputs.



## Experiment 6

### Intermediate-energy fission

The immediate objective for this experiment is the measurement of the energy distribution of alpha particles emitted in coincidence with fission fragments during the de-excitation of nuclei produced by 500 MeV protons incident on target nuclei such as Au and measurement of the coincident alpha particle angular distribution with respect to the fission fragment axis. This will shed light on when in the de-excitation chain fission takes place, a matter on which there is experimental disagreement [Wilkins *et al.*, Proc. American Chemical Society Meeting, Chicago, August 1975]. A secondary objective is a study of the influence of elevated nuclear temperature on fission parameters.

This year the angular correlation between the fission fragments from 500 MeV p + Au has been measured, with the result shown in Fig. 26. The mean correlation angle of  $81^\circ \pm 2^\circ$  translates into a c.m. velocity of 47% of the value for complete momentum transfer, consistent with the results of nuclear cascade calculations via the VEGAS code and independent measurements via nuclear track detectors [Dautet and Pate, LAMPF experiment 104]. Figure 27 shows the angular distribution with respect to the beam direction of fission fragments from 500 MeV p + Au. The distributions appear symmetric around  $90^\circ$  in the c.m., a feature of results of measurements at lower energies [Blok *et al.*, Nucl. Instr. & Meth. 122, 329 (1974)]. Such data will be subjected to analysis to extract the fission moment of inertia, once the de-excitation process is known in more detail.

The energy spectra for the fragments from 500 MeV p + Au have also been measured. The mean of the total kinetic energy release distribution,  $128.5 \pm 1.5$  MeV, is lower than the 135 MeV found for lower energy Au fission. The width of the distribution, 21 MeV FWHM, may be compared with that predicted by liquid drop calculations [Nix, Nucl. Phys. A130, 241 (1969)], 18 MeV for a fissioning nucleus of 190 amu at 235 MeV of excitation.

The mass distribution of the fission fragments from 500 MeV p + Au was obtained from their differential time of flight, plus the assumption that the distribution in fissioning system mass was narrow and equal in mean to the average mass calculated for the residual nucleus from the corresponding nuclear cascade process. The fragment mass distribution is Gaussian with FWHM of 30 amu. Earlier measurements for 60-120 MeV  $\alpha$ 's plus Au have given 38 amu, while liquid drop calculations predict 42 amu for a fissioning temperature of 3 MeV (excitation energy of 235 MeV). The presently observed narrow mass distribution is surprising and not understood. It may result from fission occurring after extensive evaporative nuclear cooling, while the average c.m. velocity is unchanged.

An initial attempt was made at the end of the year to observe triple coincidences between alpha-fragment-fragment signals. This was unsuccessful due to an unfavourable true-to-random coincidence ratio.



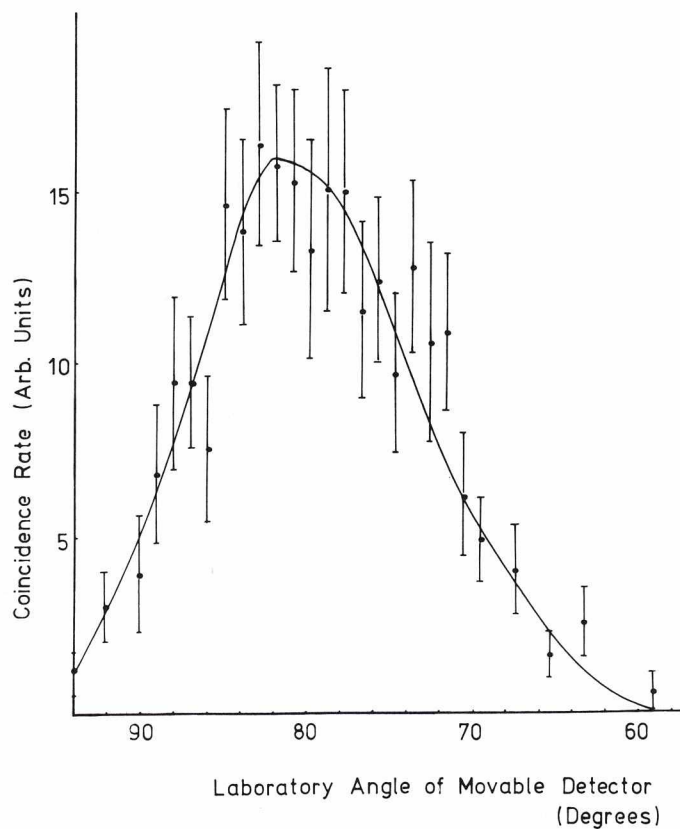


Fig. 26. Laboratory angular correlation of binary fission fragments from Au + 500 MeV protons (one fragment detector being fixed at  $90^\circ$  in the laboratory to the beam direction).

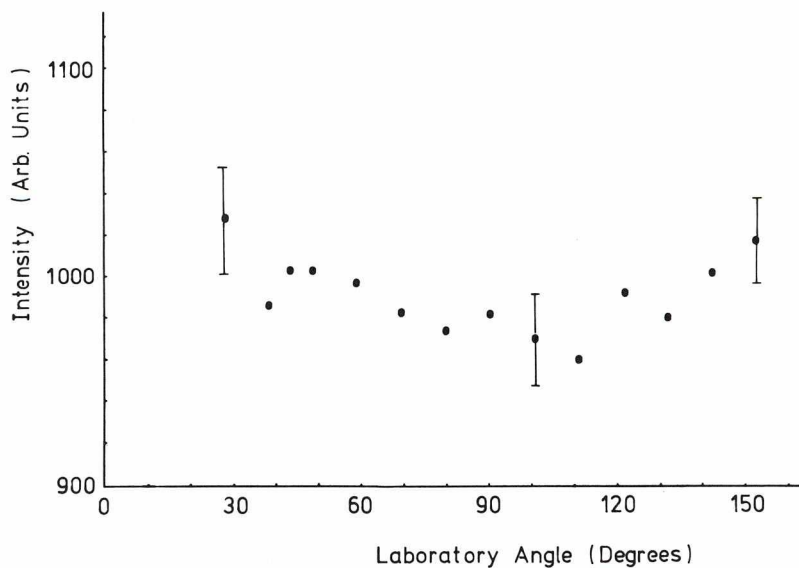


Fig. 27. Laboratory angular distribution, with respect to the beam direction, of fission fragments from Au + 500 MeV protons.

## Experiment 11

### Gas jet

A major part of the activity this year was devoted to a survey of the behaviour of the gas-jet system in different product nuclide mass regions, for different types of target systems, and particularly with fast transport times for delivering nuclides far from beta stability. Targets of different physical form including gases, solids and aerosols (e.g. droplets of  $\text{CH}_2\text{I}_2$ ) were used successfully. Cluster agents such as methanol and ethylene when added to carrier gases such as  $\text{N}_2$  and He carried the radioactive products from proton-induced fission and spallation reactions rapidly and in good yields. Half-lives as short as 760 msec and nuclides as far as 13 nucleons from beta stability were clearly observed.

A collection of detection systems, including Ge(Li) and Si(Li) spectrometers for photon spectroscopy, a  $\Delta E$ -E beta telescope for studying beta particles up to 10 MeV, and a  $\Delta E$ -E solid-state telescope for charged particle studies, were assembled to perform spectroscopic measurements of products collected on a moving tape system at the end of the gas-jet system. The feasibility of performing alpha spectroscopy studies on spallation products of heavy targets was demonstrated despite relatively low yields resulting from the low recoil ranges of such heavy spallation products. A multiple target assembly was designed to obtain greater yields.

Specific studies were attempted or performed on neutron-rich Mo and Tc nuclides, in the neutron-rich and neutron-deficient Te-Sb region, and in the neutron-deficient Zr-Mo region.

Utilizing the fission of uranium as a nuclide source, studies by ( $\gamma$ - $\gamma$ ,  $\gamma$ -x,  $\gamma$ - $\beta$ ) techniques were undertaken on the decay of heavy Mo-Nb nuclides, specifically  $^{100-104}\text{Nb}$  and  $^{104-108}\text{Mo}$ . Analysis of these data is in its final stages. This region is predicted to comprise transitional nuclei, soft towards beta and gamma deformations with evidence of both spherical and deformed shapes.

Measurements of  $Q_\beta$  values from light Te-Sb nuclides ( $^{111-114}\text{Te}$  and  $^{110-113}\text{Sb}$ ) and heavy Mo-Nb nuclides were begun, to study systematic trends in the mass-energy surface in these mass regions.

Several as yet unassigned  $\gamma$ -transitions (and half-lives) were observed in products from the bombardment of a solid Mo target with 480 MeV protons. Identification of these on the basis of X-ray coincidence studies is proceeding. A thermochromographic cell is being assembled to perform on-line chemical separations to assist in such studies.

## RESEARCH IN CHEMISTRY AND SOLID-STATE PHYSICS

### *Experiment 71*

#### *$\mu$ SR — New aspects of solids revealed by muons at TRIUMF*

In metals the positive muon behaves like a light, radioactive proton stopping preferentially at interstitial sites and subsequently diffusing among these sites. The average local magnetic field of the  $\mu^+$  can be obtained from the frequency of precession of the  $\mu^+$  spin via the time evolution of the asymmetric distribution of decay positrons; local field inhomogeneities or fluctuations can be studied via the  $\mu^+$  spin depolarization which manifests in the damping of the precession signal. This is the typical ' $\mu$ SR technique'.

#### 1) Diffusion properties of the $\mu^+$

One uncertainty which plagued the interpretation of early results was the question of how the  $\mu^+$  diffuses through a crystal lattice; this uncertainty has been reduced dramatically by a TRIUMF  $\mu^+$ SR study on Fe in the crucial temperature range from 4.2 K to 1000 K. Use of a very pure single crystal Fe target enabled TRIUMF to obtain results below the previous lower limit of  $\sim 150$  K.

In bcc Fe there are two magnetically inequivalent but electrostatically identical sites, which occur with relative probability 1:2 and have dipolar fields  $2H_1$  and  $-H_1$ , respectively. If  $\mu^+$  diffusion is fast enough, the dipolar fields are averaged out to zero; for slow diffusion these inhomogeneous fields contribute to the  $\mu^+$  depolarization. Thus  $\mu^+$  diffusion can be studied by looking at the  $\mu^+$  depolarization, which is plotted logarithmically in Fig. 28 as a function of inverse temperature. The data for  $73 \text{ K} < T < 720 \text{ K}$  are well represented by a simple exponential form exhibiting  $\mu^+$  diffusion governed by an Arrhenius law with an activation energy of 17 meV. This is three times smaller than the activation energy for hydrogen diffusion in Fe, suggesting a  $\sqrt{m}$  law, consistent with empirical tendencies between  $D$  and  $H$  but inconsistent with the theoretical predictions of a quantum theory of diffusion.

Surprising deviations from the Arrhenius law were found for  $T < 73 \text{ K}$  and for  $T > 720 \text{ K}$  (see also Fig. 29). Below 44 K  $\mu^+$  diffusion stops slowing down, suggesting that quantum tunneling dominates over thermally activated diffusion at low temperature. This interpretation is also consistent with the failure of our attempt to 'freeze' the muons in their separate sites at 4.2 K. At high temperatures (above 720 K) the depolarization rate increases again:  $\mu^+$  diffusion, which is expected to speed up, is suppressed. Perhaps the  $\mu^+$  is being trapped by vacancies or defects due to Fe self-diffusion at high temperatures.

The above investigations were made in zero field; also studied was  $\mu^+$ SR in single crystal Fe in an applied external field, extending the studies to a polycrystalline sample which was the source material for the single crystal. It was found that  $\mu^+$  diffusion does not depend on



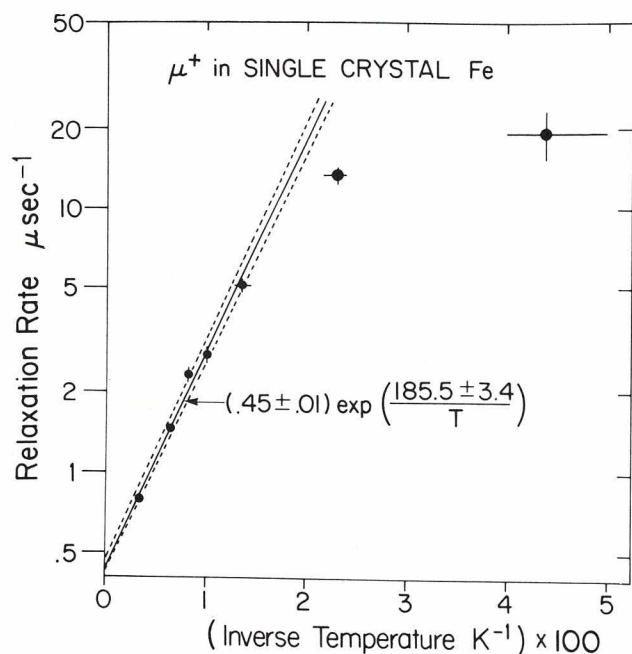


Fig. 28. Temperature dependence of  $\mu^+$  relaxation rate in Fe at low temperatures.

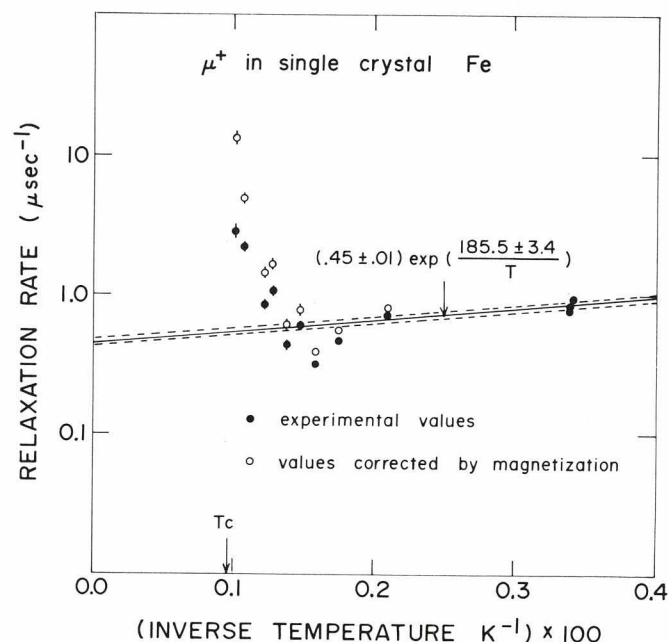


Fig. 29. Temperature dependence of  $\mu^+$  relaxation rate at high temperatures. (Extension of Fig. 29)

the density of domain walls but *does* depend on the density of grain boundaries. More systematic studies are in progress.

## 2) Studies of $\mu^+$ hyperfine fields

a) Systematics. Successful measurements of the  $\mu^+$  hyperfine fields for Fe, Co, Gd and paramagnetic Pd at very low temperatures have revealed systematic trends which are especially interesting in the context of existing data on Ni from SREL and Berkeley. In Table IV are shown the measured values of the  $\mu^+$  contact hyperfine fields, corrected for the classically predicted Lorentz fields and dipolar fields in Co and Gd. For comparison,  $H_{\text{int}}/(8\pi/3)M$  and  $M_{\text{int}}/M$  are defined, where  $M_{\text{int}}$  is the local magnetization due to the interstitial spin-density measured by polarized neutron scattering. ( $H_{\text{int}}$  should equal  $(8\pi/3)M_{\text{int}}$  if there is no spin-dependence of the conduction electron screening around the  $\mu^+$ .) There is a strong enhancement of  $H_{\text{int}}$  in all cases except Ni. These two conclusions show the importance of spin-dependent screening and that this spin-dependence is affected by the details of d-band structure as manifested in the difference between Ni and Pd.

b) Temperature dependence of  $\mu^+$  field in ferromagnets. The  $\mu^+$ SR experiment in Fe and the earlier study of Ni at Berkeley have shown that the temperature dependences of local hyperfine fields felt by the  $\mu^+$  in these two most popular ferromagnets have shown qualitatively different deviations from the temperature dependence of the magnetization, both in sign and magnitude. A term  $A(T)$  is introduced to characterize this deviation of finite temperature:  $H_{\text{int}}(T)/H_{\text{int}}(0) = A(T) M(T)/M(0)$ . The extracted values of  $A(T)$  for  $\mu^+$  in Ni and Fe below 300 K are shown in Fig. 30. The deviation for Ni is clearly opposite to and much

Table IV.  $\mu^+$  Contact Field in Magnetic Metals

	Fe (bcc)	Co (hcp)	Ni (fcc)	Gd (hcp)	Pd (fcc)
$H_{\text{int}}$ (gauss)	-11.099(10) (73.4 K)	-6185 (4.2 K)	-641 (0.1 K)	-7502 (4.2 K)	$-0.040(2) \times H_{\text{ext}}$ (300 K)
$M$ (gauss)	1749	1458	510	2115	$-0.00655 \times H_{\text{ext}}$
$H_{\text{int}}/\frac{8\pi}{3}M$	-0.76	-0.51	-0.15	-0.42	-0.74
$M_{\text{int}}/M$	-0.074	-0.16	-0.152	-0.12	$\sim +0.057$
$H_{\text{int}}/\frac{8\pi}{3}M_{\text{int}}$	10	3.2	1.0	3.5	$\sim -13$

stronger than that for Fe. The deviations of the nuclear hyperfine fields at lattice sites, on the other hand, have the *same* sign for Ni and Fe; the deviation at lattice sites in Fe is similar to that of the interstitial  $\mu^+$ .

One rather straightforward conclusion can be drawn from these features: the presence of the interstitial impurity in Ni perturbs the host magnetic structure, producing an anomalous deviation of the interstitial fields from the unperturbed local magnetization; in Fe this effect is absent. This result seems relevant to well-known impurity effects in Ni and Fe. Other possible explanations have been considered.

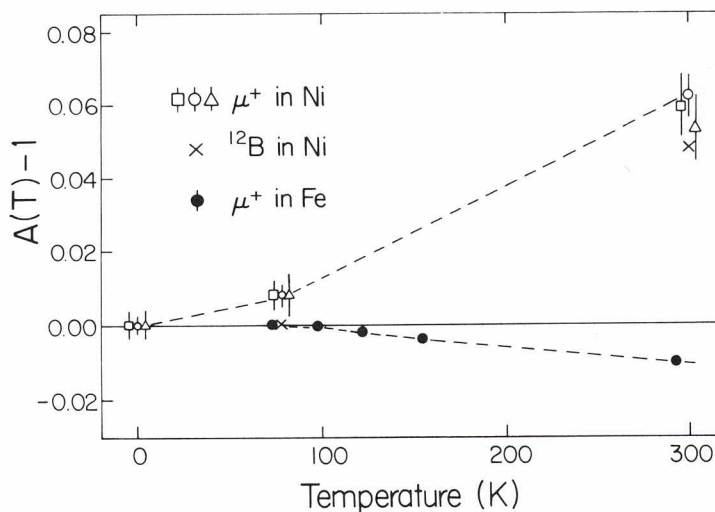


Fig. 30. Deviation of interstitial hyperfine field temperature dependence from that of host magnetism in Ni and Fe.

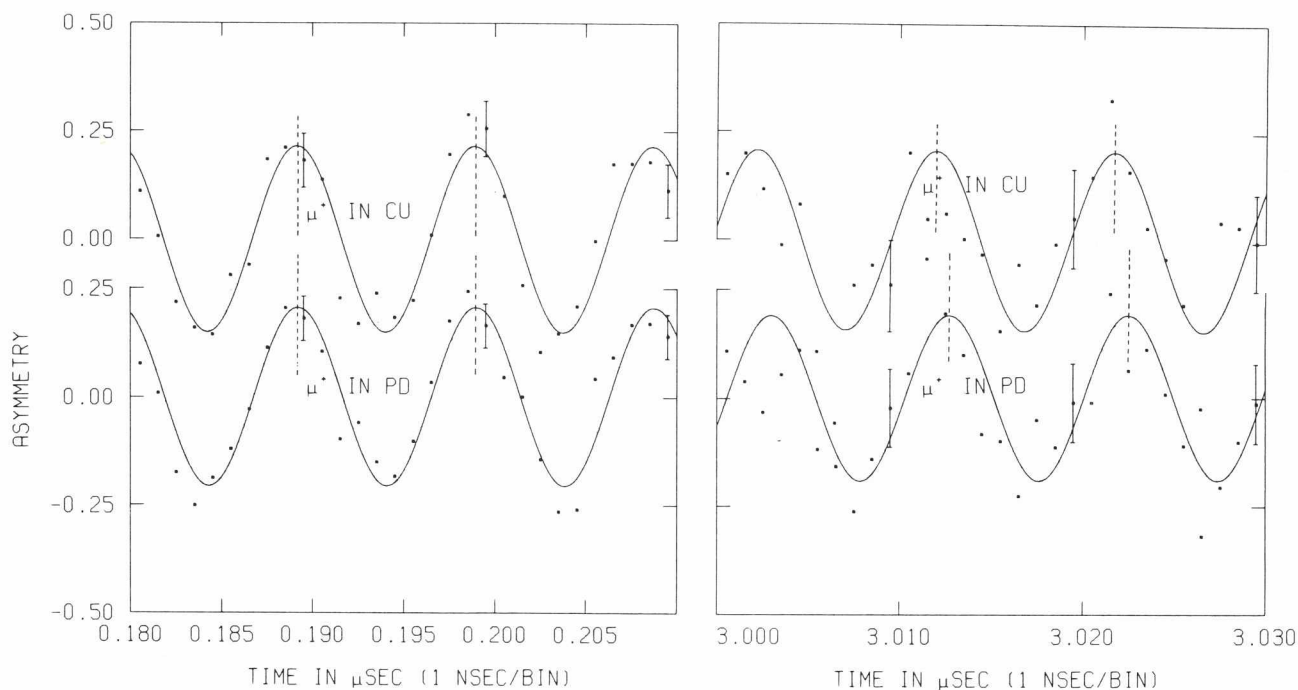


Fig. 31.  $\mu^+$ SR precession signals in Cu and Pd at very early times (left) and very late times (right). The curves are drawn from a computer fit in which the frequency is determined very precisely by the many oscillations in between the two regions shown.

c) Direct comparison between  $\mu^+$  field and  $H^+$  field. It is essential that the picture of the  $\mu^+$  as a 'light proton' impurity in metals be validated if one wishes to confidently interpret other  $\mu^+$ SR results on internal magnetic fields. Motivated by recent measurements of the Knight shift for extremely dilute hydrogen in Pd, the group made a precise measurement of the  $\mu^+$  precession frequencies in Pd (impurity concentration below 5 ppm) and (as a reference) in pure Cu at 300 K. In Fig. 31 the earliest and latest regions of the fitted time spectra are shown in an expanded scale so that the shift of the Pd precession pattern can be seen in the later portion. The measured frequency shift and the corresponding  $\mu^+$  Knight shift due to the contact field (corrected for the Lorentz field) are  $-0.013(2)\%$  and  $-0.040(2)\%$  at 300 K. These values agree remarkably well with the corresponding values for dilute H in Pd,  $-0.012(1)\%$  and  $-0.035(1)\%$  at 343 K.

### 3) Magnetic dipolar field at $\mu^+$

In some magnetic metals a dipolar field from the surrounding atoms contributes to the local magnetic field at interstitial  $\mu^+$  sites. It is important to know whether such a field component obeys classical predictions or has some nonclassical enhancement such as an anisotropic contact field with dipolar symmetry. This problem has been studied for hcp Co and Gd because of the following advantages: 1) an uncanceled, unique dipolar field always contributes to the interstitial  $\mu^+$  field; and 2) because of the directional changes in the easy magnetization axis in a specific temperature range, it is possible to isolate and identify the dipolar contribution.



The observed  $\mu^+$ SR precession patterns in Co are shown in Fig. 32, which clearly shows the temperature variability of  $B_\mu$ , the field of the  $\mu^+$ ;  $B_\mu$  is plotted vs. temperature in Fig. 33. Abrupt changes in  $B_\mu$  correspond to dipolar field variations due to rotation of the easy axis of magnetization. These effects are clearly visible between 518 K and 598 K in Co. A similar situation is observed between 50 K and 220 K in Gd.

The lattice sum of the dipolar fields was calculated by the Ewald method. Best fits to the data were obtained for both Co and Gd by assuming that the  $\mu^+$  is located at the octahedral site and that the dipolar field nearly obeys classical predictions. The resulting hyperfine fields ( $H_{int}$ ) were found to follow the magnetization within 10%. The same behaviour was observed in Co at SiN.

### Experiment 35 Muonium chemistry

#### 1) Gas phase studies

A simple and unambiguous technique has been developed for measuring muonium (Mu) reaction rates in the gas phase. This technique is made possible by the 'surface muon' beam (see M20 report, p.91), which stops completely in about 10 in. of argon at 1 atm. Mu atoms in the spin triplet state are precessed in a weak magnetic field (MSR technique), and the amplitude of the precession is observed to decay at a rate which depends upon the concentration of Mu-scavenging impurities. Chemical rate constants thus obtained are now being compared with H atom rate constants in an unparalleled test of dynamic isotopic effects in elementary reactions. So far rate constants have been measured for Mu reacting with  $Br_2$ ,  $Cl_2$ ,  $O_2$  and HBr at room temperature; results are listed in Table V. There is tentative evidence for quantum tunneling

Table V. Reaction rate data for Mu and H with  $X_2$  and HX

Reaction	$k_{Mu}^a \times 10^{10}$	$k_H^a \times 10^{10}$	$k_{Mu}/k_H$	$E_a$ (kcal/mole)
Mu+HF	-	0.00035	-	$35 \pm 3$
Mu+HCl	$<0.0015^b$	$0.002 \pm 0.001$	$<(0.5-1.5)$	$4.5 \pm 0.5$
Mu+HBr	$0.91 \pm 0.10$	$0.2 \pm 0.1$	3-9	$1.5 \pm 0.3$
Mu+HI	$9.9^c$	$0.9 \pm 0.1$	10-12	$0.75 \pm 0.75$
Mu+ $Cl_2$	$5.2 \pm 0.4$	$1.2 \pm 0.5$	3-8	$2.0 \pm 0.5$
Mu+ $Br_2$	$24 \pm 3$	$2.2 \pm 1.5$	6-23	$1.0 \pm 0.5$

<sup>a</sup>  $\ell$ /mole-sec at 295 K

<sup>b</sup> only an upper limit

<sup>c</sup> preliminary result

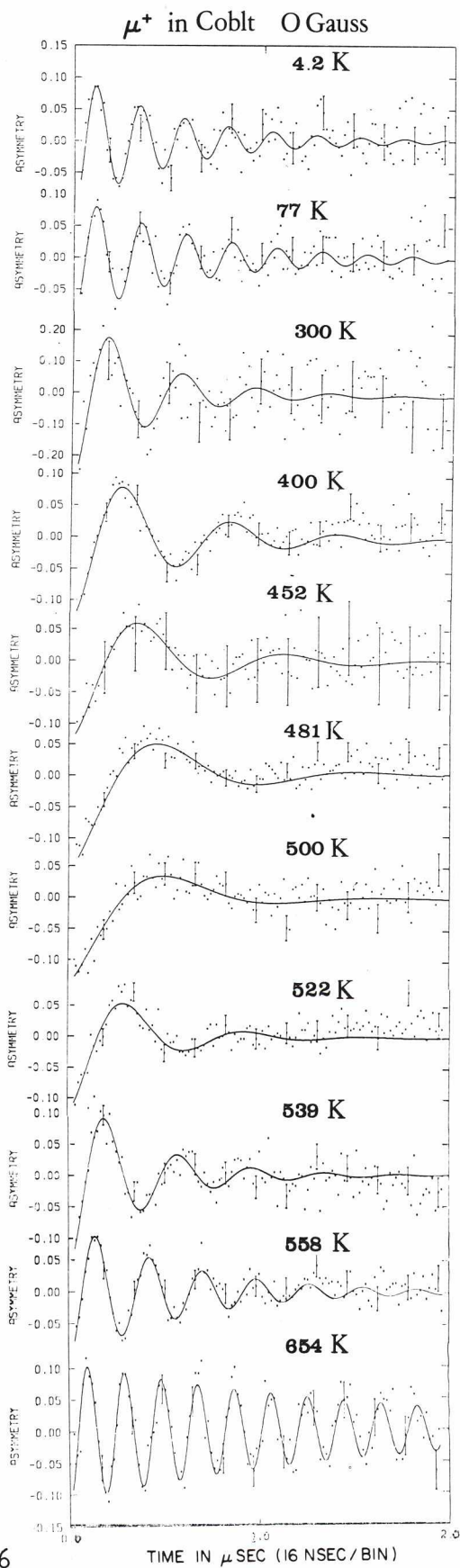


Fig. 32.  $\mu^+$ SR precession signals from Co in zero applied field at various temperatures.

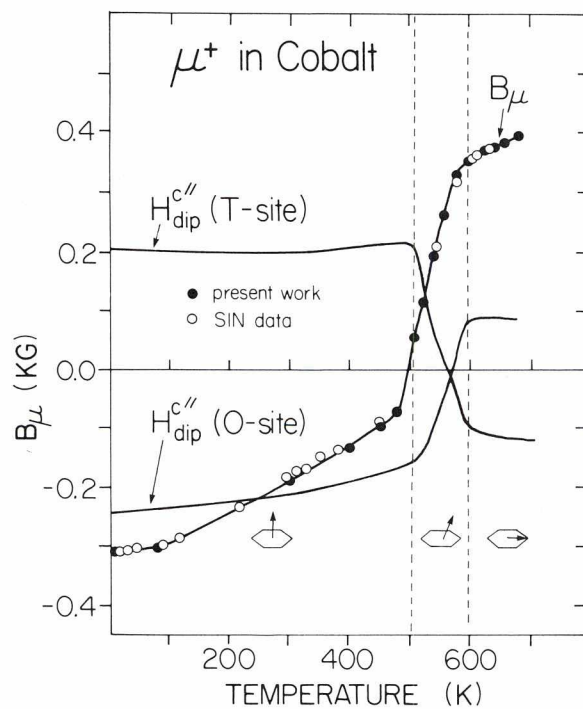


Fig. 33. Temperature dependence of the local field of the  $\mu^+$  in Co.

in the reactions of Mu with Br<sub>2</sub> and Cl<sub>2</sub>: Mu, being nine times lighter than H, will have a mean thermal velocity three times as fast, and so will collide with the same 'hard sphere' reagent molecules three times as often as H. This accounts for a 'trivial' enhancement factor of three for Mu + X<sub>2</sub> over the equivalent H atom reaction; any additional enhancement must be due to a 'dynamic' effect such as tunneling. This effect is expected to be dramatic in the Mu + F<sub>2</sub> reaction, which will be studied in 1977.

## 2) Liquid phase chemistry

Another major breakthrough in 1976 was the observation by the SIN  $\mu$ SR group of triplet Mu precession in pure liquids, permitting (in principle) direct measurement of Mu reaction rates in the liquid phase by the same MSR relaxation method used so successfully in gases (see above); however, the very small amplitudes in liquids will necessitate high-statistics runs. Preliminary tests of a TRIUMF apparatus using ultra-pure water seem to confirm the SIN results.

While this 'direct MSR method' in liquids is a vitally needed tool for reducing the ambiguity of liquid-phase Mu chemistry results, the more indirect 'residual polarization method' is still a necessary (and very convenient) way of exploring the chemical behaviour of Mu. In this method one observes the precession of muons which have reacted very shortly after the formation of Mu, placing the still polarized muons in diamagnetic molecules. This is the only known way to study the *hot-atom* reactions of Mu, which have been another focus of the muonium chemistry program at TRIUMF in 1976. A few of the epithermal reaction probabilities (h) measured in this way are listed in Table VI.

Much of the effort in this branch of the program has gone into solving systematic problems associated with the normalization of the asymmetry, the key observable in this method: the degree of correlation of decay positrons with the  $\mu^+$  spins depends dramatically upon the energy of the positrons detected, as well as the residual polarization of the muons. A typical apparatus rejects low-energy positrons ( $E_e \leq 20$  MeV) by absorbers, raising the experimental asymmetry (good) but destroying the normalization (bad, at least for residual-polarization measurements). The finite thickness of a typical stopping target for conventional muons has a similar effect, and so *density* variations in the liquid targets are translated into intolerable *asymmetry* variations. An apparatus using 'surface muons' on a thin target is now ready and should eliminate these difficulties, allowing more precise measurements of residual polarization than have hitherto been possible.

## 3) Solid-state chemistry

A TRIUMF search for muonic radical precession has, like the parallel search at SIN, met with only tantalizing results. A muonium-like signal is barely visible in solid CS<sub>2</sub> at 20 G, but it does not last long enough to tell whether it is 'split' into the anomalous two-frequency precession expected as the signature of a radical such as  $\cdot\text{MuS}$  or  $\cdot\text{MuCS}_2$ . This phenomenon will be studied further in 1977.



Table VI. Measured asymmetries and deduced hot fractions for liquids with varying physical and chemical properties

Target	Asymmetry <sup>a</sup>	Hot Fraction h	Density g/cm <sup>2</sup>
Bromine (L)	0.203 ± 0.003	0.95 ± 0.03	3.119
SnCl <sub>4</sub>	0.217 ± 0.009	1.02 ± 0.05	2.226
TiCl <sub>4</sub>	0.214 ± 0.004	1.00 ± 0.04	1.726
CCl <sub>4</sub>	0.214 ± 0.005	1.00	1.594
SiCl <sub>4</sub>	0.103 ± 0.003	0.48 ± 0.02	1.483
CHCl <sub>3</sub>	0.166 ± 0.004	0.78 ± 0.03	1.489
DMSO	0.141 ± 0.009	0.66 ± 0.04	1.095
Water	0.110 ± 0.004	0.52 ± 0.02	1.00
MeOH	0.102 ± 0.004	0.48 ± 0.02	0.792
2-propanol	0.099 ± 0.006	0.49 ± 0.03	0.752
Acetone	0.075 ± 0.003	0.37 ± 0.02	0.789
2-2,4-trimethyl- pentane	0.070 ± 0.003	0.35 ± 0.02	0.692
Nonane	0.088 ± 0.005	0.44 ± 0.03	0.718
Decane	0.090 ± 0.007	0.45 ± 0.04	0.730
Tetradecane	0.082 ± 0.003	0.41 ± 0.02	0.764
Benzene	0.05 ± 0.009	0.25 ± 0.03	0.879

<sup>a</sup>The errors in the asymmetries are standard errors obtained from programs such as MINUIT.

A search for different Mu formation efficiencies in D- and L-quartz crystals has so far yielded negative results. Any difference would constitute evidence for a possible natural selection between optical isomers in Earth's prebiotic organic chemistry.

### Experiment 73

#### Artificial negative muon polarization

The aim of this experiment is to polarize negative muons during their lifetime in the ground state of muonic atoms, using high magnetic fields and low temperatures, and thus hopefully to produce an enhanced polarization larger than the natural residual polarization (<1/6).

For the first series of experiments the group tried to utilize the strong hyperfine fields at lattice sites in rare earth metals: in Er or Dy one would expect a large enhancement of the  $\mu^-$  polarization even at liquid helium temperature, as long as the  $\mu^-$  spin-lattice relaxation time is short compared to the  $\mu^-$  lifetime ( $\sim 80$  nsec). It was first

attempted to polarize the  $\mu^-$  bound in Er at 1.5 K with a magnetic field applied vertically, perpendicular to the muon beam direction. Here the ( $\mu$ -Er) muonic atom looks like an exotic Ho impurity in the Er host. Polarization effects were monitored via the decay electron asymmetry in 'up' and 'down' electron counters. The resultant asymmetry turned out to be smaller than 5%, in contrast to the expected value of 18%. This result must be due to a suppression of the  $\mu^-$  spin relaxation mechanism in Er. In order to detect such a small effect with a reduced experimental asymmetry, the apparatus has been reconfigured using a 50 kG longitudinal field superconducting magnet. The experiment will soon continue with single-crystal Er and Dy.

## APPLIED RESEARCH

### Experiment 61

#### Biomedical experimental program

The biomedical experimental program in 1976 has been concentrated on three areas: clinically important measurements of the physics of the pion beam, dosimetry of the pion beam, and *in vitro* biological measurements of the relative effectiveness of pion radiation.

Measurements of the pion yield from the channel as a function of channel momentum have shown a continuously increasing pion flux up to 220 MeV/c (the maximum channel momentum). Integral range curves have shown a constant loss of pions due to in-flight interactions in water of  $1.62 \pm 0.05\%/cm$  for 210 MeV/c incident pions. This causes the number of pions reaching the stopping peak as a function of channel momentum to have a maximum at 200 MeV/c, as is shown in Fig. 34. A knowledge of the width of the stopping peak for full momentum acceptance allows the calculation of the pion stopping density, also shown in Fig. 34.

Investigation of the electron contamination of the beam has shown that it decreases sharply with increasing momentum. Furthermore, it is dependent on the configuration of the proton beam on the pion production target, decreasing to a minimum as the proton beam grazes the proximal surface of the target. Further work to minimize the electron contamination is being carried out.

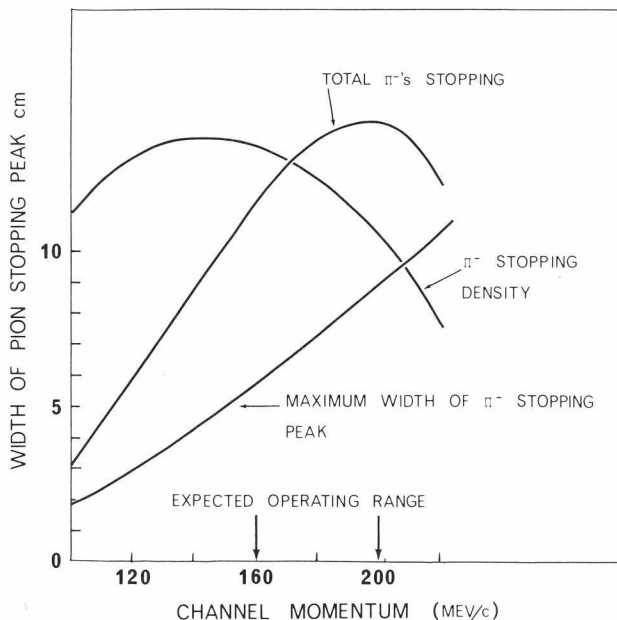


Fig. 34. The relative pion flux reaching the stopping region, the stopping flux density and the thickness in depth of the stopping region for full momentum acceptance as a function of the channel momentum.



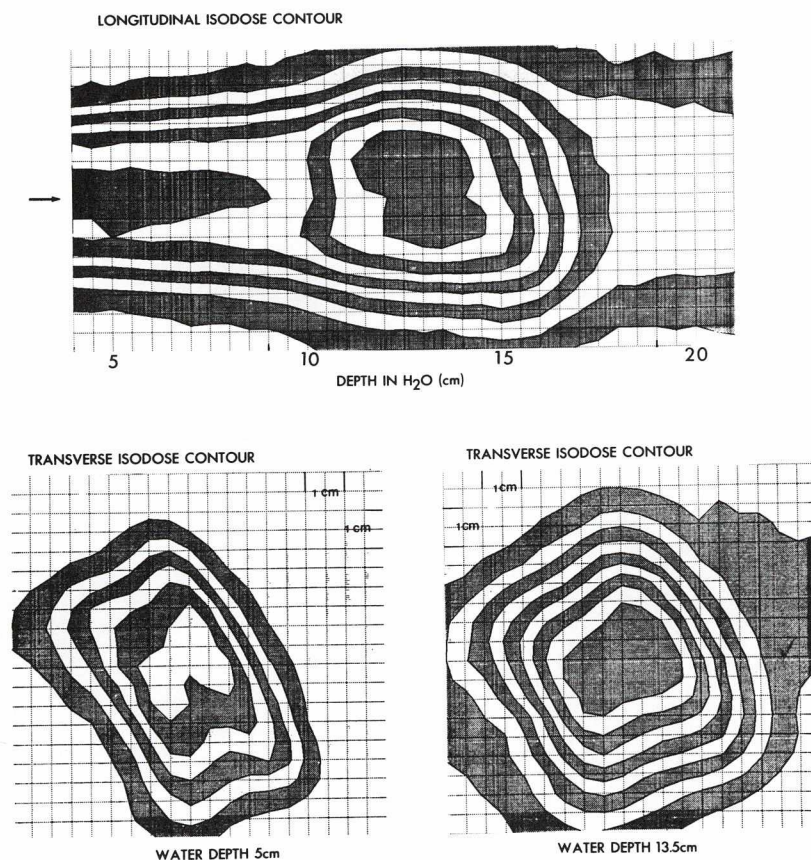


Fig. 35. Isodose contours for a 148 MeV/c midline momentum time showing a longitudinal section in the plane of the beam line and two transverse sections—one in the plateau at a depth of 5 cm and the other at the peak at a depth of 13.5 cm.

Dosimetry of the pion beam dose distribution has been done using tissue-equivalent ionization chambers. A computer-controlled x-y-z scanner coupled with an automatic integrating readout allows a spatial matrix of the dose to be measured. Each dose point is normalized to a constant number of pions, using a transmission chamber. By software interpolation isodose contours are generated, as shown in Fig. 35.

Using the beam tune which is shown in Fig. 35, initial biological irradiations have been done using CH<sub>2</sub>B<sub>2</sub> cells suspended in a 25% gelatin matrix. The gel cylinder has been irradiated from the end at 0°C with pions and then has been extruded and sliced at 1 mm intervals. Cells from each slice are plated and grown to assay the fraction of cells that have survived the radiation. The results of two such irradiations are shown in Fig. 36 with the corresponding depth-dose profile.

During 1977 further biological research will be directed towards investigating the RBE and OER of several cell systems *in vitro* and of several tissue systems *in vivo*.

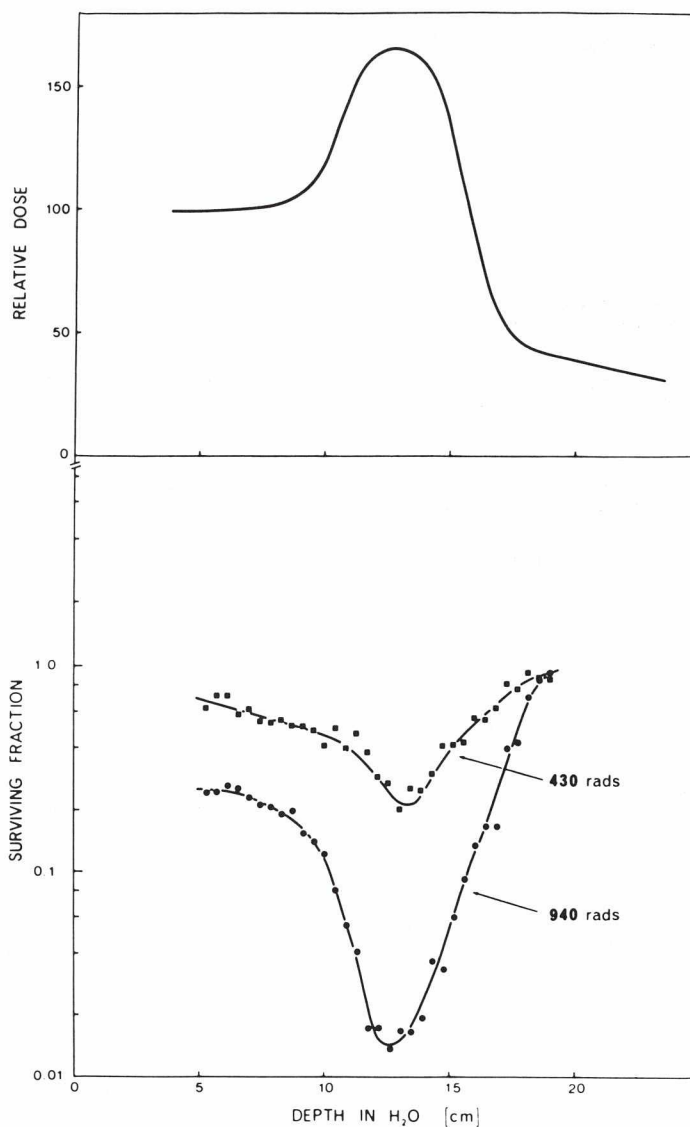


Fig. 36. Survival of Chinese hamster cells ( $CH_2B_2$ ) irradiated with pions. Top: The depth-dose profile for pions with momentum between 138-158 MeV/c. Bottom: Depth survival curves for two different total peak doses 430 and 940 rad. The dose rate at the peak was approximately 2 rad/min.

**Experiment 87**  
**Proton radiography**

Charged particles such as protons have a well-defined range in matter. A detector placed near the end of the range of a monoenergetic proton beam will see a large intensity change for a small density or thickness change in the material which the beam has traversed. This property of charged particles can be exploited to make radiographs of solid objects with improved density resolution over conventional radiographs with X-rays. For instance, a 1% change in the transmitted intensity for 200 MeV protons in the most sensitive part of the range curve corresponds to a 0.02% density.

The transmitted proton intensity can be measured with film to produce a picture similar to an X-radiograph or, as will be described here, scintillation counters can be used to give better accuracy together with the possibility of three-dimensional reconstruction.

The experimental arrangement used for most of the measurements is shown in Fig. 37. A pencil beam of protons with an energy of 200 MeV and an intensity of  $10^4$ - $10^6$ /sec is obtained by inserting a pair of collimators 1 mm diam separated by 2.6 m, a beam spot of 2 mm diam base width is obtained after a drift distance of 4 m. A pair of standard horizontal and vertical steering magnets just downstream of the second collimator are programmed to scan the beam in a raster fashion over the test object. A range telescope consisting of four scintillators each 6 in.  $\times$  6 in.  $\times$  0.25 in. thick is used to detect the transmitted protons. A pair of thin scintillators before the test object determine the incident beam intensity and a variable thickness absorber is used to put the range telescope into the sensitive region of the proton range curve. At each point as the beam is scanned over the test object the counts in each of the telescope counters are scaled for

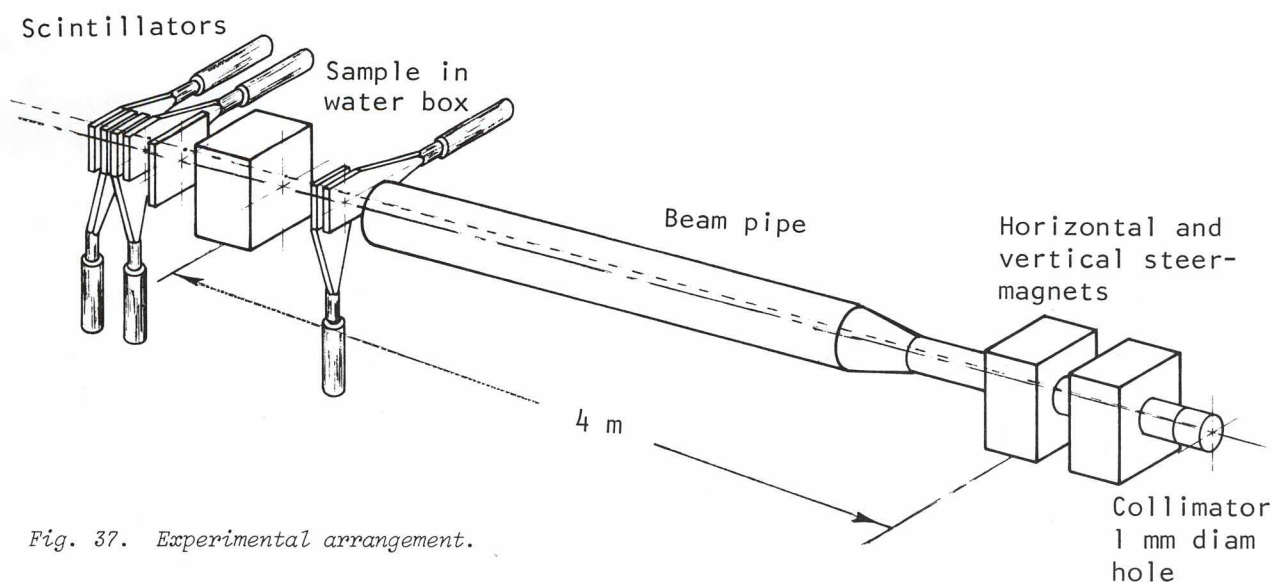


Fig. 37. Experimental arrangement.



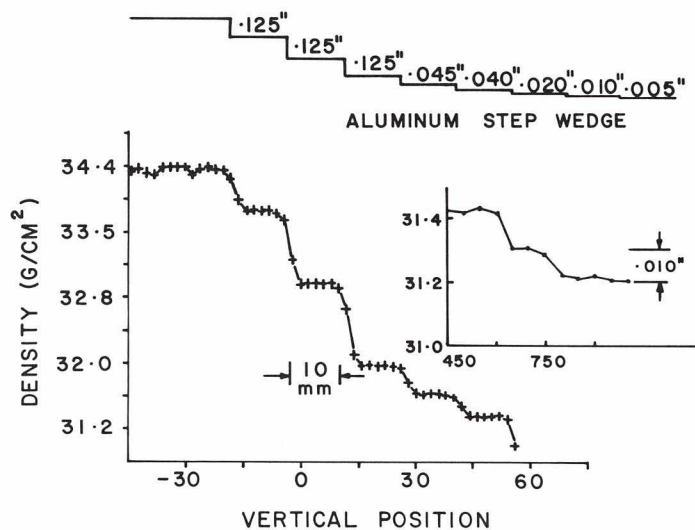


Fig. 38. Scan across a step wedge.

a fixed number of counts in the front counters. This provides four points which can be fitted to the proton range curve to determine the density of material through which the beam has passed.

The first experimental runs used a proton beam passing through the 0° line of the BASQUE neutron collimator. A number of Polaroid film radiographs were taken of test objects and samples in a water bath to develop some expertise in this new field and to demonstrate the sensitivity of the technique. A 0.010 in. step in a perspex sheet is observable on film with 210 MeV protons. The experimental equipment was then shifted to the 'FERFICON' position in beam line 4A to develop the scanned beam technique. The beam size was determined to be 2 mm diam by scanning over a step in a test block.

Using 190 MeV protons the transmission curves for the different counters in the range telescope were obtained by varying the thickness of a copper absorber in front of the detectors. Each curve should have the same shape, and the separation between each curve should be the thickness of the scintillation counters. From these curves the sensitive region of the four counters is 6 g/cm<sup>2</sup> or about 16% of the proton range. For this reason the test object must be fairly uniform. In the case of biological samples the usual technique is to place them in a water bath or to use specially shaped absorbers.

A one-dimensional scan across an aluminum step wedge is shown in Fig. 38. At each point the density has been calculated from the transmission data. A step of 0.010 in., which is 0.2% of the proton range, can be seen. The non-uniformity at this level is due to irregularities in the taping of the scintillation counters and is being corrected for later measurements.

To demonstrate a viable diagnostic technique for medical applications a full scan over at least a 10 cm × 10 cm area should take not more than 10 sec and should give a total dose of less than 100 mrem. At

present the speed is limited by both the data-handling system and the scanning magnets. The data-handling problem will be solved shortly by using the 'data interface' system being installed at TRIUMF for rapid transmission of data to the UBC 370. Programs are presently being developed for the analysis and display of the radiographic information. Fast scanning magnets capable of delivering the required fields with response times of 60 Hz are available commercially. Improvements in the sensitivity for a given dose will come with a better understanding of the factors affecting the sensitivity, variations in counter efficiency or thickness, beam energy or emittance fluctuations, etc.

### Experiment 77 Isotope production

The aim of this work was to establish a small but viable radioisotope production program at TRIUMF by concentrating on  $^{123}\text{I}$ , a highly desirable isotope for diagnostic nuclear medicine. The requirements were 1) operation in the high energy and intensity beam line 1; 2) minimal radiochemistry processing as no facility exists 'on site'; and 3) production which was continuous and orthogonal to the physics program.

The system investigated consists of a metallic cesium heat pipe target (Fig. 39) which produces radioxenon and many other species by spallation. Xenons are floated a distance of 18 m on a helium jet to a 77 K trap where they are allowed to decay to their respective iodine daughters. Evaporation of cesium metal provides a convenient method of removing beam power from the target. Twelve separate tests have been performed with a  $2 \text{ g/cm}^2$  cesium target in beam line 4A, and about 100 h of beam time have been used since February 7, 1976. For early runs supplementary electrical heating was supplied to evaporate cesium as beam currents were limited to 100 nA. Activity was transported to the freezing trap and many xenon species plus their daughters were observed. Long-lived

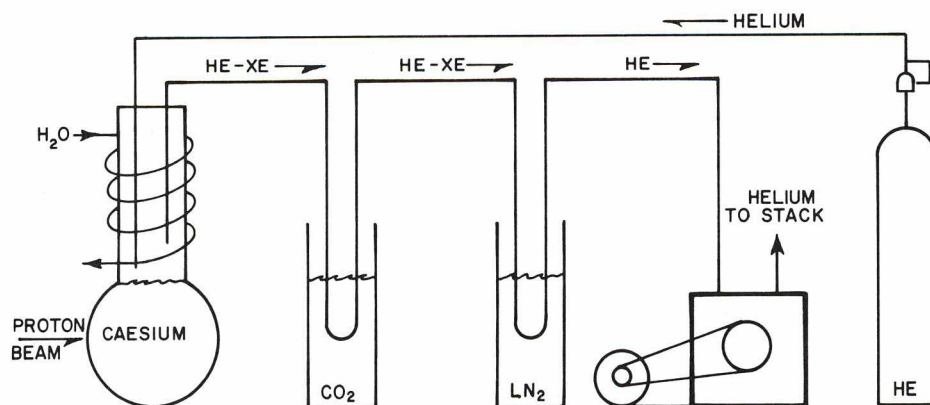


Fig. 39. Functional diagram  $^{123}\text{I}$  generator.

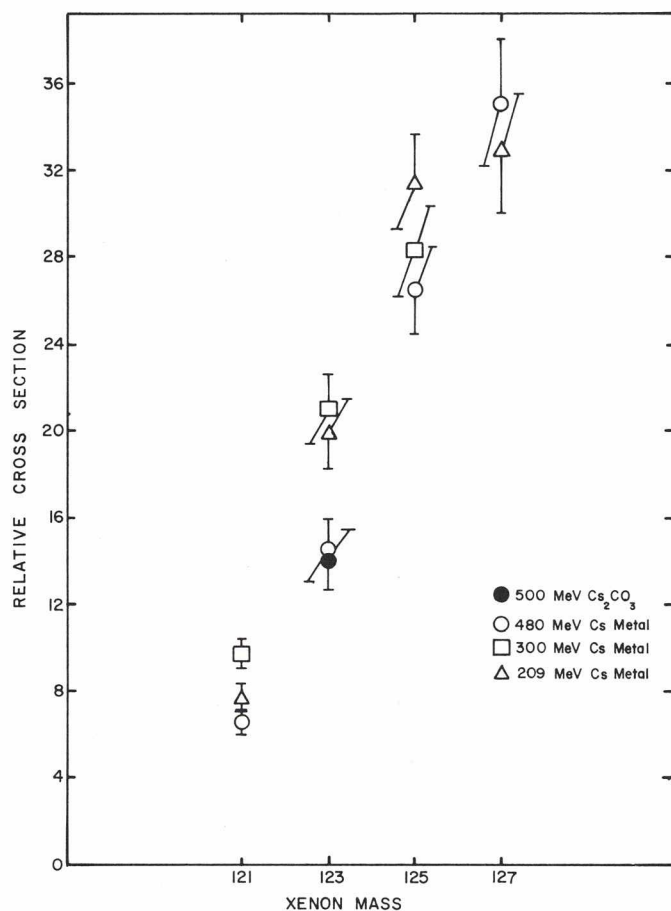


Fig. 40. Mass yield of radiocesium from spallation of Cs.

xenons were removed from the freezing trap by warming and cryopumping after three  $^{123}\text{Xe}$  half-lives. At that time the principal contaminants were  $^{121,125}\text{I}$  and  $^{119,121}\text{Te}$ . After a second decay period to clear  $^{121}\text{I}$ , sulphuric acid and hydrogen peroxide were admitted to release  $^{123}\text{I}$  from the trap walls, and the free iodine was distilled from the tellurium admixture. Trap extraction efficiencies between 78% and 88% were achieved without the use of a carrier. The distillate proved to have no detectable tellurium activity at the 1% level.

At this point the principal contaminant was  $^{125}\text{I}$  (35 keV, 59 days). It was essential, therefore, to measure cross-sections for the  $^{125}\text{Xe}$  precursor relative to the  $^{123}\text{Xe}$  precursor to see if improvements could be made. In fact, cross-sections for  $^{121,123,125,127}\text{Xe}$  were measured at energies of 209, 300 and 480 MeV relative to the  $^{27}\text{Al}(p,3p)^{24}\text{Na}$  cross-section. The mass yield curve shown in Fig. 40 indicates that no significant improvements can be made in the  $^{125}\text{I}/^{123}\text{I}$  ratio in the range of available bombarding energies. However, the point at 480 MeV for  $^{123}\text{Xe}$  from Cs was compared with a measurement at 500 MeV from  $\text{Cs}_2\text{CO}_3$ . If the energy dependence is small, as seems to be the case, it can be concluded that the xenon extraction efficiency is at least 90%.

From a typical 4 h run on cesium at 480 MeV the  $^{125}\text{I}/^{123}\text{I}$  ratio is calculated to be 0.275% at the end of bombardment, and it will reach the



dose-doubling fraction of 1.65% at EOB + 28 h. Although this result is somewhat inferior to that obtainable from the  $^{127}\text{I}(p,5n)^{123}\text{Xe}$  reaction at 60 MeV, the product quality compares favourably with the commercial  $^{123}\text{I}$  from the  $^{124}\text{Te}(p,2n)^{123}\text{I}$  reaction and is thought to be quite satisfactory for administration up to 28 h after EOB. Therefore, permission was obtained for patient trials at the end of September, and two thyroid scans were taken. These first tests have been judged to give medically acceptable results by the staff at Vancouver General Hospital who are co-operating in this development.

#### Experiment 48

##### Fertile-to-fissile conversion (FERFICON)

Under contract with Atomic Energy of Canada Ltd. Simon Fraser University is conducting an experimental program to measure the neutron leakage and fertile-to-fissile conversion reaction rates in a variety of heavy element targets. Table VII lists the target configurations for which neutron leakage measurements were made during the past year. The neutron yields for all targets were made at incident proton energies of 480 MeV and 350 MeV.

The neutron leakage is measured by two techniques simultaneously. In the first case the neutron capture activity in gold foils is measured by  $\beta$ -counting to map the thermal neutron flux distribution in the water moderator surrounding the targets. From this flux map the total neutron capture rate in the water is estimated and compared to the integral proton beam current determined by  $\beta$ -counting the  $^{24}\text{Na}$  activity induced in a thin aluminum foil located upstream of the target. A secondary measure of the neutron flux is derived from the current through a thin

Table VII. FERFICON target configurations. (All targets are 12 in. in length.)

Target material	Number of nested cylinder	Diameter of cylinder (inches)
Pb	1	4.00
Pb	7	1.51
Th	1	1.65
Th	7	1.65
Th	19	1.65
U (depl)	1	1.28
U (depl)	7	1.28
U (depl)	19	1.28
UO <sub>2</sub> (nat)	37	1.00

MgO insulator surrounding a thin vanadium wire embedded in the water moderator around the target. Most of the current in this system is due to  $\beta$ -particles emitted by the 3.7 m half-life  $^{52}\text{V}$  activity following neutron capture; the total charge collected during and following target bombardment by protons is directly proportional to the neutron fluence associated with the bombardment.

After analysis of these irradiations is complete, the results will be compared with calculated values generated by CRNL.

Neutron leakage from other target configurations are currently under way, to be followed by measurement of the conversion reaction rates.

## THEORETICAL PROGRAM

A theoretical group has been formed at TRIUMF, and it is the eventual intention to have a number of theorists at the main site working in various areas of theoretical medium-energy physics. It is hoped that the presence of an active theoretical group will provide stimulus for, and in turn be stimulated by, the various experimental groups. Thus both theoretical and experimental programs can benefit from the interchange of ideas.

Currently there are only two full-time staff in the group, H.W. Fearing and A.W. Thomas, who arrived this last fall. There is one graduate student, R. Sloboda of the University of Alberta, associated with the group, and a number of outside collaborators have contributed to the research described below, including I.R. Afnan, R.H. Landau, F. Myhrer and A.S. Rinat. There have also been a number of theoretical visitors during the past year, including N. Austern, B. Gibson, A.N. Kamal, R.H. Landau, G. Miller, R. Rockmore, R. Seki and others.

Research areas which have been of interest include the following:

### *$\pi$ -nucleus scattering*

One of the very fundamental strong interaction processes under investigation at TRIUMF is low-energy pion elastic scattering. Active interest in this process was recently aroused when a group at LAMPF measured the angular distribution for 50 MeV  $\pi^+$   $^{12}\text{C}$  scattering and found that it disagreed with currently accepted theory by a factor of four [Amann *et al.*, Phys. Rev. Lett. 35, 425 (1975)]. Several groups have since attempted to explain this discrepancy by improving the theory. In particular, it has been shown that a rather simple re-examination of the energy at which the  $\pi\text{N}$  t-matrix should be evaluated (based on a three-body formulation of the optical potential) can lead to a drastic improvement in the agreement with experiment [Landau and Thomas, Phys. Lett. 61B, 361 (1976)]. (Unfortunately our present ignorance of the isospin-1/2  $\pi\text{N}$  phases in this region forbids more than semi-quantitative predictions.)

Recent investigations at TRIUMF have exploited the low-energy pion beam to extend this picture down to 30 MeV (see pp.37-39). In parallel with this effort, we are working to include further corrections of higher order in the nuclear density (e.g. absorption, Pauli effects,...). The lower energy range is extremely interesting for reasons shown in Fig. 41. There it is clear that the effect of the semi-phenomenological absorptive contribution to the optical potential becomes much more significant as the energy is lowered. One of the primary aims of the investigation is to develop a single consistent picture of the interaction of pions with nuclei, from zero energy (i.e. pionic atoms) through the resonance region, based on the  $\pi\text{N}$  interaction and nuclear structure information. The necessity for this absorptive contribution, with its energy dependence taken from  $\pi d \rightarrow pp$  experiments, and its



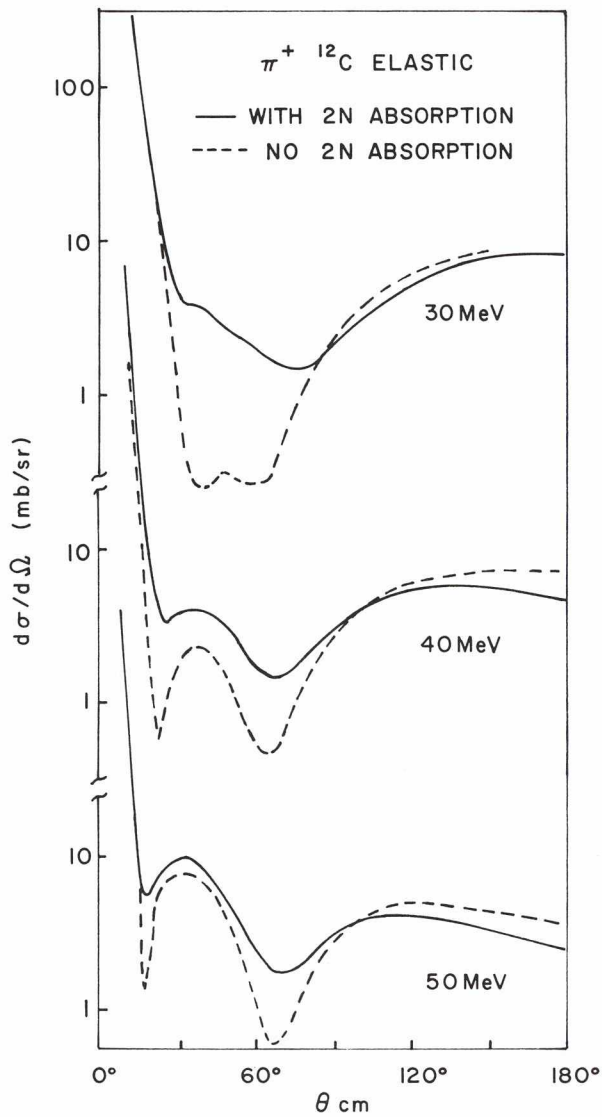


Fig. 41. This illustrates the growing importance of the term in the optical potential which describes the effect of true pion absorption as the energy is lowered. (Note that Coulomb-nuclear interference is only included here in an approximate way, and these curves are therefore preliminary.)

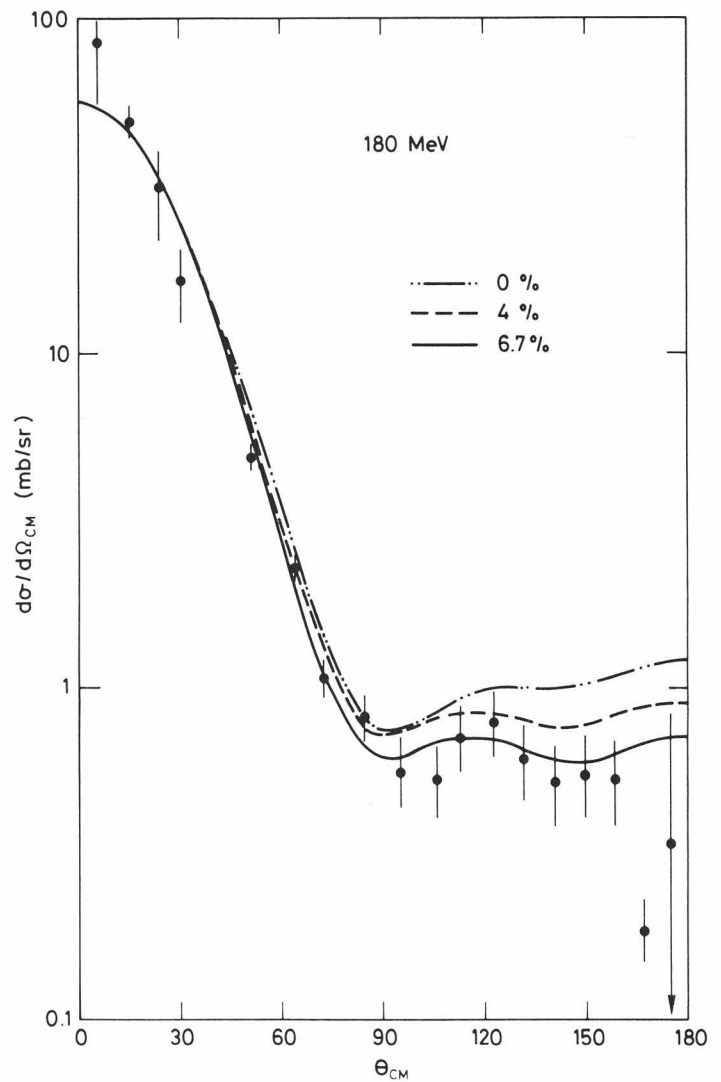


Fig. 42. Comparison of the elastic  $\pi D$  differential cross-section calculated within our relativistic three-body scattering theory with the data of Norem.

overall strength adjusted to match the pionic atom results, is just one indication that this program has good chances of success.

### $\pi D$ scattering

The 'simplest' example of a  $\pi$ -nucleus system, namely the  $\pi D$  system, is of considerable fundamental significance. Freed from the many necessary approximations of a many-body system,  $\pi D$  scattering has been studied as a relativistic three-body problem. Using the Bethe-Salpeter equation, in the quasi-particle approximation, as a starting point, one can reduce the problem to a set of one-dimensional coupled integral equations (after angular momentum decomposition) [Aaron *et al.*, Phys. Rev. **174**, 2022 (1968); Rinat and Thomas, CERN report #TH-2275 (1976)]. At the expense of certain truly relativistic aspects of the problem (such as crossing and non-instantaneous exchange), these equations provide a Lorentz-invariant description of the  $\pi D$  system, including nucleon motion and all orders of multiple scattering.

The completeness of this theory, which enables many approximations (e.g. impulse approximation, fixed scatterer approximation [f.s.a.], etc.) to be tested, is extremely valuable. For example, within a model calculation (which neglected spin and isospin) it has been shown that the f.s.a. is quite poor, even at forward angles [Woloshyn *et al.*, Phys. Rev. **C13**, 286 (1976)]. The same group also emphasized the importance of the so-called 'TS' terms (involving N-N scattering in intermediate stages) for backward scattering. Our calculations, which include isospin and spin (Pauli spinors only), have qualitatively confirmed the importance of 'TS' terms. It has also been found that it is essential to use a relativistic choice of relative momentum at the  $\pi N$  interaction vertices. (However, the results appear insensitive to which relativistic choice is made, if these are equivalent in the physical region.)

The agreement with existing experiments is rather good at 142 and 180 MeV. The latter results are shown in Fig. 42 because the interference effects of the non-resonant  $\pi N$  waves are negligible in this case. There is, however, a significant discrepancy in the  $90^\circ$ - $160^\circ$  region at 256 MeV. Several possible explanations are at present being investigated. Work is also proceeding, in collaboration with the LAMPF theory group, to include the effects of the small  $\pi N$  partial waves. In addition, calculations are under way to determine the model dependence of various  $\pi D$  polarization parameters, as well as the total cross-section.

### $(p, \pi)$ and $(p, \gamma)$ reactions in light nuclei

Several experimental groups both at TRIUMF and at Los Alamos have been investigating  $(p, \pi)$  reactions in light nuclei. Such reactions are of great interest in that one hopes to learn about the basic pion production/absorption mechanism and about high-momentum components of nuclear wave functions. Work on such reactions, particularly  $pd \rightarrow t\pi$ ,  $pd \rightarrow {}^3\text{He}\pi^0$ , and  $p{}^3\text{He} \rightarrow \pi{}^4\text{He}$ , has been continued, based on a distorted-

wave impulse approximation model [Fearing, Phys. Rev. C11, 1210 (1975); Phys. Rev. C11, 1493 (1975); Phys. Lett. 52B, 407 (1974)]. Several interesting new results have emerged. It has been suggested [Locher and Weber, Nucl. Phys. B76, 400 (1974)] that if one use three-body wave functions which reproduce the dip in the electromagnetic form factor, such dips should be reflected in similar dips in the  $(p,\pi)$  cross-sections. This does happen if crude wave functions are used, but it has been found at TRIUMF that if one includes either correct antisymmetrization of the wave functions or puts the D-state into the deuteron wave function then the dip is filled in and qualitatively the results are similar to those originally obtained using analytic wave functions which do not give the dip in electromagnetic form factors. There are quantitative differences, however, and with the new more sophisticated wave functions agreement with experiment is good (Fig. 43).

Another interesting aspect of the problem concerns the position of the resonance bump in the fixed angle cross-section. Naively one expects such a bump, resulting from the presence of the  $\Delta(1232)$  resonance, at roughly 450 MeV, but such a bump was not seen in a recent experiment [Fredrikson *et al.*, Lawrence Berkeley Lab report LBL-3636 and to be published; Dollhopf *et al.*, Nucl. Phys. A217, 381 (1973)]. In the context of our DWIA model we can show, however, that distortion effects move the bump to lower energies, 325-375 MeV. We thus predict a gradual fall-off with energy in the 450 MeV region, rather than a jump, in qualitative agreement with experiment. Quantitatively, however, the rate of fall-off is too great, and we are investigating possible mechanisms which might improve this aspect of the theory.

Pion distortion is an important ingredient of this calculation, and we have also investigated how the results change when one replaces the Glauber distorted wave functions used earlier with wave functions calculated in a realistic optical potential [Landau, private communication]. Results are preliminary, but seem to indicate little change for forward pions but a fairly significant enhancement of the cross-section at backward angles.

Finally, a number of the experiments made in the original DWIA calculation of  $(p,\pi)$  reactions are being incorporated into a calculation of the analogous  $(p,\gamma)$  reactions. Such reactions are very similar to  $(p,\gamma)$  reactions, and yet simpler since no pion distortion is required. Hence they serve as a useful check on the model.

### *Nucleon-nucleon bremsstrahlung*

In principle nucleon-nucleon bremsstrahlung is one of the cleanest ways to investigate off-shell aspects of the nucleon-nucleon force, since there are only two strongly interacting particles present. Currently an experiment (#66, p.34) is under way at TRIUMF to look at the bremsstrahlung process for small opening angles between the scattered protons. We have investigated bremsstrahlung in this geometry using a model-independent, soft-photon approach. This approach cannot predict



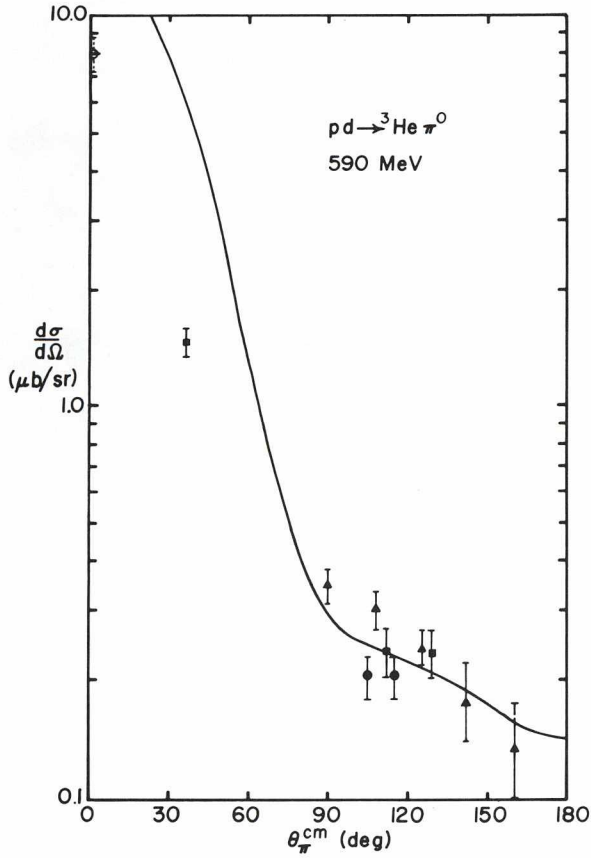
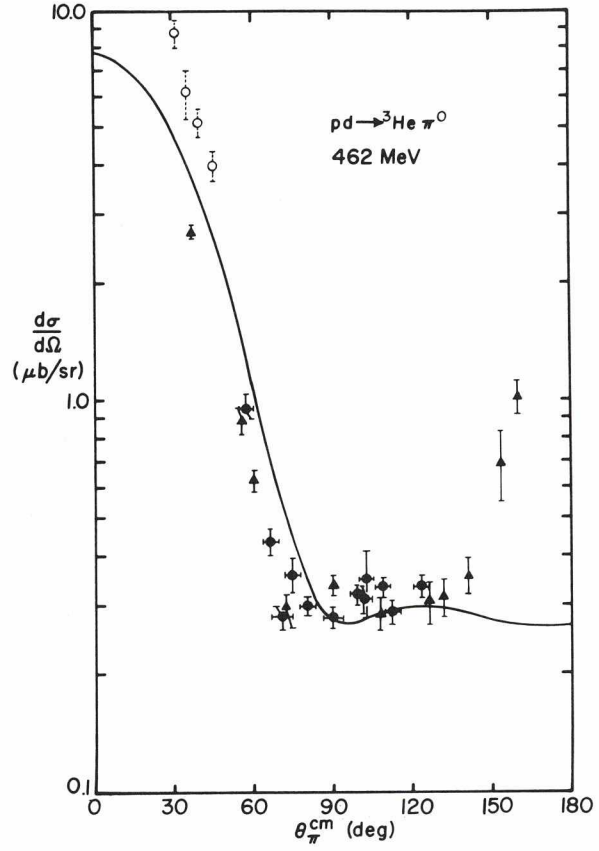
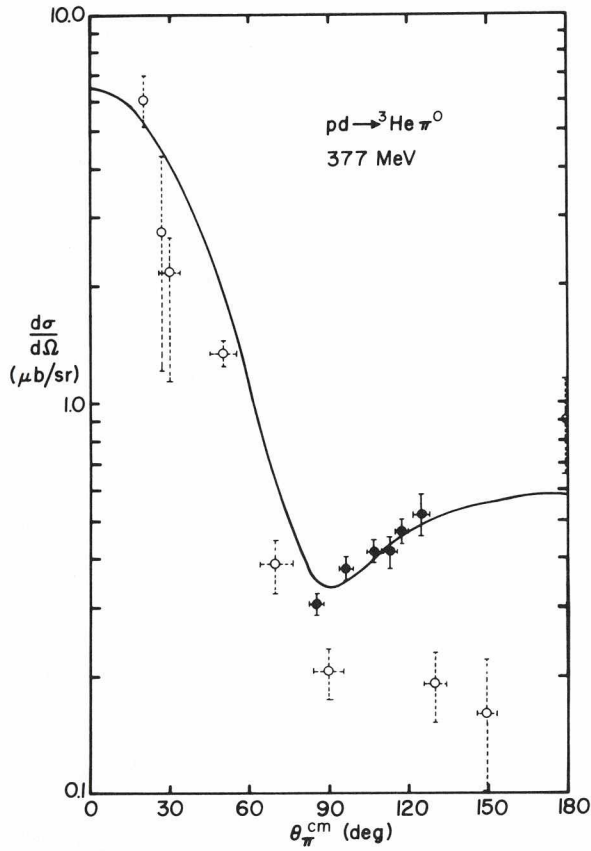


Fig. 43. Comparison of DWIA model for  $pd \rightarrow {}^3\text{He} \pi^0$  with available data.

off-shell terms but it can give some indication where such terms might be important. Individual terms in the expansion of the cross-section in power of the photon momentum  $k$  have been kept separately, which apparently has not previously been done, and as a result some very interesting features have emerged. Conventionally one writes the NN amplitude as  $M \sim A/k + B + Ck$  and the cross section as  $d\sigma \sim kM^2 \sim A^2/k + 2AB + (B^2 + 2AC)k + 2BCK^2 + \dots$ , where  $A$  and  $B$  contain only on-shell information and  $C$  contains both off-shell information and higher-order on-shell terms. We have found that for the equal angle geometry the  $AB$  term is small and the cross-section is dominated by the  $A^2$  piece or by the  $B^2$  piece which is of the same order as the off-shell term of interest. Furthermore, at forward and backward photon angles and at one intermediate point  $A \equiv 0$ , and the entire cross-section is given by the  $B^2$  term which was previously thought to be small. At these points the  $AC$  term vanishes, and one must go to still higher orders in  $k$  to get a contribution from off-shell terms.

We intend to explore these results further by looking at a very simple model which allows explicit calculation of the individual terms. It will also be interesting to investigate the possibility of obtaining new information by using polarized protons.

#### *Radiative muon capture*

The radiative muon capture process is particularly sensitive to the value of the induced pseudoscalar coupling constant  $g_p$  of the weak interaction and presumably also sensitive to the second-class term  $g_T$  for which there now may be some evidence from  $\beta$ -decay. Currently published experimental results both for the photon spectrum and asymmetry with respect to the muon spin are in gross disagreement with the theory. Thus it is quite important to look more carefully at the theory to make sure that it is correct.

Recently it was shown [Fearing, Phys. Rev. Lett. 35, 79 (1975)] that for a correct calculation of the asymmetry one needs to include in the Hamiltonian certain higher-order terms which had been previously neglected. Most of these terms have now been calculated, and we are in the process of squaring the matrix element of this new Hamiltonian to obtain the spectrum and asymmetry. This process, while straightforward in principle, is extremely complicated in practice because of the large number of terms, and it has been necessary to use one of the available computer systems for carrying out the algebraic manipulations.

The results for radiative capture are also very sensitive to the average maximum photon energy, or equivalently the average excitation energy of the nucleus, and it has been difficult to unravel this dependence from the dependence on  $g_p$ . We have investigated the possibility of extending a sum rule approach previously used for ordinary muon capture to the radiative process. Our results, while preliminary, indicate that a sum rule can be derived for radiative capture, and it may help soften

the dependence on this average excitation energy and thus allow a cleaner separation of the dependence on  $g_p$ .

#### *Absorption of soft pions*

The process of muon capture on nuclei leading to the emission of fast neutrons can be related (using PCAC) to pion absorption—for a pion off its mass shell. In particular, in the highly time-like region ( $q^2 \sim m_\pi^2$ ) the  $\bar{V}$ ,  $\bar{A}$  and  $A_0$  contributions to  $\mu^-$  capture add incoherently, and the  $A_0$  term, for example, can be related to the rate of s-wave pion absorption in a model-independent way. At least, it would be model independent if the extrapolation off-shell ( $q^2 = m_\pi^2$  to  $m_\mu^2$ ) were smooth. In view of the failure of soft-pion theory for  $pp \rightarrow \pi d$  this did not appear to be the case. Therefore, the invariant matrix element for the latter process at threshold has been studied as a function of the mass of the produced pion [Thomas and Afnan, in *Meson Nuclear Physics-1976 (Carnegie-Mellon Conference)*, AIP Conference Proceedings No. 33 (AIP, New York, 1976), p.472]. It is a remarkable fact that over a wide range of masses this matrix element does seem to be constant within a few per cent. As a consequence, the evaluation of the  $A_0$ -contribution to  $\mu$ -capture can proceed in a model-independent fashion (as described above).

#### *$N\bar{N}$ states*

Finally, while the project was not directly relevant to TRIUMF, we report some work on possible  $N\bar{N}$  states. Within a rather simple analytic model, we have shown that it is most unlikely that any bound states or resonances predicted by the OBEP models (of NN scattering) would survive the inclusion of  $N\bar{N}$  annihilation—which experimentally is very strong [Myhrer and Thomas, Phys. Lett. **64B**, 59 (1976)]. If the 'S'-meson at 1932 MeV (with a highly elastic width  $\leq 9$  MeV) really exists, it is indeed a challenging theoretical problem to understand its origin.



# THE STATUS OF EXISTING FACILITIES

## ION SOURCE AND INJECTION SYSTEM

### *Polarized ion source*

In early January a vertical polarized beam emittance of  $10\pi$  mm-mrad was measured in the Wien filter region. This is comparable to the emittance of the unpolarized source without limiting apertures. The Wien filter was then installed and beam transmitted through it with no difficulty.

The first attempts at measuring the polarization of the extracted beam were made in February. The maximum polarization observed at that time was 20%, and measurements were terminated due to source solenoid failures. Some efforts were made to improve beam current and transmission through the injection line which resulted in 250 nA at the end of the POLISIS line and 140 nA at the fast target.

By mid-March the solenoids were repaired and a second attempt at polarized beam extraction was made. Some problems were encountered with the source hardware; however, it was possible to do extensive measurements of the polarization as a function of source parameters. Although maximum polarizations were only 20% these measurements allowed an analysis of the Wien filter behaviour which showed the predictions to be substantially correct. A modification to the Helmholtz coil support structure was made which allowed the rotation of these coils about the beam axis and therefore a better compensation of the transverse fringe field in the zero-crossing region of the source. With this modification polarizations of 73% were measured during trials at the end of March. The previous Wien filter results were checked with these higher polarizations and the Wien filter parameters fixed.

Since April 1 the source has been producing beam extensively for experiments, with more than 1000 h of beam delivered on target. Nominal operating conditions are 250 nA from the source, with 30 nA extracted with 75% polarization. Maximum beam currents observed are 300 nA from the source, with 50 nA extracted. The source running time was originally limited to approximately five days due to cesium contamination in the accel-decel region. This problem has been greatly reduced, and runs of 7-8 days are now possible, with the filament lifetime becoming the limiting factor. The polarization can now be monitored continuously in the control room with polarimeter signals supplied by the experimenters. This allows the operators to check and improve the source operation.

### *Unpolarized $H^-$ source and injection system*

During the year the source, the 300 kV accelerator and the injection system have been functioning satisfactorily without serious breakdowns. The main effort has been to consolidate the existing system so it

could be operated routinely and reliably at low currents (below 15  $\mu\text{A}$ ). At the same time the system had to be upgraded such as to become compatible with higher currents. During a test in November 400  $\mu\text{A}$  continuous current was transported through the 40 m long electrostatic injection line with 90% transmission; 7% loss due to vacuum ( $10^{-7}$  to  $10^{-6}$  Torr), 2 or 3% loss on water-cooled collimators. Slits in the 12 keV region, right after the ion source, were restricting the beam emittance to  $\sim 0.25\pi$  mm-mrad horizontally and  $0.1\pi$  mm-mrad vertically. Since at lower currents and with buncher on this emittance was compatible with 25% overall transmission between 12 keV and the 500 MeV regions, it is plausible that 400  $\mu\text{A}$  at injection will be adequate for achieving the design goal of a 100  $\mu\text{A}$  proton beam at 500 MeV. In fact, during the 50  $\mu\text{A}$  500 MeV test in November the beam required at injection was about 200  $\mu\text{A}$ .

Slight modifications of the original 'Ehlers type' Cyclotron Corporation ion source were performed in order to lengthen the life of the filament, reduce the arc oscillation amplitude and the arcing rate. Under favourable conditions and for currents of about 500  $\mu\text{A}$  through the emittance slits, a filament life of about 100 h with arc oscillations of less than 10% and an arcing rate of about 10-20 per hour could be obtained.

Along the injection line the reproducibility is now very good; a good master tune can normally be restored and optimized in about half an hour.

Two inductive monitors, each consisting of a toroidal tape wound core of 1.75 in. i.d., 2.75 in. o.d., and 1 in. long with 41 coil windings, were installed at the beginning and at the end of the line. 124  $\Omega$  shielded balanced lines were used to transport the signal. In order to provide the current-versus-time variation necessary for detecting a signal, the beam was pulsed in a 99% duty cycle mode at the 12 keV region with beam off for 10  $\mu\text{sec}$  every millisecond.

## SAFETY

The TRIUMF Safety Group was restructured to facilitate the cyclotron operating schedule. Early in the year five crews were organized consisting of one shift supervisor, one cyclotron operator and one safety operator. The shift supervisor is the one ultimately responsible to ensure safe operation of the facility. During the year all of the operators have learned the proper lock-up procedures and the routine radiation-monitoring procedures. The three remaining safety officers are primarily concerned with health physics but are also responsible for all other aspects of safety.

The TRIUMF Safety Executive Committee met 16 times and received the results of many radiation surveys and approved submissions of seven experimental proposals. The thermal neutron facility (TNF) design was under review by TSEC for several meetings in the latter part of the year, and this facility is now under construction.

In the early part of the year a major effort was put into producing documents to support a licence application that would permit operation at 100  $\mu$ A. In July TSEC met with the Accelerator Safety Advisory Committee of the Atomic Energy Control Board to review the licence application. AECB granted the operating licence on August 25.

### *Radiation protection*

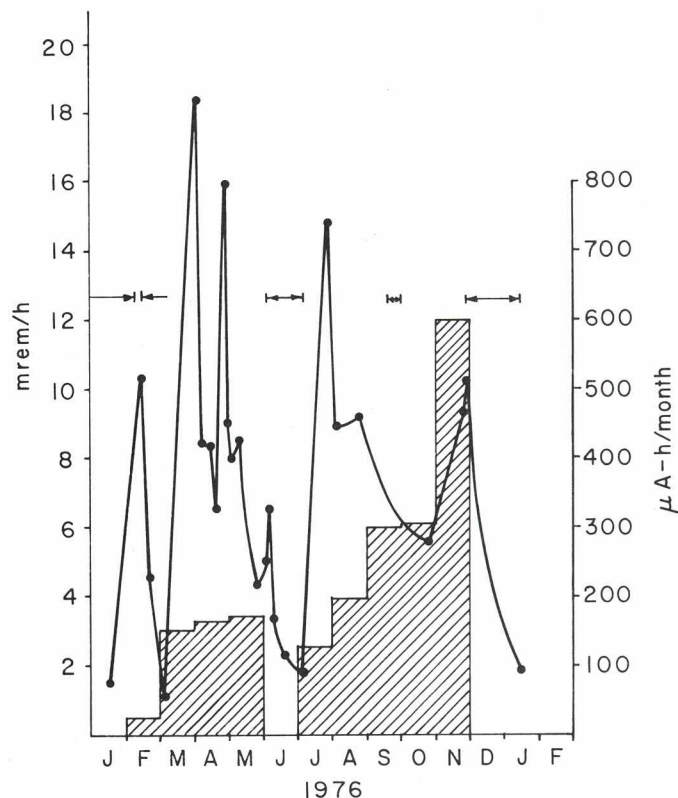
The tuning of the beam lines and the cyclotron improved considerably during the year, and the 22 beam-spill monitors have proved to be extremely useful for minimizing beam losses in the proton beam lines. Beam lines 1, 4A and 4B have been routinely operated 2  $\mu$ A, 1  $\mu$ A and 20 nA, respectively, and there were six shifts of operation in beam line 1 at currents at or above 10  $\mu$ A.

The residual activity at 1 m from most of beam line 1 ranged from 2 to 10 mrem/h one hour after shutdown. This is the same as the levels a year previously even though the beam current increased from 90  $\mu$ A h in 1975 to 2070  $\mu$ A h in 1976. Figure 44 shows the average contact dose rate on beam line 1 during 1976 compared with the number of micro-ampere hours per month. As the current has been increased the beam line tuning has also increased so that the residual activity in beam line 1 has not changed significantly. There have been increases in the residual activity of beam line vacuum windows and the beam dump. The copper beam dump had an activity of 350 mrem/h at 1 m two months after shutdown at the end of 1976. The activity level a year previously was 30 mrem/h at 1 m two months after shutdown.

Radiation surveys of the tank can now be performed remotely using the service bridge and a radiation detector trolley designed for this purpose. The residual activity in the central area of the cyclotron vacuum tank was about 5 mrem/h on June 8, eight days after termination of a three-month period in which there were 500  $\mu$ A h of beam operation.



Fig. 44. Average contact dose rate on beam line 1 (15 points outside vault, excluding  $p, \pi$  window).



Carbon blocks encased in aluminum were installed between the vacuum tank and the return yoke, and their immediate effect was to reduce the dose rates by a factor of 5 to 10 in various parts of the tank. In December two weeks after a five-month period in which 1500  $\mu\text{Ah}$  of beam were accelerated, the residual activity in the central region of the tank was only 2 mrem/h (see Fig. 45). This reduction in residual radiation levels is due to reduced spill and the effect of the carbon blocks. The radiation levels in the cyclotron tank are, however, expected to increase by a factor of 100 after a few years' operation at 100  $\mu\text{A}$ . In order to reduce such levels two-inch-thick lead shields are being fabricated for mounting at the tank edge.

Several shielding tests were performed on beam line 1 at 10  $\mu\text{A}$ . The first 10  $\mu\text{A}$  test was on August 5 and the last was on November 24. The shielding was modified slightly for each test, and the beam losses were reduced significantly during this period. Table VIII shows various neutron dose rates observed in the initial and final 10  $\mu\text{A}$  tests normalized to 10  $\mu\text{A}$ . The beam spill monitor readings are shown in rads/h since the response of this detector is not well known.

There were several weak points found in the shielding in November which will be strengthened with the additional shielding blocks that were being fabricated at the end of the year.

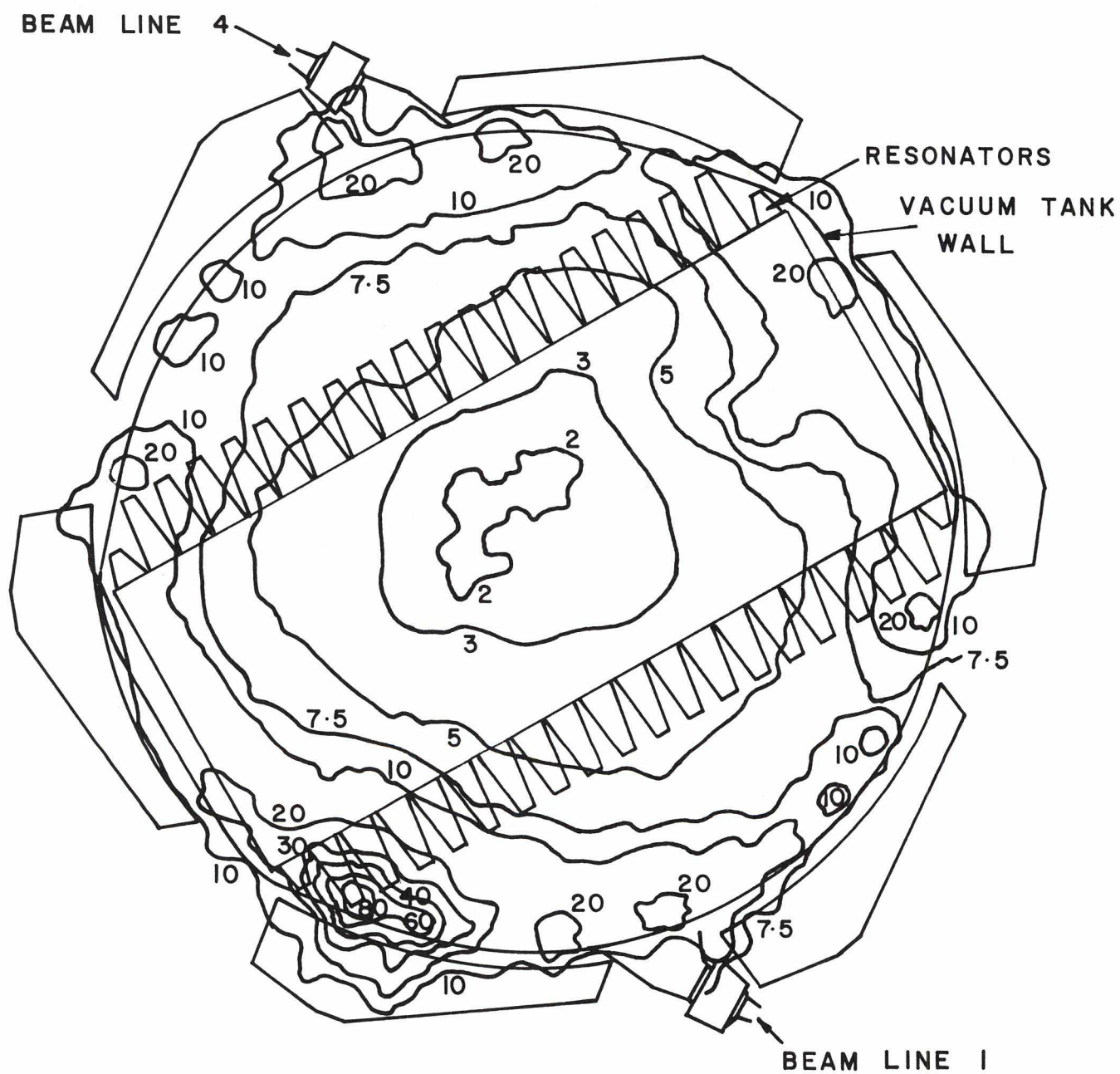


Fig. 45. Isodose curves in cyclotron (mrem/h) in December, 15 in. above beam plane.

Table VIII. Radiation Fields During 10  $\mu$ A Operation in Beam Line 1

Location	Radiation Field	
	August 5	November 24
Average of five beam-spill monitor readings along beam line 1	60 rad/h	1.5 rad/h
Above vault wall	150 mrem/h	4 mrem/h
NW corner of medical cave	300 mrem/h	30 mrem/h
Meson hall generally	2 mrem/h	0.5 mrem/h
Above beam line 1 T2	20 mrem/h	12 mrem/h
Above (p, $\pi$ ) shielding	200 mrem/h	5 mrem/h
South boundary fence	20 $\mu$ rem/h	20 $\mu$ rem/h

During 1976 there were 344 individuals on the RPB and neutron monitoring service. In September the  $\gamma$ -film service was replaced by a TLD service. In addition, persons who enter the vault or the proton beam line tunnels were issued quartz fibre pencil dosimeters. A total of 15 persons were issued finger ring TLD's for maintenance work near the edge of the cyclotron or on active beam line components. The finger ring doses were all less than 50 mrem. 10% of the personnel received an annual whole body dose of more than 100 mrem, and the highest single whole body dose was 329 mrem. The total dose received by all of the radiation workers was 6.7 man/rem.

#### *Accident record*

1976 was the first full year of operating experience for the TRIUMF Accident Prevention Committee, whose formation proved to have a remarkable effect on TRIUMF's accident record. For example, 200 working hours were lost to 'on-the-job' accidents in 1975 whereas this year the total was 88. Of the 19 accidents and injuries reported to and treated by the six first-aid attendants, nine were referred to the employee's own doctor.

The committee has endeavoured to make the site as safe as possible in all areas of industrial safety although improvements are still needed in some minor areas.



## REMOTE HANDLING

The major developments in the group's three areas of activity are:

### *Cyclotron servicing*

Construction of a family of service bridge trolleys has continued throughout the year. A lower resonator removal trolley and a new manned trolley are now being lab tested. A lift trolley with a lifting attachment has been commissioned. The lift trolley prototype was originally used for installation of the graphite/borax-filled shielding cans between the tank wall and the main magnets, and it was later updated to install remotely the peripheral shadow-shield frames. Sixty shadow shields have been fabricated and will be used from now on for discrete peripheral tank shielding each time the lid goes up for any length of time.

The remote handling system makes extensive use of video monitoring, and x,y,z positioning within  $\pm 1/16$  in. is now routine. A typical example is the lift trolley when set up to install shadow shields which uses five TV cameras. One is for general viewing (tilt/pan/zoom) from the centre-post end of the service bridge. One is a pick-up tool alignment camera that locates the pick-up tool directly over the pick-up socket (via a  $45^\circ$  flip-up mirror). Two cameras are mounted vertically to view the two inner corners of the shadow shields, to make sure they are properly aligned and not liable to damage other equipment. A fifth camera is mounted vertically to position the trolley into a pre-established location by sighting a target. This camera is not used when picking up and removing the shields. Later four more cameras will be mounted on outrigger trolleys for general viewing and troubleshooting. The outrigger trolleys are actually service bridge-mounted manipulators that can hold TV cameras, place and retrieve small parts, leak test, nudge or push, etc.

TRIUMF's remote video system is well ahead of the international state-of-the-art in TV-monitored manipulation, with considerably less cost. The control centre (which is duplicated in the lab for continuing development and training) has a six-monitor video display and can be located anywhere on site if the vault levels turn out to be higher than estimated.

### *Beam line servicing*

The T2 components (IM9, T2, M8, M9, M20) have been updated for fast handling. The LD<sub>2</sub> target has still not been commissioned for remote handling because of the experimental nature of the target design and the projected low-level radiation expected in the near future. One indium remote-operable seal (M20 T2 to Q1) has given unexplained leakage problems, but the beam pipe is badly aligned. It has become apparent that M9 Q1 and Q2 were not installed as originally agreed (also M20 which was to use the same design philosophy set for M9), and these two

areas will have to be updated to allow remote servicing before full-power operation.

Quick disconnects for power and water have been installed in all 'radiation-hard' areas.

The existing target flask was found to be deficient in 'steering' ability for reinstalling components into the T2 shield and too small to handle the new TNF components, so it is now being used as a test bed for trying out new mechanisms and will be replaced next year by a larger and mechanically superior design.

All monitor boxes have been redesigned for rapid servicing, and all radiation-hard areas in the vault beam lines have been updated for quick handling (except for the beam line tube clamps which will be updated next year).

#### *Hot cell area*

A low-level 'warm cell' has been designed and fabricated for handling such components as resonators, magnets, etc. It is a large shielded area with good visibility (4 ft high  $\times$  12 ft wide  $\times$  4 ft thick water window). Two 'donated' model D manipulators are being modified to give extra-extended reach in the warm cell. It is anticipated that in the long run the warm cell will be used for setting up low- to medium-radiation level repair jobs so that technician contact repair time will be minimized. It will also be available for temporary active storage. The warm cell fabrication was accelerated as it will be used through the next year as an interim hot cell while the first of a new permanent hot cell complex is being installed. The development of the permanent hot cell(s) has been delayed a few months awaiting more definitive information on the future requirements of isotope production.

A 'hot shop' has been installed (and used) for machining and processing of components that exceed the radioactive limits allowable in TRIUMF's Machine Shop. It includes a small precision lathe, a large 'rough' lathe, a small mill, horizontal and vertical bandsaws, a drill press, tig welding, and nickelplating. It will be updated with demand.

## RF SYSTEM

In order to improve the reliability of the fundamental RF system major modifications were made in the following areas:

- 1) Centre quadrants
- 2) Resonator tips
- 3) Resonator water cooling system
- 4) Transmission line and amplifier system
- 5) Centring probe housing

The phenomenon which caused the overheating and melting of the centre quadrants in November 1975 is still present, and quadrant temperatures are now continuously monitored to prevent further damage. It was observed that heating of the centre quadrants only occurred when the magnetic field on. Computer studies showed that the heating could be due to electron bombardment from electrons trapped in the cross electric and magnetic fields around the quadrants, although the source of electrons was not clear. The electron bombardment theory led to the fabrication of two new quadrants (II and III) from copper, modified so as to reduce the volume in which the electric equipotentials were parallel to the magnetic lines of force. The effect of the new quadrants was that the phenomenon shifted to quadrant IV; here, however, it is less active and it is now possible to operate for weeks without the quadrant heating. When heating does occur it usually lasts for only a few hours (and does not reach melting temperature) and usually disappears after a few sparks and vacuum bursts in the tank. Further tests are still being carried out in an effort to understand the phenomenon.

During tests and repair of the centre quadrants a major misalignment of the resonator tips due to sagging of the resonator skin near the tip, and also burning of the tip-to-tip connections (tulips), was observed. Both problems were due to poor mechanical design, and temporary solutions were incorporated. When the RF system became operational again a 20% increase in the quality factor (Q) of the resonators was observed. However, the temporary solution for the resonator tip sagging deteriorated, and the system is now operating again with a decreased Q. The permanent designs for the tip tulips and the tip supports were installed during the November shutdown and will be tested out in the new year.

In June cooling channels in three of the resonator segments were ruptured due to the clogging of an inlet strainer with remnants of the resin used in the ion-exchange column. Resonators were repaired and modifications made to the ion-exchange system.

The resonator fine tuning system using movable 'foils' had to be abandoned, and tuning of the resonators is controlled by the resonator water cooling temperature and pressure. Water cooling data were collected over the past year to enable determination of the behaviour of the resonator system due to water temperature and pressure changes. However, when the resonator tip supports (temporary solution) were



installed, the behaviour of the resonator system due to water temperature and pressure changes was completely changed, and the previous cooling data were not applicable. New cooling data are in the process of being acquired. In order to make the water cooling system more stable the resonator cooling return line is being isolated from the common return manifold; the effect of this will be tested out in the new year.

In August major downtime was caused by the burning of two polystyrene insulators in the tuned section of the transmission line. The local damage was insignificant; however, the nature of the air circulating system was such that it caused a layer of soot to be deposited along the transmission line and into the RF cabinets. Most of the downtime was spent in cleaning the transmission line and the RF amplifier components. Three observations were made: pitting of spark gaps in the area, a scotch-brite pad lying in the transmission line, and a small water leak in the cooling system of the inner conductor. The only conclusion could be that the failure was a result of the above problems, the most likely one being the water leak in the cooling system.

Major water leaks in the RF amplifiers and waster loads also caused some considerable downtime, but these failures were mainly due to lack of available maintenance time.

The November shutdown was premature by two days due to RF problems that prevented voltage being maintained on the resonators. On opening the tank it was found that the probe housing, which runs down the centre of the accelerating gap, had melted due to RF heating. The cause is not known but the best guess is that thermal expansion of the housing caused poor resonator ground arm fingerstock contact. This would then cause localized heating resulting eventually in melting the housing. The probe housing was reinstalled in sections to allow for greater thermal expansion, and modifications were made to improve the thermal and electrical contacts.

### *Third harmonic RF system*

Some progress was made this year with the third harmonic RF system. The coupling loop and the standing wave section of transmission line were installed. Measurements of isolation between the two RF systems were made. The amount of fundamental RF power penetrating back down the third harmonic transmission line is less than 100 W with full fundamental RF power of approximately 1000 kW coupled into the resonator system. The quality factor ( $Q$ ) of the resonators at the third harmonic frequency was measured to be approximately 6400 (compared to a fundamental frequency  $Q$  of approximately 5500). Whether a third harmonic to fundamental frequency ratio of 3:1 can be achieved without major modifications to the resonators is still unknown, since the third harmonic frequency has never been measured with full fundamental RF power applied to the resonators.

## VACUUM SYSTEM

There have been no significant changes in the cyclotron vacuum chamber system during the past year. Operation has been satisfactory and the total downtime for the year was 40 h, primarily due to failure of lead grain regenerators in the Philips B-20 cryogenerator used to cool the cryopanel.

The indicated vacuum chamber pressure, read on a Bayard-Alpert ionization gauge located behind the resonators, has reached a minimum pressure of  $2 \times 10^{-8}$  Torr with the RF off. With RF on, after about three days on conditioning, the vacuum chamber pressure is about  $1 \times 10^{-7}$  Torr. The bulk of the difference is due to hydrogen. This hydrogen is presumably produced by dissociation of hydrocarbons by the RF field and can be pumped by a liquid helium cryopump operating at a temperature below 3°K. Such a pump (nominal speed 25,000 l/sec) has been built and is being tested.

## M9 CHANNEL

The stopped  $\pi/\mu$  channel (M9) has now been tuned to approximately the design specification for 30 MeV pions. In the channel shown in Fig. 46, Q1 and Q2 collect the  $\pi$ 's from the target and bring them to a momentum-dispersive focus as the position of the midplane slits. The second part of the channel from Q3 to Q5 brings the image defined at the vertical and horizontal slits to an achromatic focus labelled 'primary  $\pi$  focus'. Q6, Q7 and Q8 are mounted as a triplet on a stand fitted with air pads and can be readily removed and inserted to produce a 'secondary  $\pi$  focus' further along. The measurements reported here have been taken at the primary  $\pi$  focus with Q6-Q8 removed.

Tuning of the channel to optimize resolution and spot size has been done so far using the copper target, since it is short and therefore presents a small source size to the channel compared to the 10 cm long beryllium target. The copper target, however, produces more electrons which contaminate the  $\pi$  beam.

A number of flux measurements have been made using both the copper and beryllium targets. For these one has normalized to a Čerenkov counter (shown as Č in Fig. 46) which is calibrated, for each target and incident proton energy, to stripping-foil currents. This monitor has proved helpful in final tuning of the proton beam; a factor of two or

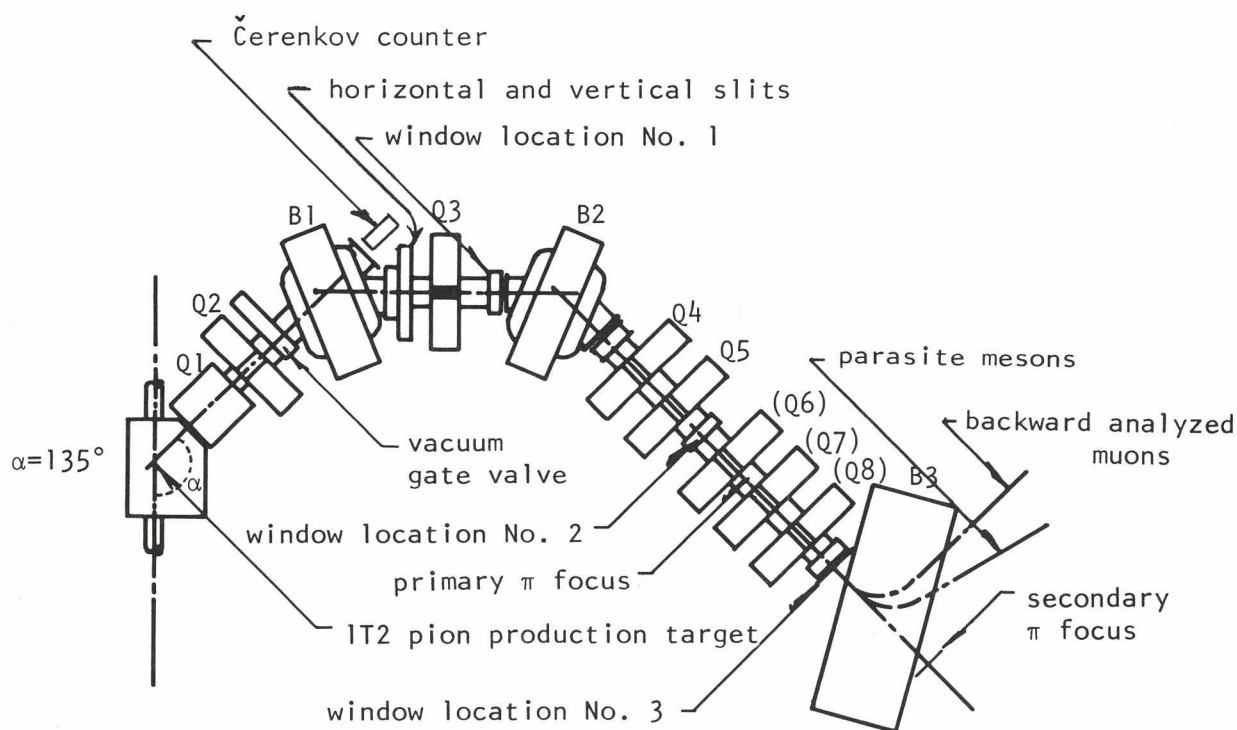


Fig. 46. Layout of M9 channel. The B3 dipole is a 12-in. gap cyclotron magnet obtained from Oregon State University.



so in  $\pi$  flux can be obtained by optimizing using  $\tilde{C}$  rather than the scintillator on the production target.

Figures 47 to 49 show the results of measurements taken on the channel. Figure 47 shows a measurement of the dispersion at the midplane slits made after tuning Q1 and Q2 to maximize the flux through 1 cm  $\times$  1 cm slits. The dispersion obtained compares well to the design value. In Fig. 48 is shown a measurement of the energy resolution made with a Ge(Li) counter for 30 MeV  $\pi$ 's. As the horizontal slits are decreased below 10 cm width, the resolution improves in a linear way, yielding an optimum for 1 cm slits of  $\Delta p/p \sim 2.5\%$ , near the design value. The maximum acceptance of  $\Delta p/p \sim 14\%$  is not consistent with the design value of  $\sim 21\%$ , and the discrepancy is being investigated.

Figure 49 illustrates some flux measurements made for the copper and beryllium targets. The maximum  $\pi^+$  flux of  $1.5 \times 10^6/\text{sec}/\mu\text{A}$  from the 10 cm Be target compares well with the calculated value of  $1.7 \pm 0.3 \times 10^6/\text{sec}/\mu\text{A}$ . Muon fluxes for the Be target are not shown, but preliminary indications suggest the curve is of a similar shape to the copper result and that the ratio of  $\pi/\mu$  is somewhat higher.

Spot sizes at the primary  $\pi$  focus have been measured using two-dimensional multi-wire proportional chambers. To date, the best achieved is about a 3 cm diam spot, but it is believed this can be improved with further tuning.

Finally, some stopping efficiency results have been obtained using a  $\sim 1 \text{ g/cm}^2$  stopping scintillator. Results at 30 MeV pion kinetic energy indicate that with the midplane slits at 15 cm 76% of the flux remains with a maximum stopping efficiency of  $\sim 37\%$ . The corresponding result for 50 MeV pions is 19%.

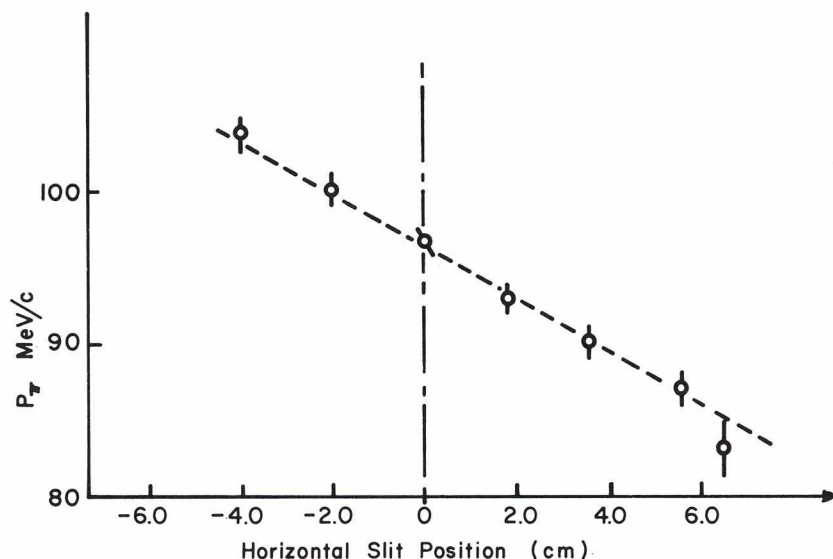


Fig. 47. The M9 dispersion at the midplane slits measured with a slit width of 1 cm and the 1 cm Cu target at T2. The momentum dispersion is 0.6 cm/%p.

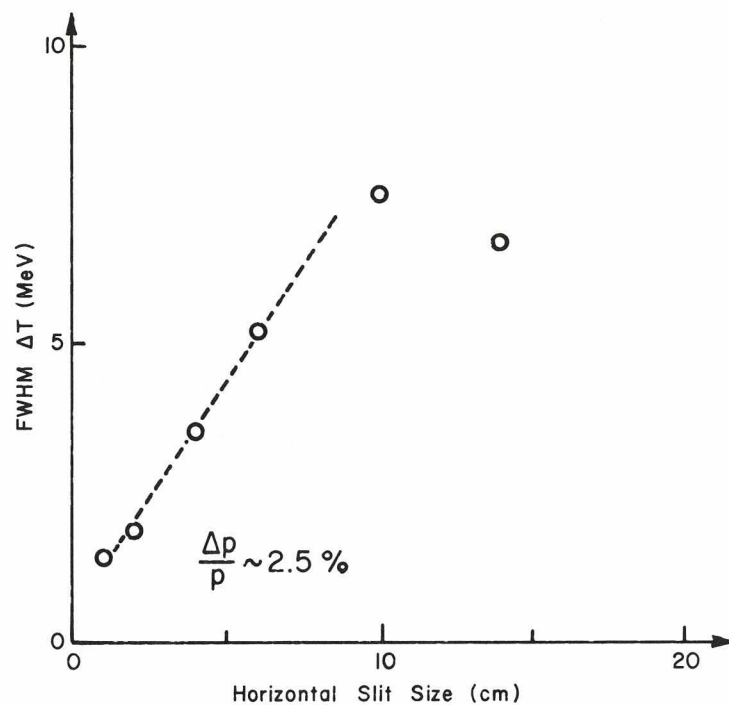


Fig. 48. The M9 energy resolution at the primary  $\pi$  focus. The T2 target was 1 cm Cu, the vertical slits were set at 1 cm width, and  $T_\pi = 30$  MeV.

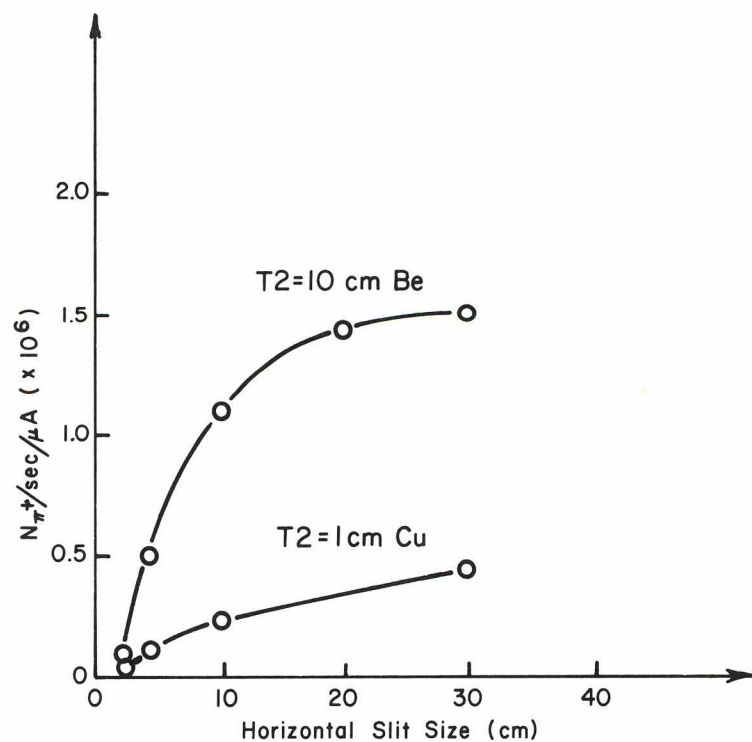


Fig. 49. Pion fluxes in M9 for the 10 cm Be and 1 cm Cu targets at T2.

## M8 CHANNEL AND BIOMEDICAL FACILITY

The M8 channel is a negative pion beam line dedicated to the investigation of the clinical efficacy of pion radiotherapy. The beam line collects pions which are produced at the T2 target and delivers them into the irradiation room of the Batho Biomedical Facility. The facility provides office and laboratory space for the physics research group associated with the beam line. Cellular and animal radiobiology laboratory space occupy the top floor of the three-storey building. An animal colony housed in a commuting trailer has become operational this year. A 250 kV X-ray machine for providing a standard comparative source of radiation has also been installed in the facility.

Continuing work on the development of the beam line has consisted primarily of measuring and understanding the optical properties of the channel. The dispersion and momentum resolution have been deduced from telescope measurements of differential range curves in a water phantom. The momentum acceptance has been measured with positive pions in a total-energy plastic-scintillator detector. Achromaticity in both position and slope have been determined with an amplifier per wire multiwire proportional counter. Effects on the uniformity of beam profiles have been investigated with the use of two sextupole magnets in the beam line. The parameters which have been measured this year are included in the following table:

Table IX. Parameters of the biomedical channel

Angle of channel to proton beam	30°
Length of channel	7.2 m to vacuum window
$\pi^-$ flux at 150 MeV/c pion 10 cm Be target 1 $\mu$ A 500 MeV proton beam	$1 \times 10^6 \pi^-/\text{sec}$
Momentum range	0-220 MeV/c
Dispersion	0.62 cm/% $\Delta p/p$
Momentum resolution	1.5% $\Delta p/p$ FWHM
Momentum acceptance	$\pm 6.7\%$ $\Delta p/p$
Momentum spot size	2.0 cm $\times$ 2.6 cm FWHM



## M20 CHANNEL

Most experiments on M20 have used so-called 'cloud muons' from pion decay near the T2 production target. When tuned for 170 MeV/c, M20 produces  $\sim 10^4$  'cloud'  $\mu^+$ /sec on a 50 cm<sup>2</sup> spot for 1  $\mu$ A of 500 MeV protons on the 10 cm Be production target. These muons are only about 60% polarized but have served admirably for a number of  $\mu$ SR experiments where pions are separated by a degrader.

For both cloud and backward muons the rates for  $\mu^-$  are about a factor of four less than for  $\mu^+$ .

Since July M20 has also produced 'surface muons' for experiments. These 4.1 MeV (29.8 MeV/c) positive muons arise from  $\mu^+$  decay at rest in the 'skin' of the production target and so are nearly 100% polarized. The difficulty of transporting such low-energy muons through thin counters and vacuum windows is compensated by their incomparably high stopping densities. The  $\mu$ SR group routinely stops the entire surface muon beam in <30 cm of argon gas at 1 atm. When tuned for 29.8 MeV/c (commonly referred to as 'Arizona mode' in deference to the group which developed the concept originally), M20 produces 6000  $\mu^+$ /sec for 1  $\mu$ A on the 10 cm Be target in T2. Unfortunately, negative surface muons are not available, since the pions capture upon coming to rest.

## CONTROL SYSTEM

At the end of 1975 the consolidation of the TRIUMF control system into one large CAMAC system was complete. In 1976 this unified system was used to implement several operational improvements, new scans and interlocks, and improved logging. Progress was slightly slowed by the August reassignment of one programmer to development of the TRIUMF data interface.

### *Operational improvements*

'Master solutions' for all cyclotron systems have been placed on disc. This means that commonly used cyclotron set points can be restored on command, without recourse to paper tape. Two injection line solutions, corresponding to the two ion sources, are maintained as are several external beam line solutions corresponding to the most commonly used energies. Experience has shown that the master solutions almost always produce a beam, with only minor adjustments required for optimization. On request, deviations of actual operating conditions from the master solutions may be typed out, or displayed on a CRT.

Control and/or display of several cyclotron systems not previously accessible through the main console have been implemented. These include the ISIS injection line, the tank correction plates, the meson production target (T2), and a large fraction of the beam line and tank vacuum systems. Selection of the mode of operation of the trim and harmonic coil controls has been facilitated by the addition of a numeric pad on the main console. Some remote control of the polarized ion source has been added, including a system of four remote 'spin flip' control panels which allow the experimenter using polarized beam (and none other) to control the spin state either manually or using his data acquisition computer.

An increased number of histogram-type storage scope displays—of skimmer currents in the injection line and radiation spills in the vault and along the high-energy beam lines—have proved a useful beam tuning aid. In addition, use of the alphanumeric CRT display ('Tel Term') has been greatly expanded. There are now over 80 pages which may be called up, ranging from status displays of all major systems through 'checklists' of conditions which may prevent successful beam extraction, to pages of operator-modifiable messages for transmission from shift to shift.

A major development has been the installation of an autonomous CAMAC controller which continuously reads all of the 0-5 mV shunt levels from the trim and harmonic coil power supplies, storing them in an associated CAMAC memory. The low-level multiplexed analogue-to-digital system used for the measurements results in extremely stable readings; and the combination of autonomous—meaning without computer intervention—scanning and CAMAC memory greatly reduces the CPU overhead in the acquisition of this data. The CAMAC memory module designed for this

application has also been incorporated separately in the system and is used to store several parameters which may be required by all control system computers, or must be preserved through control system reloads.

### *Scans and interlocks*

Some interlocks required for machine protection at higher beam intensities have been implemented, or backed up, using control system software. Thus the program prevents beam from entering either the ISIS injection line or the cyclotron unless they are set up to receive it. Several conditions, such as excessive beam loss along the injection line, cause the beam to be cut off at the source. Excessive temperatures detected at any of 88 points on the resonator panels result in the RF system being disabled.

In addition, the number of cyclotron parameters which are routinely scanned has been increased. The value of these scans, however, continues to be adversely affected by a large number of anomalous messages, due in general to measurement errors. This situation has been improved somewhat with the introduction of new multiplexer cords; however, much remains to be done in this area.

### *Logging*

The higher intensity operation during 1976 has resulted in a requirement for routine logging of radiation levels. This has been implemented on magnetic tape, at intervals specified by the operator. Analysis of these logs is performed off line.

One teletype has been dedicated to the logging of all scan and error conditions, as well as of some operator actions. This log has proved useful in analyzing control system faults.

The logs of cyclotron operating conditions taken routinely by each shift have been rendered more useful by including comparisons with the master solutions, as well as an indication of when measured outputs do not correspond with values calculated from their set points.

### *Reliability*

In 1976 two important improvements affecting system reliability were made to the CAMAC system. Power monitors have been installed in each crate permitting annunciation in the control room of failed or failing CAMAC power supplies; and a modification to prevent oscillations on a branch in the case of a crate power failure has been made to all differential branch drivers. The latter modification prevents a recurrence of the most serious control system fault in 1976, when branch oscillations generated valid CAMAC commands, which in turn caused spontaneous motion of probes in the tank.



The most frequent control system failure continues to be of CAMAC power supplies, followed by multiplexer cords in the analogue-to-digital monitoring system. Computer and peripheral hardware has generally performed reliably, with the exception of the six KSR 37 teletypes, which require almost continuous service. Two of these were replaced with 'Decwriters' in 1976, and the remainder will be phased out in 1977 and 1978. Software errors introduced with new programs continue to cause some system downtime, and this can be expected to continue for some time.

In spite of these difficulties, cyclotron operating records indicate that in 1976 control system failures have been responsible for only 42 h, or <5%, of unscheduled cyclotron downtime.

## INSTRUMENTATION

For the second year instrumentation was rented to experimental groups from the TRIUMF Instrumentation Pool, which in 1976 was funded to the extent that about two-thirds of the instrumentation requested could be provided. A major change in the operation of the Pool, announced at the TRIUMF Users Meeting in December, is the intention to make rental payments (at the level of 1% of the initial value of a unit per month) a continuing cost to the user. This change will be implemented in (fiscal) 1977 and is intended to defray the cost of maintenance of Pool instrumentation.

The current list of TRIUMF standard instrumentation is shown in Table X.

Table X. TRIUMF Pool Standard Instrumentation

1. RACKS			4. NIM MODULES (cont'd)		
Premier Metal Housings (Montreal)	Type 000003070		Variable attenuators (50Ω)	LRS A101 L	
2. POWER SUPPLIES, BINS AND CRATES			Fast pulse generator: (Berkeley)	BNC 8010	
NIM bins			High resolution ADC		
Bin and power supply: B.L. Packer	Bin NB10		10-bit amplitude encoder (requires scaler for read-out)	EGG EA 101/N	for replacement only
CAMAC crate	200 W power supply 1001-3		High resolution TDC		
Crate: GEC Elliott	VC0011/CP1		10-bit time encoder (requires scaler for read-out)	EGG ET 102/N	
Power supply: B.L. Packer	1031 BC (300 W)		Spark chamber TDC (routing unit)		
Photomultiplier high voltage	Power Designs 1570		Clock generator (up to 200 MHz) and scaler required. Dual unit:	TRIUMF B00100	
High voltage distribution	TRIUMF THV100				
3. PHOTOMULTIPLIERS AND HOUSINGS			Slow NIM		
2 in. 12-stage, bi-alkali photomultipliers	RCA 8575R		Gate biased amplifier	ORTEC 444	
housings	N.P.W. England Ltd.		Research amplifier	450	
3 in. 14-stage, 118 spectral response* photomultipliers			Timing filter amplifier	454	
housings			Delay line amplifier	460	
			Delay amplifier	427A	
			Linear gate	426	
			Linear gate and stretcher	442	
			Fast coincidence	414A	
			Universal coincidence	418A	
			Time-to-pulse-height converter	467	
			Gate and delay generator	416A	
			Precision pulse generator	419	
			5 kV power supply	459	
			Constant fraction timing SCA	455	
			Digital current integrator	439	
			Biased amplifier	408A	
4. NIM MODULES					
Fast NIM			5. CAMAC MODULES		
Discriminators, quad updating	LRS 621L		Coincidence buffer (pattern unit)	EGG C212	
bridged input version	LRS 621L/4		dual 12-fold		
quad zero-cross	EGG T140/NL		Multi-ADC		
constant fraction	ORTEC 473A (requested for evaluation)		octal 8-bit units	LRS 2248 or NE 9040	
AND (coincidence) gates			Multi-TDC		
Triple 4-fold logic	LRS 465		quad 9-bit	LRS 2226A	
[Dual 4-fold majority logic LRS 364 and 365 accepted but not recommended for new purchases]			octal 10-bit	LRS 2228	
Dual 4-fold overlap	TRIUMF B024 } for special		Scalers: hex 24-bit, 100 MHz	Kinetics 3615**	
Quad 2-fold overlap	TRIUMF B042 } order only		Crate A controller	Kinetics 3900	
Quad 2-fold and/or (updating)	LRS 622		[GEC Elliott accepted but not recommended for new purchases]		
[LRS 322A accepted but not recommended]			Dedicated crate controller (NOVA)	EGG NC 023C	
OR gates and logic fan-out			TTY output	NE 7061-1	
Logic 8-fold fan-out	TRIUMF 14X295		16-bit (relay-type) output register	GEC OD 1606	
OR gate: Dual 4-fold	LRS 429		24-bit (TTL) output register	SEC PR 612	
Linear Fan-in/Fan-out	LRS 428		24-bit in/out (TTL) register	NE 9017	
[LRS 127 and 128 accepted but not recommended for new purchases]			24-bit input gate SEC	SEC PG 604	
Linear gate			16-fold fast NIM out	SEN	
Linear gate and stretcher (integrator)	Borer 330 (for replacement only)		256-bit input gate (for MWPC)	GEC	
Level converter (NIM Fast ↔ TTL)	EGG LG 105/N				
Gate pulse and delay generator	LRS 688 AL and (EGG L1380/WL)				
Scaler (visual display): 100 MHz, 6 digit	LRS 222 (EGG GG 202)				
Dual unit					
[accepted but not recommended]	Joergers VS				
Variable delay units (cable-switched)	ORTEC 772				
Passive '64 nsec'	TRIUMF B007				

\*Complete with face plate adaptor AJ 2142  
 \*\*[LRS-2550 quad units accepted but not recommended for new purchases]

# PROGRESS TOWARDS ULTIMATE PERFORMANCE

In addition to the performance objectives already achieved, including variable energy of 180-520 MeV and simultaneous extraction of beams of differing energy and widely varying intensity, there are still two important objectives yet to be attained. They are the acceleration of proton beams  $\geq 100 \mu\text{A}$  and the use of separated turn acceleration to yield beam energy spreads of 100 keV or less.

In order to co-ordinate the work towards these objectives, two task forces were appointed and their reports constitute this section of our Annual Report.

A third important objective—reliable operation—has at least been partially achieved, and its influence permeates a large part of the Report.

## 100 $\mu\text{A}$ TASK FORCE

The task force was set up in June 1975 to plan, oversee and effectuate the timely achievement of the design goal of 100  $\mu\text{A}$  along beam line 1 with the thermal neutron facility as a beam dump. Since the task involves the collaboration of various groups, one of the major concerns has been communication, information and co-ordination between the groups. Results of this co-ordinated effort are reported below but listed as milestones only, the details being covered in the group reports.

In general most of the problems encountered in bringing a meson facility to full intensity can be grouped into four categories:

- 1) Problems connected with producing the required intensity of the ion source and in transporting it to higher energies without losses due to space charge effects

That the ion source and the injection system are capable of delivering enough current to the cyclotron had already been demonstrated when 120  $\mu\text{A}$  were injected into the full-scale central region cyclotron and accelerated successfully to 2.5 MeV. In addition, at the end of 1976 the required current was produced and transported through the TRIUMF 40 m long injection line for several hours as a test. The details of this work are described in the ISIS report.

- 2) Problems arising from the need to avoid thermal damage due to beam losses on non-cooled elements

The power involved in these losses can be of several tens of watts along the 300 keV electrostatic injection line, with possible melting of the electrodes and metallization of the insulators. Even



worse, at higher energies beam losses can be associated with kilowatts of power, and the damage may involve large machine structures or regions where repairs are difficult due to high local residual activity. In order to avoid beam losses for a substantial fraction of the time, non-intercepting current monitors have been built to function along the injection line and the external lines. Beam-spill measuring systems have been built or designed for the injection system (skimmers), cyclotron (scrapers) and beam lines (halo monitors). In addition, for the higher energies the radiation-spill monitors were set so as to trip the machine before any damage could occur. The interlocking of these devices to the ion source output has been gradually implemented while the current was raised at higher levels.

- 3) Problems related to the radiation produced by the high-energy beam at places where casual losses or deliberate beam dumping occur

There are two aspects: a) keeping the radiation below the permissible level in access areas, and b) keeping the residual activity in the cyclotron and beam lines under control for safe maintenance. Shielding around the cyclotron and the beam lines and remote handling for hot equipment maintenance are the obvious solutions to these problems. However, improved transmissions and proper collimation or dumping arrangements can greatly reduce the cost involved in shielding and remote handling. Localizing inevitable beam losses will mean that remote handling may be limited to specific regions only and that heavier shielding structure may be used in these confined regions. Further comments about these aspects can be found under Safety, Remote Handling, Shielding, Beam Development and Beam Lines reports.

- 4) Problems which may occur in systems that are bound to become active when operating at higher currents

All foreseeable tasks in regions bound to become hot must be studied and possibly completed before raising the intensity. If this is not possible, enough flexibility for changes has to be provided through remote handling and remote handleability of the components. The completion of the beam line 1 system to the thermal neutron facility as a 100  $\mu$ A beam dump is essential for the achievement of the 100  $\mu$ A goal, since the temporary dump at T2 is compatible only with a few tens of microamperes. Along beam line 1 new facilities which should preferably be installed before the line is too active are the front end of the high resolution pion line and the front end of beam line 1B. In the tank RF modifications for third harmonic flat-topping of the wave form, and RF, probes and vacuum improvements for higher reliability, remote handleability and better performance, are items which had to be taken into account in the general planning. This situation required close collaboration between the 100  $\mu$ A task force and the TNF, M11 and beam line 1B task forces.

The complexity and inter-dependency of the various problems required a major planning effort. As outlined in last year's annual report, the plan consisted in proceeding towards the goal through two phases. During phase one the aim was to increase the current from a few hundred nanoamperes at the end of 1975 to an operating current of 10  $\mu\text{A}$  by the end of 1976. The 10  $\mu\text{A}$  limit was compatible with hands-on maintenance in most of the vacuum tank and beam line 1, with the exception of the tank wall and the target T2 regions where remote handling was required. Phase two was to result in 100  $\mu\text{A}$  with remote handling, the completion of beam line 1 beyond T2, and the construction of the 100  $\mu\text{A}$  thermal neutron facility having highest priority. Upgrading the machine and the beam line 1 to meet reliability and improvement requirements, monitoring beam transmissions and beam losses, making the injection system suitable for high currents, and upgrading the shielding structure were activities contemplated in both phases.

By the end of 1976 almost all the activities which had been planned for phase one were completed, and several 10  $\mu\text{A}$  shifts, plus one demonstration of 30  $\mu\text{A}$  for several hours plus 50  $\mu\text{A}$  for a few minutes, had been achieved. Thermal protection on the '10  $\mu\text{A}$ ' temporary dump behind T2 prevented running 50  $\mu\text{A}$  any longer.

At the same time a detailed plan had been prepared for phase two. It was decided that a PERT schedule involving almost all activities at TRIUMF would be useful in order to monitor the progress, emphasize the constraints, estimate and allocate the resources, define the priorities and maximize the output. By the end of 1976 three detailed PERT schedules were drawn. PERT 1 included about 325 activities involving the cyclotron and the commissioned facilities, PERT 2 (540 activities) concerned the meson area, PERT 3 (200 activities) concerned the proton area. The analysis of the resources suggested that the installation of the front end of beam line 1B and of the M11 line be attempted during the same shutdown (fall 1977) where the beam line 1 would have been extended to the TNF ready for the 100  $\mu\text{A}$  beam. These PERTs suggested that with a few additional resources and some luck the beam line 1 extension, the TNF, the front end of beam line 1B and M11, and the corresponding safety and shielding structures will probably be installed by the end of 1977. The system will then be ready for 100  $\mu\text{A}$ , initially for short periods, becoming gradually longer during 1978 depending on the success of the remote handling devices and on the reliability achieved in all systems.

The major milestones achieved towards the completion of phase one along with the dates of achievement are as follows:

During January currents of 1  $\mu\text{A}$  were made available to the users. The beam transmission between the central region and the 500 MeV extraction had been brought close to the design value of 80% and the beam spill along beam line 1 minimized such that the limited amount of shielding available by that date was actually adequate for this current. Also, the vacuum in the cyclotron tank improved gradually, due to long-term outgassing of components and to a constant leak detection and repair



effort. In March the operating pressure went below  $10^{-7}$  Torr, consequently reducing the priority on the construction of two 25,000 l/sec hydrogen-pumping cryopumps.

After a rearrangement of the shielding structure above beam line 1, a 5  $\mu$ A beam was accelerated in March for 1.5 h. More accurate measurements of the restriction in working areas and along the fence were performed, and in general the measurements agreed with predictions within a factor of two and indicated clearly the additional shielding required for the 10  $\mu$ A operation (about a 3 ft layer on beam line 1 and additional blocks on the vault walls and downstream T2). At that time a very welcome injection of funds, specifically related to the 100  $\mu$ A goal, mobilized the laboratory. Additional shielding was immediately ordered and detailed designs were started on the thermal neutron facility and the beam line 1 extension for phase two.

In June a special system of graphite absorbers surrounded by boriated gypsum sheets was installed around the cyclotron tank in order to degrade the beam spilled horizontally through the thin (1/22 in.) portion of the tank wall. Being inserted between the tank wall and the magnet yokes these shields also partially protect the tank area from the residual activity induced on the yokes. A factor five to ten of reduction of the tank activity was achieved with 2.5 mrem/h on average at the tank periphery and 0.5 mrem/h at the centre.

The radiation measurements performed by the Safety group during the 5  $\mu$ A test and the encouraging situation inside the tank proved the validity of our programs and predictions, and prepared the layout for the extension of the safety licence regulations from the rather limiting 1  $\mu$ A average initial licence to a new type of licence where the new 100  $\mu$ A limit was associated with a number of criteria limiting the radiation in working areas (August).

As soon as the first part of the new shielding blocks arrived on site the system was ready to accept 10  $\mu$ A. Along the injection line the skimmer system designed to protect the line from excessive beam losses had been commissioned, and 50 to 100  $\mu$ A could be safely transmitted to the inflector. Three 10  $\mu$ A shifts were successfully performed between September and November and dedicated to spill minimization and shielding optimization. By the end of November everything was ready for increasing the current to the thermal limits of the T2 beam dump. The chart recorder graph showing the achievement of 50  $\mu$ A for the first time at TRIUMF is given in Fig. 50. The current as derived from the stripping foil reading was 47  $\mu$ A, but there were clear indications that the amplifiers used to display this current in the control room had started saturating just below 50  $\mu$ A and that the current to be believed was the indication from the spill monitor placed very close to the beam dump. During the same day several hours of 30  $\mu$ A operation enabled the mapping of the radiation distribution in the working areas. It became clear that except for a few weak regions easy to correct the shielding system was actually adequate for 20-30  $\mu$ A.



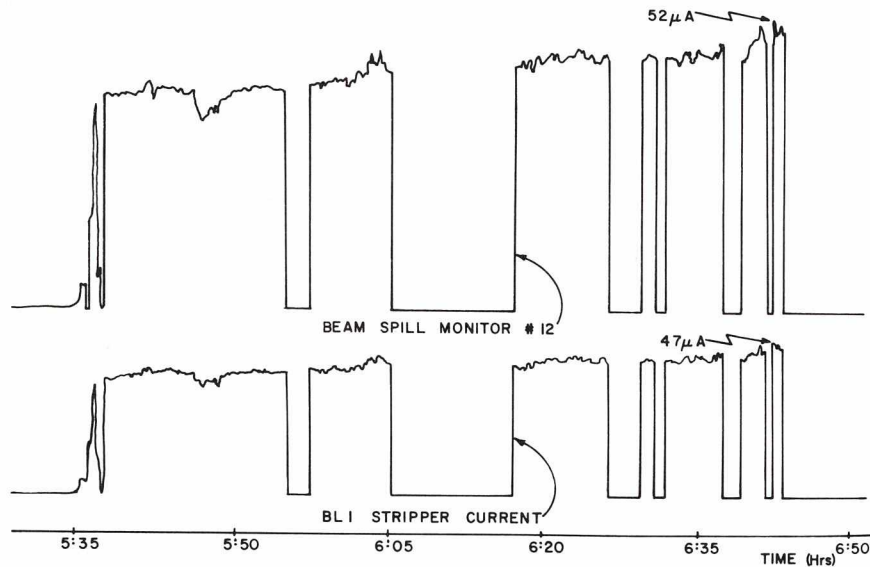


Fig. 50. Strip chart recording showing first 50  $\mu\text{A}$  to temporary beam dump T2.

For 50  $\mu\text{A}$  of extracted beam about 200  $\mu\text{A}$  had been injected along the injection line. A few days later 400  $\mu\text{A}$  required for 100  $\mu\text{A}$  extracted beam was maintained along the injection line for several hours, without any thermal damage but with some instability at the source.

Before the end of the year all essential interlocks for operating 10  $\mu\text{A}$  regularly, and including a non-intercepting transmission system in ISIS, were implemented. The system was ready for standard beam production at 10  $\mu\text{A}$ . A set of 2 in. thick lead shields to be inserted during shutdowns at the inner surface of the tank wall, to reduce the radiation inside by another factor of five, was in an advanced stage of fabrication to be ready for installation during the first 1977 shutdown.

## SEPARATED TURNS TASK FORCE

With the emphasis on operating at higher beam intensities this year, work towards separated turns has not been favoured with high priority. Nevertheless, significant progress has been made in the crucial areas of RF third harmonic, magnet stability and beam dynamics.

In the case of the RF the feasibility of coupling third harmonic into the resonators simultaneously with the fundamental while there is good isolation between them has now been tested and seems assured. The third harmonic coupling loop and transmission line (with uncooled stubs) were installed during the summer. Tests at signal level with the fundamental off showed that the third harmonic Q-value was higher than for the fundamental. There remained some doubt, however, as to whether the frequency ratio could be brought to exactly 3.0 without either modifying the resonators in a major way or changing the fundamental frequency and spoiling the isochronism. [This question was resolved satisfactorily in the first weeks of 1977, when third harmonic tests were made in the presence of fundamental at full power; it appears that a frequency ratio of 3.0 can be obtained by adjusting the tie rods, without dropping the frequency more than 30 kHz, a quite acceptable amount.]

The next step is to raise the third harmonic power level using the 3 kW driver; this should provide 2.5 kV on the dee tips and provide observable effects on the beam. Work is proceeding on the design and construction of the 100 kW amplifier and water-cooled stubs for the transmission line as fast as priorities allow.

The stability of the magnetic field has been investigated and found satisfactory so far in a series of tests begun during the year. These began with 'quiet site' tests when all other work was banned over two week-ends to determine the background and the stability of the undisturbed power supply. The field changes were monitored by integrating the emf induced in the outermost trim coil. A later test under normal site operating conditions showed short-term 'noise' of  $\pm 1.3 \times 10^{-6}$  and longer-term 'drifts' of up to  $\pm 1.5 \times 10^{-6}$  over periods of 20 min. This comes close to meeting the assigned tolerance of  $2.5 \times 10^{-6}$  and is particularly encouraging in view of the 2% changes in site voltage which occurred during the test. [Observations by one of the experimental groups have confirmed these values; they timed an external proton beam relative to the RF and found it to be stable within  $4^\circ$  RF (i.e.  $\pm 1.8 \times 10^{-6}$  in field) over an hour.] Measurements on temperature drift of the power supply subsystems are proceeding. In the coming year it is hoped to complete these tests and design and test an improved stabilization system. Present plans call for the slow drifts to be corrected via the main power supply, while the faster fluctuations will be dealt with by a small supply in parallel.

The most critical development this year has been in beam dynamics—the discovery of a method of achieving separated turns and good energy resolution with the cyclotron's existing field, a possibility which had

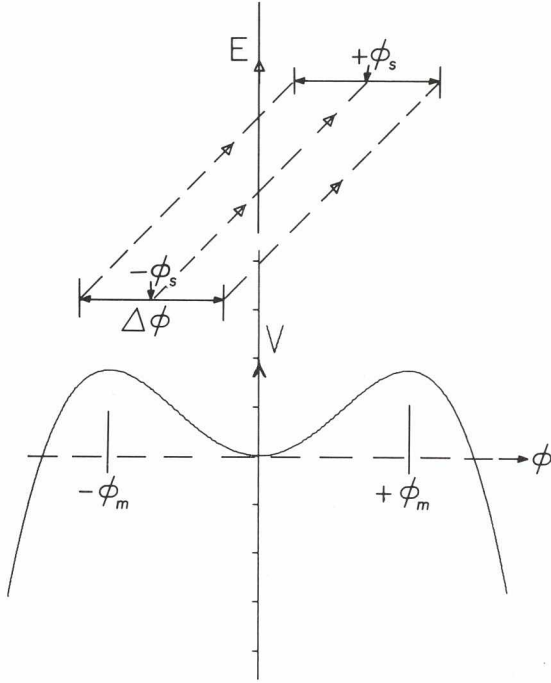


Fig. 51. RF wave form with third harmonic flat-topping and linear phase ramp.

seemed very doubtful in 1974 and 1975. To achieve separated turns for a finite phase spread  $\Delta\phi$ , it has generally been assumed that extremely good isochronism is necessary. Thus to achieve an energy resolution  $\Delta E/E \simeq 10^{-4}$  for TRIUMF, even with the aid of RF third harmonic flat-topping, the phase errors tolerable were determined to be only  $\pm 1.1^\circ$ . In the limited time available for shimming the magnet it was not possible to meet these tolerances everywhere, and phase oscillations of up to  $\pm 20^\circ$  were left (cf. Fig. 7, p.19). However, the technique which has now been found makes such a stringent isochronous requirement unnecessary.

The basis of the technique [Craddock *et al.*, in Proc. 1977 Particle Accelerator Conf., Chicago, IEEE Trans. Nucl. Sci. (to be published)] is to use the phase oscillations to average out the phase-dependency in the dee voltage. Just as in the case of perfect isochronism, the fraction  $\epsilon$  of third harmonic used is a little greater than the nominal  $1/9$ , creating two humps in the RF wave at phases  $\pm\phi_m$  (Fig. 51). In the case of a linear phase ramp from  $-\phi_s$  to  $+\phi_s$  the exact value of  $\epsilon$  which minimizes  $\Delta E$  is such that the two humps occur at phases slightly outside  $\pm\phi_s$ , the amount outside depending on the phase spread  $\Delta\phi$  in the beam. The minimum value of  $\Delta E$  turns out to depend only on  $\Delta\phi$  and not on  $\phi_s$ ; in fact it is the same value  $\Delta E_0$  that could be obtained for the same phase spread  $\Delta\phi$  in the case of perfect isochronism. In that case  $\epsilon$  is chosen so that  $V(\pm\Delta\phi/2) = V(0)$ ; then the energy resolution  $\Delta E_0/E = 1 - V(0)/V(\phi_m) = 3(\Delta\phi)^4/512$ . Numerical integration turn by turn has confirmed this; thus for  $\Delta\phi = 20^\circ$ ,  $\Delta E_0/E = 0.87 \times 10^{-4}$ , independent of  $\phi_s$  and  $\epsilon$ .



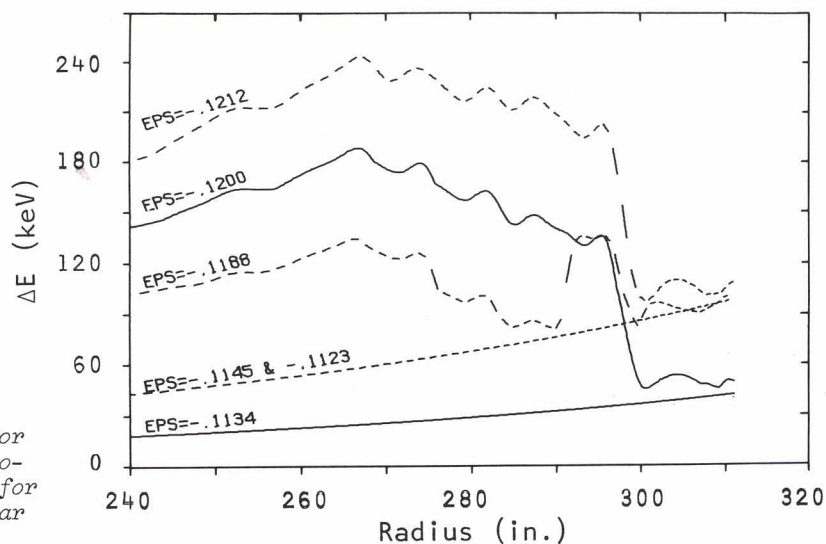


Fig. 52. Energy spread for  $\Delta\phi=20^\circ$  for perfect isochronism (smooth curves) and for actual situation (irregular curves).

If the energy spread can be reduced to  $\Delta E_0$  for a single ramp, then so it can for a succession of alternating ramps with a common amplitude. The technique also works for purely sinusoidal phase oscillations, bringing  $\Delta E$  down to  $\Delta E_0$  at each extreme of the phase. TRIUMF's phase oscillations of course vary in amplitude, so that the optimum value of  $\epsilon$  will vary in radius; nevertheless it has been possible to find a value of  $\epsilon$  (0.120) which, for  $\Delta\phi = 20^\circ$ , makes  $\Delta E < 1.2 \Delta E_0 = 52$  keV between 450 and 500 MeV. Figure 52 illustrates these results. The effect of varying  $\epsilon$  by 1% of its value is also shown; as expected theoretically the sensitivity to  $\epsilon$  is independent of isochronism. It should be noted that the discussion above completely neglects the effects of instabilities on  $\Delta E$ ; for TRIUMF these are expected to add an additional 50 keV.

# FACILITIES UNDER DESIGN AND CONSTRUCTION

## M11 CHANNEL

The M11 channel is designed for production of  $\pi^+$  and  $\pi^-$  of energies 30 to 350 MeV at rates up to  $10^8 \text{ sec}^{-1}$  for a  $4 \text{ g/cm}^2 \text{ H}_2\text{O}$  target and a  $100 \text{ }\mu\text{A}$  proton beam. The channel will look at  $\pi$ 's produced at  $2.5^\circ$  which have been spatially separated from the proton beam by the dispersive effect of the quadrupole IQ9. The proton beam having a higher momenta is not dispersed as much spatially and is recombined for transport down the rest of beam line I by the doublet IQ10 and IQ11. The  $\pi$ 's having been separated from the proton beam are then picked off by the septum magnet IIS1 and directed through the doublet IIQ1 and IIQ2 which produce a dispersive focus at the midplane through the dipole IIB1. The rest of the beam line, IIQ3, IIQ4 and IIB2, is a repeat of the first section, IIQ1, IIQ2 and IIB1.

The advantage in not having any quadrupoles following IIB2 is that three experimental lines can be defined without the expense of having to purchase quadrupoles for each line. The three experimental lines are designated as follows:  $L60^\circ$ , an achromatic focus;  $0^\circ$ , a moderately dispersive focus; and  $R60^\circ$ , a strongly dispersive focus of  $4.2 \text{ cm}/\%$ .

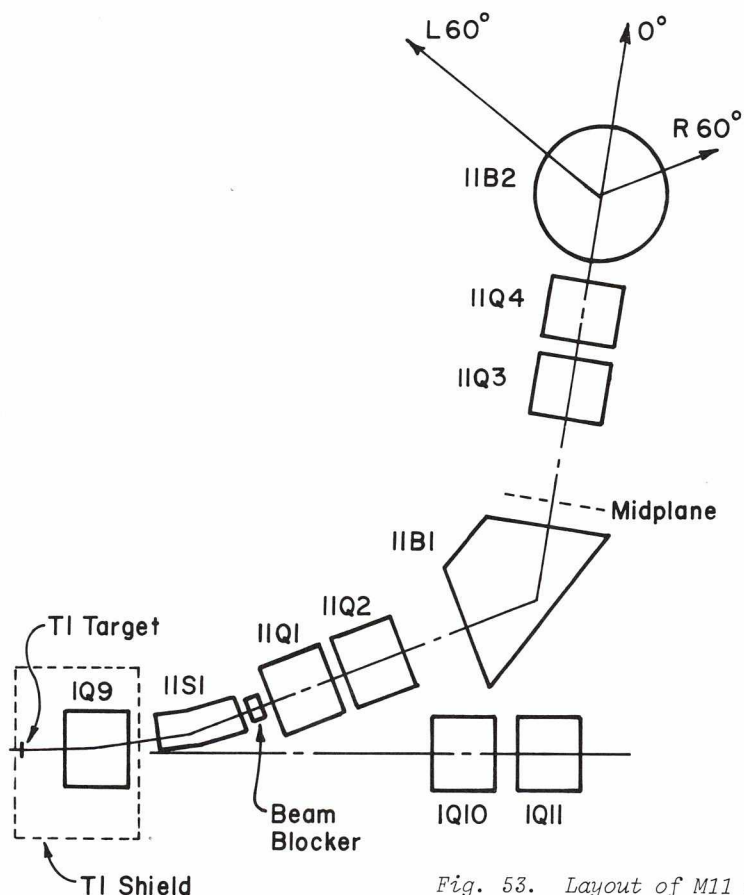


Fig. 53. Layout of M11 channel.

Calculation of beam optics to second order predicts a momentum resolution of 0.75% can be achieved at the midplane focus. This resolution can be improved later by the addition of sextupoles and trim coils. Ultimate resolution of the line should be 0.03%.

At present all magnets should be on hand by June 1977. The magnets 1Q9, 1Q10, 11Q1, 11Q2 and 11B2 are on site. The dipole 11B2 is commonly known as the Corvallis magnet, and it is presently residing at the end of beam line M9. The septum magnet 11S1, which is being built at the University of Victoria, is proceeding without any significant snags. The coils have been bent and are almost ready to be brazed. Provisions for doing so are being made at LAMPF.

The future schedule for M11 calls for installing the line up to 11B1 by the end of TNF installation shutdown which begins late summer 1977. With this minimum installed, the rest of the line can go together without significant interference with the running of beam line 1.

## PROTON SPECTROMETER

The dipole magnet for the medium resolution spectrometer (MRS) has been assembled (with its vacuum vessel and special pole pieces), mounted and aligned in the MRS support structure. Cooling water, air and electrical services have been installed on the support structure. The multi-wire proportional chamber (MWPC) support structure and service platform have also been completed.

The air-pad lifting system has proved to be satisfactory, and the mechanical drive system for the MRS is under construction. The angle measurement encoding system is also under construction and will provide a precision of  $\pm 0.01^\circ$  in the MRS angular position. The normal angular range of the spectrometer, with the downstream beam line in place, will be from approximately  $15^\circ$  to  $165^\circ$  (but see below).

To permit the full angular range of the spectrometer the quadrupole lens, located in front of the dipole on the MRS support structure, must be movable. To accomplish this a special moving mechanism for the quadrupole lens has been designed and is under construction.

A survey of the magnetic field in the main dipole has been made using a 19-element flip-coil cart which can be stepped through the vacuum chamber. This cart permits measurements to be made in the median bend plane and  $\pm 5/8$  in. off the median bend plane. Surveys were made for fields of 6 kG to 16 kG in 2 kG steps in the median plane and of 6, 10 and 16 kG out of the median plane. In addition, the effect of the trim coils was investigated for main fields of 6 and 16 kG and trim coil currents of 200 and 400 A. The availability of the magnetic field survey computer permitted the powering of only two trim coils; those near the exit were chosen to maximize their effect on the fringe field.



A multiwire proportional chamber system has been developed and constructed at the University of Alberta. It consists of two planes of detectors 1 m apart with the focal planes between them. Each detector is 2 m  $\times$  0.4 m and has three wire planes, x, y and diagonal. They will be triggered by large ' $\Delta E$ ' scintillation counters located behind the MWPC's. A small 5 in.  $\times$  5 in. MWPC will be located in front of the quadrupole to improve the determination of the production angle of the reaction products. This system will be transported to Vancouver some time in the spring of 1977.

The design and construction of the target chamber is being handled by D. McDaniels of the University of Oregon. The target ladder which will accommodate five targets is under construction, and the design of the chamber itself is completed and construction is under way. The chamber is 28 in. in diameter and will have Kapton windows on both sides from 12.5°-140° to permit double-arm coincidence experiments. It will be equipped with a 'horn' to replace the beam line at the exit of the chamber to allow the spectrometer to reach angles between  $\pm 15^\circ$ . The beam will be stopped in the horn.

The data acquisition system will be based on an Eclipse S200 processor with 32K core, control store, floating point processor and memory allocation and protection. It will also include an 800/1600 bpi drive and controller, a decwriter, branch driver, 10 mbyte cartridge disc system and a 32K semi-conductor memory in addition to the basic memory above. The display system will be a raster scan, refreshed graphics display. The software will be in a language based on PASCAL.

Commissioning of the MRS facility should commence during the spring of 1977. The spectrometer will be run in the 'fixed-angle' mode (22.5°) for this purpose.

## BEAM LINE 1B

In June, following a poll of experimental spokesmen and others which favoured the establishment of an alternative proton line off beam line 1, a task force was set up to design and procure a beam line to run parallel to the vault wall in the meson hall and to have shielded experimental space for at least two set-ups ( $p, \pi$ ) and one other. It was assumed that the main use of the line would be with polarized beam and that consequently it could be designed as a low-intensity ( $> 30$  nA) line. In the absence of detailed knowledge of the space requirements of 'other' experiments, it was decided to take counter experiments which have run at 4BT1 as typical of low-intensity set-ups that would be used at the 'other' position. A magnetic transport design for acromatic beam at two target locations has been produced. The solution uses two 45° bending magnets and five quadrupoles to produce required beam spots at target locations 14 ft and 28 ft south of the mezzanines, with a beam dump at the north wall of the meson hall.

## THERMAL NEUTRON FACILITY

The conceptual design as described in report TRI-71-3 and simplified in 1975 was further developed and consolidated in a detailed engineering design that is now 25% complete. Orders were placed for the iron shielding core and the vacuum tank. Installation of the iron shield was started in December.

The design combines the requirement for a 100  $\mu$ A beam stop with the following experimental facilities:

Access to the proton beam in three locations, all within the iron shield:

- just ahead of the beam stop (target)
- 90 cm ahead of the target, for isotope production
- 137 cm ahead of the target, for insertion of a muon target

Access to the fast neutron flux in three locations:

- just behind the target, inside the vacuum tank
- immediately outside the vacuum tank, but within the iron shield
- outside the iron shield, but within the concrete shielding

Access to the slow neutron fluxes by means of 'thimbles' or 'rabbits' in the following locations:

- inside the  $D_2O$  moderator surrounding the target below beam level
- inside the  $H_2O$  moderator surrounding the target above beam level

Channels for extraction of thermal neutron beams at  $\pm 60^\circ$  and  $\pm 120^\circ$  from the proton beam

The possibility of utilizing certain isotopes that will be produced in the lead target

In addition, the shielding accommodates temporary storage wells for neutron targets as well as for other radioactive objects that may be produced at TRIUMF.

For a 100  $\mu$ A beam of 500 MeV protons the maximum expected neutron fluxes are as follows:

Thermal	$8 \times 10^{12} \text{ cm}^{-2} \text{ sec}^{-1}$
Intermediate ( $0.1 \text{ eV} < E < 25 \text{ MeV}$ )	$4 \times 10^{12} \text{ cm}^{-2} \text{ sec}^{-1}$
Cascade ( $E > 25 \text{ MeV}$ )	$5 \times 10^{11} \text{ cm}^{-2} \text{ sec}^{-1}$

The construction is illustrated in Figs. 54, 55 and 56. Figure 54 is a cross-section at beam level. Before entering the iron shield the proton

beam passes a monitor station and a gas-cooled vacuum window. It then passes through a vertical tube, suitable for insertion of a muon target with neutron take-off at  $120^\circ$ . Next it passes through a similar vertical tube, suitable for insertion of isotope-production targets. Passage from the vacuum in the vacuum vessel and beam line into the lead target is via a 1-mm-thick aluminum water window and a thin layer of water which serves to cool the window.

Figure 55 is a vertical cross-section along the proton beam line. It shows how access to the proton beam line and immediate target area is mostly from above, from an area which is accessible for people after shutdown but not during operation. The same area accommodates the cooling equipment for the various target components. Access to the fast neutron flux outside the vacuum tank is by unstacking a pile of concrete blocks and removing a water-cooled iron plug from behind the target.

Figure 56 is a cross-section along the NW and SW neutron channels. The NW channel runs at 15 cm below beam level as does the SE channel. Both channels stop very close to the target. The shielding block configuration in the NW channel will accommodate a double monochromator. The SW and NE channels run at 30 cm below beam level and form one continuous channel underneath the target.

After a thorough evaluation of the merits of various target materials—uranium, lead/bismuth, lead, tungsten and copper—lead was chosen as the safest material that will still yield reasonable neutron fluxes. The lead will be contained in an alloy steel can, and the 37.5 kW of heat developed in the lead will be transferred to the surrounding moderator water through nucleated boiling at the surface of the can. A heat exchanger in the upper half of the moderator tank will remove the heat to the existing active cooling water system. The lead will be molten and helium will be flushed over the surface to remove radioisotopes. Full-scale model tests to prove the heat transfer principles are still in progress, but there is little doubt about the feasibility.



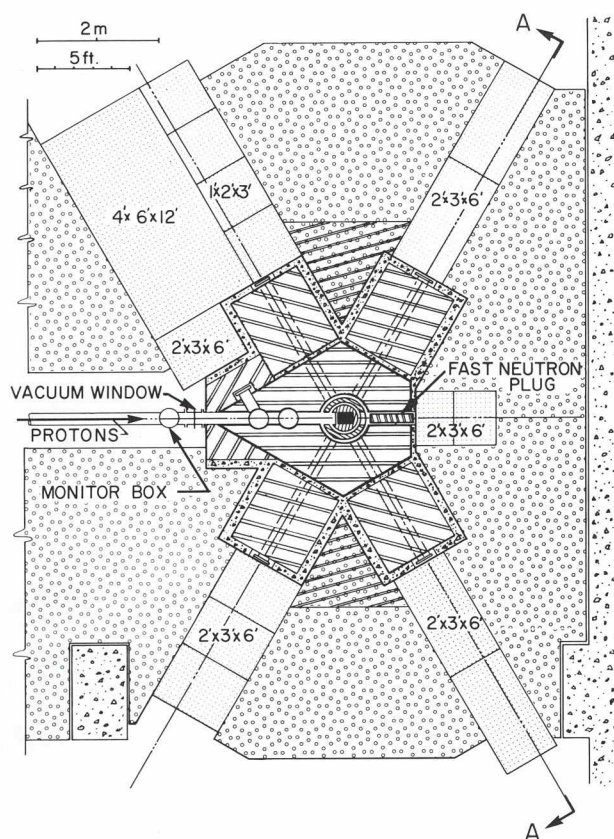


Fig. 54. The thermal neutron facility.  
Horizontal cross-section at beam level.

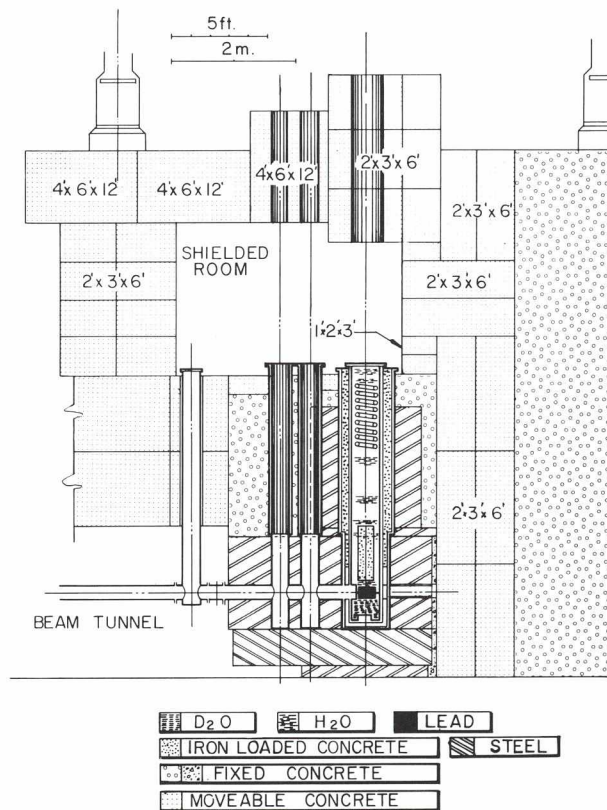


Fig. 55. The thermal neutron facility.  
Vertical cross-section along beam line.

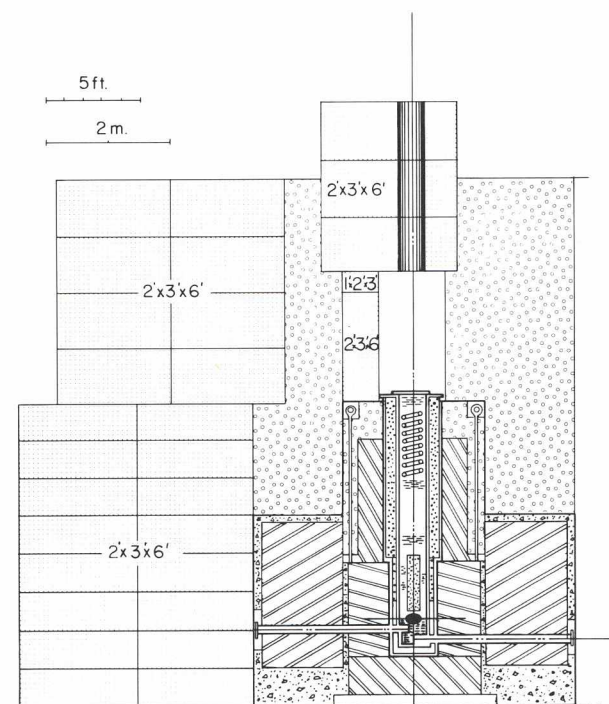


Fig. 56. The thermal neutron facility. Section A-A in Fig. 54.

## SHIELDING AND ACTIVATION

During the first half of the year shielding for the periphery of the cyclotron vacuum tank was designed, fabricated and installed. This shielding, the bulk of which is graphite, was provided to reduce the residual  $\gamma$ -radiation fields, and therefore personnel exposure, in the cyclotron tank during servicing operations. As much as possible of the approximately 20 in.  $\times$  20 in. toroidal ring—bounded on the inside by the vacuum tank wall, the top and bottom by the main magnet coil windings, and the outside by the main magnet return yokes—was filled with aluminum-clad graphite and borated gypsum. Where this space is clear of obstructions aluminum cans were fabricated with 0.020 in. side walls and 0.250 in. top and bottom plates, filled with graphite blocks and grouted with gypsum containing  $\sim$ 18% boric acid. These cans which weigh about 300 lb were installed and can be removed with the cyclotron service bridge. In the space encumbered by flanges and other components 0.75-in.-thick sheets of borated gypsum containing fibreglass were fabricated, wrapped in 0.003 in. aluminum foil, and installed at the outside of the shield ring. The centre of the ring was filled with 2 in.  $\times$  2 in. and 6 in.  $\times$  6 in. pieces of graphite bar cut to the correct length, sealed with a sodium silicate (water-glass) solution and wrapped in 0.003 in. aluminum foil to maintain clean conditions for installation.

This low-activation shielding has been effective in reducing the residual  $\gamma$ -radiation fields from activity produced by protons lost in acceleration by factors in the range 5-10, as expected from consideration of the  $\gamma$ -radiation mean-free path lengths and the vacuum tank wall thickness.

During the summer a production line for the standard 2'  $\times$  3'  $\times$  6' concrete blocks was set up using existing steel forms on the TRIUMF site, and approximately 150 concrete blocks were producing using in-house forces, primarily summer students. Also during the summer a contract was awarded (to Mutual Construction Ltd.) for the fabrication of large standard concrete blocks for experimental area shielding. The previous inventory and additional procurement to the end of 1976 are shown in Table XI.

Dose-equivalent rate measurements at a few microampere proton beam current accelerated to 500 MeV and extracted down beam line 1 with the previous shielding complement for beam line 1 and the experimental areas gave exposure rates on the order of 5-10 mrem  $h^{-1}$  on the east and west cyclotron vault walls, 5-30 mrem  $h^{-1}$  on the top of the beam line 1 roof shielding and in the M9 and M20 experimental areas, 0.5 mrem  $h^{-1}$  generally inside the main accelerator building from secondary scatter (roof and/or sky shine) and 0.05 mrem  $h^{-1}$  at the nearest site boundary, all normalized to 1  $\mu$ A proton beam current extracted down beam line 1 and stopped in the temporary beam stop immediately following the T2 target. The additional shielding available at the end of 1976 reduced

Table XI. Concrete Shielding Blocks

Size	Previous inventory	Additional to end 1976	Additional for power
1'x2'x3'	200	-	-
2'x3'x6'	630	150	-
3'x4'x12'	-	20	-
4'x6'x12'	53	114	70
4'x6'x18'	43	43	18
4'x6'x30'	5	6	-

these exposure rates generally to  $0.1 \text{ mrem h}^{-1}$  per  $\mu\text{A}$  stopped at T2 for roof shielding to elevation 284 ft (15.5 ft above the beam line) and  $0.01 \text{ mrem h}^{-1}$  per  $\mu\text{A}$  for roof shielding to elevation 288 ft (19.5 ft above the beam line). The dose equivalent rates in the M9 and M20 experimental areas had been reduced to the range  $0.1$  to  $1.0 \text{ mrem h}^{-1}$  per  $\mu\text{A}$  stopped after T2, partly by the substitution of iron for concrete shielding at strategic places.

The last column in the table is the supplementary order placed at the end of 1976 to take advantage of the low unit price for this order; it is expected to satisfy the shielding requirements for operation of beam line 1, with both T2 and the TNF installed, at the full  $100 \mu\text{A}$  beam current.



## DATA INTERFACE TASK FORCE

This task force was formed in March to oversee the 'organization and definition' of the proposed data interface—formerly referred to as the message organizer. Two meetings were held in the spring during which a system configuration and budget were established. The proposed configuration is shown in Fig. 57.

The primary purpose of the proposed system is to link the control system, experimental data acquisition computers and the UBC Computing Centre IBM 370 into a single communications network. Experimenters and the control system will then be able to use the data interface printer/plotter and, possibly, magnetic tape drives. At present only asynchronous communication at 300 baud is available with the Computing Centre directly. The data interface will provide experimenters with data communication at 9600 baud and in binary format. Communication with the Computing Centre will use the SDLC (synchronous data link control) protocol now being implemented on their front end processor; and communication with experimental systems will be via a CAMAC-to-CAMAC serial link being designed at TRIUMF.

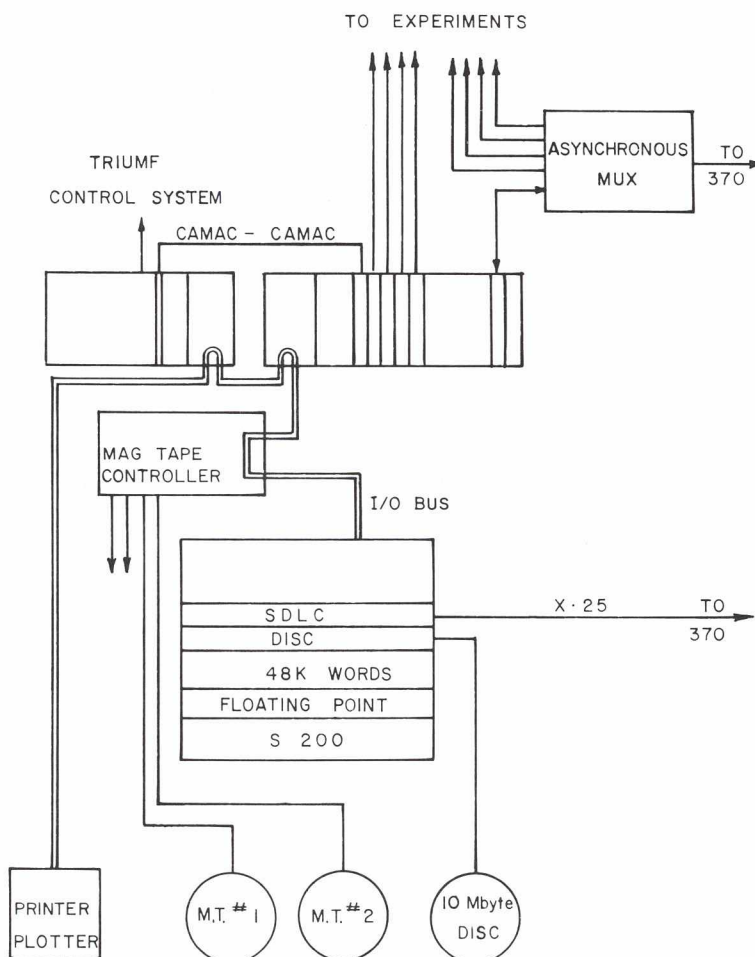


Fig. 57. Data interface system configuration.

A secondary use of the system will be to run user FORTRAN or BASIC programs for simple off-line data reduction, tape copying, or beam diagnostics. These tasks will run in a background mode while communications, operating in the foreground, will have the highest priority.

First equipment deliveries took place in August, and one control system programmer was assigned at that time to data interface software development. By December the computer, disc, printer/plotter and one magnetic tape drive were installed and operating. Both CAMAC systems had been successfully interfaced. The communications (SDLC) interface had been received but was not yet tested.

Most software development to date has been of system utility programs. CAMAC drivers for both FORTRAN and BASIC have been implemented, however, and background program development with a CAMAC test program running in the foreground has been demonstrated. By the end of the year some control system logging could be routed to the data interface line printer, thereby reducing logging time from about 15 min to two or three. It is hoped that the TRIUMF data interface will bring more such benefits in the months to come.

## NEW FACILITIES

The New Facilities group was formed to take care either of small development projects too small for the formation of a task force or relatively independent parts of larger project. Among the more important projects undertaken by the group are the following:

- 1) Faraday cup. The construction of a Faraday cup for the direct measurement of beam currents with 1% accuracy has been completed. This cup will be used to calibrate normal beam line monitors when beam time becomes available.
- 2) Radioisotopes for medicine. The results of this project are given under Applied Research (pp. 65-67).
- 3) Beam monitors. A series of gas-filled ion chambers based on an air core, high-frequency transmission cable have been used successfully to measure beam spill around the machine perimeter and along beam line 1.

Two internal multiplate secondary emission chambers were designed. These utilize the cyclotron magnetic field for electron collection and are used to monitor beam spill due to axial beam excursions.

A scintillating phase probe with a 3 m light path was designed and used to measure the phase of a 1.5 nsec bunched beam extracted at 110 MeV.

- 4) Muon production. A calculation was performed to estimate the expected flux of surface, or 'Arizona mode', muons from beam line 1 production targets including the TNF. A superconducting muon trap was also investigated.
- 5) Magnetic field measurements. Field surveys of several bending magnets including the MRS magnet have been completed. This service provided through the New Facilities group will continue in 1977.



# ORGANIZATION

## *Board of Management*

The Board of Management of TRIUMF manages the business of the project and has equal representation from each of the four universities. At the end of 1976 the Board comprised:

University of Alberta	President H.E. Gunning Dean Kenneth B. Newbound (Secretary) Mr. W.A.B. Saunders
Simon Fraser University	Mr. W. DeVries Dean J.M. Webster Dr. B.G. Wilson
University of Victoria	Dean J.M. Dewey Dr. R.M. Pearce President H.E. Petch
University of British Columbia	Dr. M. Shaw Mr. D. Sinclair Dr. E.W. Vogt (Chairman)

Until mid-year Dean S. Aronoff and Mr. G. Stuart of Simon Fraser University served on the Board in places now occupied by Dr. Webster and Mr. DeVries. Changes in University of British Columbia Board membership occurred earlier in the year when Dean G.M. Volkoff and Dr. R.R. Hearing stepped down and their places were taken by Dr. Shaw and Mr. Sinclair. The Board met four times in 1976.

## *Operating Committee*

The Operating Committee of TRIUMF is responsible for the operation of the project. It reports to the Board of Management through its chairman, Dr. J.T. Sample. It has four voting members, one from each of the four universities. The members of the committee (alternate members in parentheses) at the end of 1976 were:

Dr. J.T. Sample	Director	(Chairman)
Dr. K.L. Erdman	Associate Director	(Secretary)
Dr. W.C. Olsen	University of Alberta	(Dr. P. Kitching)
Dr. R.G. Korteling	Simon Fraser University	(Dr. A.S. Arrott)
Dr. L.P. Robertson	University of Victoria	(Dr. G.R. Mason)
Dr. J.B. Warren	University of B.C.	(Dr. D.A. Axen)

In July B.D. Pate returned to Simon Fraser University after serving as Associate Director during a year on leave at main site and was succeeded

by K.L. Erdman, on leave from University of British Columbia for the 1976/77 academic year. The Committee met twelve times during the year.

### *TRIUMF Safety Executive Committee*

Dr. K.L. Erdman (Chairman)	Dr. M.W. Greene, B.C. Dept. of Health
Dr. E.W. Blackmore	Services and Hospital Insurance
Dr. J.W. Carey	Dr. W. Rachuk, Radiation Protection and
Mr. A.J. Otter	Pollution Control Officer, UBC
Dr. J.T. Sample	Dr. L.D. Skarsgard, B.C. Cancer Foundation
Mr. P.C. Taylor	
Mr. I.M. Thorson	Mr. S.C. Frazer of the Workers' Compensa-
Dr. G.D. Wait (Secretary)	tion Board attends meetings as an observer.
Mr. M. Zach	

### *Experiments Evaluation Committee*

Dr. G.T. Ewan (Chairman)	Queen's University
Dr. R.E. Azuma	University of Toronto
Dr. J.M. Cameron	University of Alberta
Dr. R. Engfer	Universität Zürich
Dr. D.G. Fleming (until Dec 31)	University of British Columbia
Dr. M.D. Hasinoff (Jan 1977)	University of British Columbia
Dr. E.M. Henley	University of Washington
Dr. B. Margolis	McGill University
Dr. D.F. Measday (Secretary)	University of British Columbia
Dr. H. Primakoff	University of Pennsylvania
Dr. J.T. Sample	TRIUMF
Dr. L.D. Skarsgard	B.C. Cancer Foundation
Dr. E.W. Vogt	University of British Columbia
Prof. Sir Denys Wilkinson	University of Sussex

### *Biomedical Experiments Evaluation Committee*

Dr. L.D. Skarsgard (Chairman)	B.C. Cancer Foundation
Dr. M.J. Ashwood-Smith	Simon Fraser University
Dr. G.T. Ewan	Queen's University
Dr. H.E. Johns	Ontario Cancer Institute
Dr. R.R. Johnson	University of British Columbia
Dr. D.F. Measday	University of British Columbia
Dr. T.R. Overton	University of Alberta
Dr. J.T. Sample	TRIUMF
Dr. D.C. Walker	University of British Columbia
Dr. G.F. Whitmore	University of Toronto

## PUBLICATIONS

## Conference proceedings:

J.H. Alexander and H.W. Fearing, Calculation of the pion production reaction  ${}^3\text{He}(p, \pi^+){}^4\text{He}$ , in *Meson Nuclear Physics-1976 (Carnegie-Mellon Conference)*, AIPCP #33 (American Inst. of Physics, New York, 1976), p.375

M.D. Hasinoff, M. Salomon and A. Reitan, Pion charge exchange at rest, *ibid.*, p.316

M. Salomon, D. Berghofer, M.D. Hasinoff, R. MacDonald, D.F. Measday, J. Spuller, T. Suzuki, J.K.P. Lee, J-M Poutissou, R. Poutissou and P. Depommier, The TRIUMF  $\pi^0$  spectrometer and the Panofsky ratio in hydrogen and deuterium, *ibid.*, p.632

D.A. Bryman, G.A. Beer, G.R. Mason, E. Mathie, A. Olin, L.P. Robertson and J.S. Vincent, Low energy pion production by 400-500 MeV protons, *ibid.*, p.264

A.W. Thomas, Faddeev calculations of  $\pi\text{D}$  scattering, *ibid.*, p.375

A.S. Rinat and A.W. Thomas, Covariant calculations of  $\pi\text{D}$  scattering, *ibid.*, p.450

A.W. Thomas and I.R. Afnan, Soft pion production in N-N collisions, *ibid.*, p.472

R.H. Landau and A.W. Thomas, An improved optical potential for low and intermediate energy pions, *ibid.*, p.86

G. Bischoff, G. Coote, H. Dautet, J.M. D'Auria, J.K.P. Lee, B.D. Pate and W.J. Wieseahn, Studies of short-lived products of spallation fission reactions at TRIUMF, in Proc. 3rd Int. Conference on Nuclides Far From Stability, Corsica, May (CERN Report 76-13), p.55

K. Nagamine, N. Nishida and T. Yamazaki,  $\mu^+$  studies of dilute PdFe alloys, in Proc. 2nd Int. Symposium on Amorphous Magnetism, Troy, August (to be published) [TRI-PP-76-5]

K. Nagamine, N. Nishida, R.S. Hayano, T. Yamazaki, J.H. Brewer and D.G. Fleming, Temperature dependence of  $\mu^+$  hyperfine field in ferromagnets, in Proc. Int. Conference on Magnetism, Amsterdam, September (to be published in Physica) [TRI-PP-76-7]

N. Nishida, R.S. Hayano, K. Nagamine, T. Yamazaki, J.H. Brewer, D.M. Garner, D.G. Fleming, T. Takeuchi and Y. Ishikawa,  $\mu^+$  hyperfine field and relaxation in Fe single crystal, *ibid.* [TRI-PP-76-8]

K. Nagamine, N. Nishida, R.S. Hayano and T. Yamazaki,  $\mu^+$  studies of conduction electron polarization in Pd and dilute PdFe alloys, *ibid.* [TRI-PP-76-9]

M.K. Craddock, Recent developments at the TRIUMF meson factory, in Proc. V All-Union National Conference on Particle Accelerators, Dubna, October (to be published) [TRI-PP-76-10]



#### Journal publications:

- H. Dollard, K.L. Erdman, R.R. Johnson, H.R. Johnston, T. Masterson and P. Walden,  $\pi^+$  elastic scattering from  $^{12}\text{C}$  at 29 MeV, Phys. Lett. 63B, 416 (1976) [TRI-PP-76-2]
- P. Kitching, C.A. Miller, D.A. Hutcheon, A.N. James, W.J. McDonald, J.M. Cameron, W.C. Olsen and G. Roy, Observation of j-dependent effects in quasi-free scattering of polarized protons, Phys. Rev. Lett. 37, 1600 (1976) [TRI-PP-76-1]
- F. Myhrer and A.W. Thomas, The influence of absorption on possible NN resonance, Phys. Lett. 64B, 59 (1976)
- R.H. Landau and A.W. Thomas, The necessity for an improved optical potential, Phys. Lett. 61B, 361 (1976)
- A.W. Thomas, A three-body calculation of  $\pi\text{D}$  scattering, Nucl. Phys. A258, 417 (1976)

#### Preprints:

- P.W. James, D.A. Bryman, G.R. Mason, L.P. Robertson, T.R. Witten and J.S. Vincent, Production of low-energy charged pions by 580 MeV protons on various nuclei (to be published, Phys. Rev.) [TRI-PP-76-3]
- N. Nishida, H.S. Hayano, K. Nagamine, T. Yamazaki, J.H. Brewer, D.M. Garner and D.G. Fleming, Hyperfine field and diffusion of  $\mu^+$  in Fe single crystal (to be published, Solid State Comm.) [TRI-PP-76-4]
- R.M. Henkelman, L.D. Skarsgard, K.Y. Lam, R.W. Harrison and B. Palcic, Recent developments at the  $\pi^-$  meson radiotherapy facility at TRIUMF (to be published, Int. J. Rad. Oncology, Radiol. & Phys.) [TRI-PP-76-6]
- D.A. Bryman, J. Cresswell and R. Skegg, Delay line readout of the anode wires in a multiwire proportional chamber (to be published, Nucl. Instr. & Meth.) [TRI-PP-76-11]
- H.W. Fearing, DWIA (p, $\pi$ ) calculations: Effects of realistic wave functions and factors determining resonance position (to be published, Phys. Rev. C) [TRI-PP-76-12]
- R. MacDonald, D.S. Beder, D. Berghofer, M.D. Hasinoff, D.F. Measday, M. Salomon, J. Spuller, T. Suzuki, J.-M. Poutissou, R. Poutissou, P. Depommier and J.K.P. Lee, Charge exchange of stopped  $\pi^-$  in deuterium: Experiment and theory (to be published, Phys. Rev. Lett.) [TRI-PP-76-13]
- J.M. Cameron, P. Kitching, R.H. McCamis, C.A. Miller, G.A. Moss, J.G. Rogers, G. Roy, A.W. Stetz, C.A. Goulding and W.T.H. van Oers, The efficiency of counter telescopes for detecting intermediate energy protons (to be published, Nucl. Instr. & Meth.) [TRI-PP-76-14]

## STAFF

BREAKDOWN OF TRIUMF STAFF TOTAL AS OF DECEMBER 31, 1976

	Main Site	UBC	UVic	SFU	UAlta	Total
Scientists	27	3	2 <sup>1</sup>	5	2 <sup>1</sup>	39
Faculty full-time main site 1976/77 <sup>2</sup>	(4)	(1)		(1)	(2)	
Faculty part-time		12	7	3	12	34
Engineers	16					16
Operators	15					15
Programmers	5.4			3		8.4
Graduate students		18	4	5	3	30
Technicians	62	3	4	1	4 <sup>1</sup>	74
Designer-draftsmen	11		1		1	13
Machine shop staff	15		1		1	17
Plant	6					6
Administration	3					3
Office staff:						
Secretarial & clerical	11	1	1	0.6	1	14.6
Library/Information Office	1					1
Stores	4					4
	176.4	37	20	17.6	24	275

<sup>1</sup>Main site total includes five additional scientists from University of Victoria and two from University of Alberta who are based at main site. Two technicians from University of Alberta also work full-time at main site.

<sup>2</sup>Faculty members spending the 1976/77 academic year at main site have been included in appropriate category; during such leave faculty members are paid by TRIUMF rather than the respective university.





# TRIUMF Vancouver (cont'd)

## Secretarial and clerical staff

L. Balfour Clerk  
V. Cameron Accounting Assistant  
V. Hannah Clerk  
J. Jonahs Secretary  
D. Osaduk Receptionist  
N. Palmer Secretary to Director  
Library/Information Office  
A. Strathdee Asst. Information Officer

M. Stancer  
D. Staples  
L. Stewart  
M. Williams  
E. Wright  
Buyer  
Secretary & Personnel  
Liaison Officer  
Clerk  
Secretary  
Buyer

# University of Victoria (cont'd)

## Research and support staff:

D.A. Bryman Asst. Research Scientist  
M.S. Dixit Senior Research Fellow  
C.A. Fry Technician  
T.R. Gathright Technician  
B.H. Henin Technician  
T.A. Hodges Research Associate  
R.R. Langstaff Designer-draftsman  
G.A. Ludgate Research Fellow  
J.A. Macdonald Research Fellow  
J.R. McCartney Secretary  
J.T. Nelson Technician  
A. Olin Research Associate  
P.A. Reeve Research Associate  
P.G. Verstraaten Machinist

# University of British Columbia

## Faculty:

E.G. Auld Assoc. Professor  
D.A. Axen Assoc. Professor  
M.K. Craddock Assoc. Professor  
K.L. Erdman Professor  
D.G. Fleming Assoc. Professor  
M.D. Hasinoff Asst. Professor  
R.R. Johnson Assoc. Professor  
G. Jones Professor  
P.W. Martin Assoc. Professor  
D.F. Measday Professor  
E.W. Vogt Professor  
J.B. Warren Professor  
B.L. White Professor

## Graduate students:

J-M. Bangoura  
D. Berghofer  
F. Corriveau  
R. Dubois  
A. Duncan  
L. Felawka  
D. Garner  
H.R. Johnston  
R. Keeler  
M. Kent  
R. Kiefl  
R. Macdonald  
G. Marshall  
E.L. Mathie  
D. Pai  
J. Spuller  
T. Suzuki  
R. Taylor

Experimental Program  
Experimental Program  
Beam Development  
on leave to TRIUMF  
µSR Facility  
Experimental Program  
on sabbatical to Univ. of Glasgow  
Experimental Program  
Chairman, Board of Management  
Experimental Program  
Experimental Program

## Faculty:

A.S. Arrott Professor (sabbatical at TRIUMF)  
J.M. D'Auria Assoc. Professor  
R.G. Korteling Assoc. Professor  
B.D. Pate Professor  
Thermal Neutron Facility  
Experimental Program

## Graduate students:

G. Bischoff  
H. Blok  
D. Dautet  
H. Dautet  
A. Seamster

## Research and support staff:

W. Bishop Programmer  
V. Cowley Technician  
I. Duelli Secretary  
R. Green Research Associate  
F.M. Kiely Research Associate  
A. Kurn Programmer  
T. Templeton Research Scientist  
I.M. Thorson Research Associate (Shielding & Activation)  
R. Toren Programmer  
W.J. Wieseahn Research Associate

# University of Alberta

## Faculty:

J.M. Cameron Assoc. Professor  
W.K. Dawson Professor  
P.W. Green Visiting Asst. Professor  
L.G. Greeniaus Visiting Asst. Professor  
P. Kitching Assoc. Professor  
W.J. McDonald Professor  
G.A. Moss Assoc. Professor  
G.C. Neilson Professor

W.C. Olesen\* Professor  
G. Roy Assoc. Professor  
J.T. Sample\* Professor  
D.M. Sheppard† Assoc. Professor  
H.S. Sherif Assoc. Professor  
H.E. Siefken Visiting Scientist  
\*on leave to TRIUMF  
†on sabbatical at Universität Freiburg

## Graduate students:

L. Antonuk  
R.H. McCamis  
R.S. Sioboda

## Research and support staff:

A. Adolph Technician  
A.N. Anderson Research Associate  
E.B. Cairns Professional Officer  
R.M. Churchman Technician  
H.G. Coombes Technician  
J.B. Elliott Professional Officer

D.P. Gurd Research Assoc. Professor  
A. Lank Machinist Technician  
T. Lesoway Technical Assistant  
C.A. Miller Univ. Research Associate  
G.M. Stinson Research Assoc. Professor  
K. Zavazal Secretary

# University of Victoria

## Faculty:

G.A. Beer Assoc. Professor  
D.E. Lobb Assoc. Professor  
G.R. Mason Assoc. Professor  
R.M. Pearce Professor

C.E. Picciotto Assoc. Professor  
L.P. Robertson Professor  
C-S. Wu Asst. Professor

## Graduate students:

S.K. Kim  
R.P. Fryer  
E. Miller  
P.R. Poffenberger

## USERS GROUP

### *University of Alberta:*

J.M. Cameron, Chairman 1976	
A.N. Anderson	A.A. Noujaim
E.B. Cairns	W.C. Olsen
W.K. Dawson	T.R. Overton
J.B. Elliott	G. Roy
G.R. Freeman	R.F. Ruth
L.G. Greeniaus	M. Schacter
H.E. Gunning	D.M. Sheppard
A.N. Kamal	H. Sherif
P. Kitching	L.G. Stephens-Newsham
W.J. McDonald	G.M. Stinson
C.A. Miller	A. Szyjewicz
G.A. Moss	R.C. Urtasun
G.C. Neilson	J. Weijer

### *University of Victoria:*

M.J. Ashwood-Smith	G. Ludgate
G.A. Beer	J.A. Macdonald
D.A. Bryman	G.O. Mackie
G. Bushnell	G.R. Mason
T.W. Dingle	A. Olin
M.S. Dixit	R.M. Pearce
G.B. Friedmann	C.E. Picciotto
J. Haywood	P.A. Reeve
T.A. Hodges	L.P. Robertson
A.D. Kirk	C.S. Wu
D.E. Lobb	

### *University of British Columbia:*

M.D. Hasinoff, Chairman 1977	
N. Auersperg	P.W. Martin
E.G. Auld	T. Masterson
D.A. Axen	E.L. Mathie
D.V. Bates	C.A. McDowell
D.S. Beder	J.M. McMillan
J.H. Brewer	D.F. Measday
D.H. Copp	R.L. Noble
M.K. Craddock	J. Phillips
R. Dubois	M. Salomon
K.L. Erdman	J. Sams
D.G. Fleming	H. Stich
R.R. Haering	J. Trotter
L.G. Harrison	L. Vaz
R.R. Johnson	E.W. Vogt
G. Jones	D.C. Walker
R. Keeler	I.H. Warren
B. Larkin	J.B. Warren
K.C. Mann	B.L. White

### *Simon Fraser University:*

A.S. Arrott	M. Kiely
J.M. D'Auria	R.G. Korteling
B.L. Funt	B.D. Pate
R. Green	I.M. Thorson
C.H.W. Jones	W.J. Wieseahn

### *TRIUMF:*

J. Beveridge	J.G. Rogers
E.W. Blackmore	J.T. Sample
H. Fearing	A.W. Thomas
D.R. Gill	J.S. Vincent
D.P. Gurd	G.D. Wait
D.A. Hutcheon	P. Walden
G.H. Mackenzie	G. Waters
L. Moritz	

### *B.C. Cancer Foundation:*

B. Douglas	J. Nordin
J.M.W. Gibson	B. Palcic
C.J. Gregory	K.R. Shortt
R.W. Harrison	L.D. Skarsgard
R.M. Henkelman	D.M. Whitelaw
*R.O. Kornelsen	*M.E.J. Young
K.Y. Lam	

\*B.C. Cancer Control Agency

### Visiting experimentalists:

J-M Poutissou, R. Poutissou, *Université de Montréal*  
 C. Amsler, *Queen Mary College, University of London*  
 K. Nagamine, R. Hayano, N. Nishida, *University of Tokyo*  
 B.T. Murdoch, *University of Manitoba*  
 D. Gibson, *University of Surrey*

Other institutions:

- J. Matthews, S. Rowlands, *University of Calgary*  
R. Cobb, T. Walton, *Cariboo College*  
R.L. Clarke, E.P. Hincks, *Carleton University*  
G.A. Bartholomew, E.D. Earle, J.S. Fraser,  
O. Häusser, F.C. Khanna, P. Lee,  
A. McDonald, *Chalk River Nuclear Laboratories*  
W.W. Scrimger, S.R. Usiskin, Dr. W.W. Cross  
*Cancer Institute, Edmonton*  
B.S. Bhakar, N. Davidson, W. Falk, M. de Jong,  
J. Jovanovich, A.M. Sourkes, K.G. Standing,  
W.T.H. van Oers, D.O. Wells, *University of Manitoba*  
J.K.P. Lee, B. Margolis, K. Scott, *McGill University*  
J. McAndrew, *Memorial University of Newfoundland*  
P. Depommier, B. Goulard, J-P Martin,  
*Université de Montréal*  
G.T. Ewan, H.B. Mak, B. McKee, B.C. Robertson,  
A.T. Stewart, *Queen's University*  
P. Egelstaff, *University of Guelph*  
H.S. Caplan, *University of Saskatchewan*  
M. Krell, *Université de Sherbrooke*  
J.M. Daniels, T.E. Drake, *University of Toronto*  
A. Cone, *Vancouver City College Langara Campus*  
R.T. Morrison, *Vancouver General Hospital*  
L.W. Reeves, *University of Waterloo*  
W.P. Alford, *University of Western Ontario*
- D.V. Bugg, J.A. Edgington, C. Oram,  
K. Shakarchi, *Queen Mary College, London*  
N. Stewart, *Bedford College, London*  
A.S. Clough, *University of Surrey*  
R. Brown, *Rutherford Laboratory*  
I.M. Blair, *AERE Harwell*  
A.N. James, *University of Liverpool*  
D. Wilkinson, *University of Sussex*  
N. Tanner, *Oxford University*  
S. Jaccard, *Université de Neuchâtel*  
J.P. Blaser, *Schweizerisches Institut für Nuklearforschung*  
R. Frascaria, *Institut de Physique Nucléaire, Orsay*  
Cl. Perrin, *Institut des Sciences Nucléaires, Université de Grenoble*  
R. van Dantzig, *IKO Amsterdam*  
M. Furic, *Institute R. Boskovic, Zagreb*  
S. Okada, T. Ono, K. Sakamoto, T. Ono,  
T. Yamazaki, *University of Tokyo*  
G.E. Coote, *INS, Dept. of Science & Industrial Research, New Zealand*  
I.R. Afnan, *Flinders University of South Australia*
- K.W. Jones, *Brookhaven National Laboratory*  
R. Eisberg, J.R. Richardson, *University of California, Los Angeles*  
F.P. Brady, *University of California, Davis*  
L. Wolfenstein, *Carnegie-Mellon University*  
H. Plendl, *Florida State University*  
M. Rickey, G.T. Emery, *Indiana University*  
T.R. Witten, *Kent State University*  
J.M. Crowe, F.S. Goulding, S.N. Kaplan,  
R.H. Pehl, V. Perez-Mendez, *Lawrence Berkeley Laboratory*  
J.W. Blue, *Lewis Research Center, NASA*  
C.A. Goulding, L. Rosen, T.C. Sharma, *Los Alamos Scientific Laboratory*  
N.S. Wall, *University of Maryland*  
C. Schultz, *University of Massachusetts*  
M. Bardon, *National Science Foundation*  
L.M. Lederman, *Nevis Laboratories*  
J.K. Chen, *State University of N.Y. Geneseo*  
D.K. McDaniels, *University of Oregon*  
K.A. Krane, R. Landau, A.W. Stetz, A. Smith,  
L.W. Swenson, *Oregon State University*  
H. Primakoff, *University of Pennsylvania*  
R.F. Carlson, A. Cox, *University of Redlands*  
L. Church, *Reed College*  
J. Va'vra, *Stanford Linear Accelerator Center*  
R. Bryan, R.B. Clark, *Texas A&M University*  
W. Denig, E.N. Hatch, V.G. Lind, R.E. McAdams,  
O.H. Otteson, *Utah State University*  
K. Ziock, *University of Virginia*  
M. Blecher, K. Gotow, *Virginia Polytechnic Institute and State University*  
H. Bichsel, J.S. Blair, V. Cook, I. Halpern,  
E.M. Henley, J.E. Rothberg, K. Snover,  
P. Wooton, *University of Washington*  
H.B. Knowles, *Washington State University*  
W.C. Sperry, *Central Washington State College*  
R.R. McLeod, *Western Washington State College*  
C.F. Perdrisat, *College of William and Mary*



## EXPERIMENT PROPOSALS

The following lists experiment proposals received up to the end of 1976 (missing numbers cover proposals that have been withdrawn, replaced by later versions, or combined with another proposal). Page numbers are given for those experiments which are included in this annual report.

[Spokesman underlined]	Page
1. Low-energy $\pi$ nuclear scattering, K.L. Erdman, <u>R.R. Johnson</u> , T. Masterson ( <i>Univ. of British Columbia</i> ), P. Walden ( <i>TRIUMF</i> )	37
2. Investigation of the $D(p,2p)n$ reaction, J.M. Cameron, <u>P. Kitching</u> , W.J. McDonald, G.A. Moss, W.C. Olsen ( <i>Univ. of Alberta</i> )	
3. The study of fragments emitted in nuclear reactions, R. Green, <u>R.G. Korteling</u> , A. Seamster ( <i>Simon Fraser University</i> ), L. Church ( <i>Reed College</i> )	46
4. A study of the reaction $p + p \rightarrow p + p + \pi^0$ near threshold, <u>D.F. Measday</u> , J.E. Spuller ( <i>Univ. of British Columbia</i> )	
6. Studies of the proton- and pion-induced fission of light to medium mass nuclides, H. Blok, D. Dautet, F.M. Kiely, <u>B.D. Pate</u> ( <i>Simon Fraser University</i> ), Z. Fraenkel ( <i>Weizmann Institute</i> )	48
9. A study of the reaction of $\pi^- + p \rightarrow \gamma + n$ at pion kinetic energies from 20-200 MeV, M.D. Hasinoff, <u>D.F. Measday</u> , M. Salomon ( <i>Univ. of British Columbia</i> ), J-M Poutissou, R. Poutissou ( <i>Univ. de Montréal</i> )	27
10. Positive pion production in proton-proton and proton-nucleus reactions, E.G. Auld, R.R. Johnson, <u>G. Jones</u> , T. Masterson ( <i>Univ. of British Columbia</i> ), P. Walden ( <i>TRIUMF</i> )	31
11. A study of new, high neutron excess nuclides, G. Bischoff, <u>J.M. D'Auria</u> , H. Dautet, R.G. Korteling, B.D. Pate, W. Wieseahn ( <i>Simon Fraser University</i> ), G.E. Coote ( <i>INS, Dept. of Science &amp; Industrial Research, New Zealand</i> ), J.K.P. Lee ( <i>McGill University</i> )	50
12. An experiment to measure the mass of new elements with isospin $T_z = -2$ and $T_z = -5/2$ using $(p, {}^8\text{He})$ and $(p, {}^9\text{Li})$ , <u>J.M. Cameron</u> , G.C. Neilson, G.M. Stinson ( <i>Univ. of Alberta</i> ), D.R. Gill, D.A. Hutcheon ( <i>TRIUMF</i> )	
13. Measurement of the electromagnetic size of the nucleus with muonic X-rays, particularly the 2s-2p transition, G.A. Beer, G.R. Mason, <u>R.M. Pearce</u> , C.E. Picciotto, C.S. Wu ( <i>Univ. of Victoria</i> ), D.G. Fleming ( <i>Univ. of British Columbia</i> ), W.C. Sperry ( <i>Central Washington State College</i> )	
14. The interaction of protons with very light nuclei in the energy range 200-500 MeV, <u>J.M. Cameron</u> , R. McCamis, C.A. Miller, G.A. Moss, G. Roy ( <i>Univ. of Alberta</i> ), B.S. Bhakar, C.A. Goulding, M. de Jong, B.T. Murdoch, <u>W.T.H. van Oers</u> ( <i>Univ. of Manitoba</i> ), A.W. Stetz ( <i>Oregon State University</i> ), D.A. Hutcheon, J.G. Rogers ( <i>TRIUMF</i> )	40
15. A proposal to study quasi-free scattering in nuclei, J.M. Cameron, W.K. Dawson, P. Kitching, <u>W.J. McDonald</u> , C.A. Miller, G.C. Neilson, W.C. Olsen, J.T. Sample, G.M. Stinson ( <i>Univ. of Alberta</i> ), D.A. Hutcheon ( <i>TRIUMF</i> ), A.N. James ( <i>Univ. of Liverpool</i> ), E.D. Earle ( <i>CRNL</i> ), A.W. Stetz ( <i>Oregon State University</i> )	42
16. Proton-deuteron quasi-elastic scattering, <u>P. Kitching</u> , W.J. McDonald, C.A. Miller, <u>G.A. Moss</u> , W.C. Olsen, D.M. Sheppard ( <i>Univ. of Alberta</i> ), D.A. Hutcheon, J.G. Rogers ( <i>TRIUMF</i> ), A.W. Stetz ( <i>Oregon State University</i> ), A.N. James ( <i>Univ. of Liverpool</i> )	44
17. Cross-section measurements for $p(p,2p)\gamma$ , $p(p,2p)\pi^0$ and $D(p,2p)n$ reaction, <u>J.V. Jovanovich</u> ( <i>Univ. of Manitoba</i> )	
18. Influence of chemical environment on atomic muon capture rates, G.A. Beer, T.W. Dingle, D.E. Lobb, G.R. Mason, <u>R.M. Pearce</u> ( <i>Univ. of Victoria</i> ), D.G. Fleming ( <i>Univ. of British Columbia</i> ), W.C. Sperry ( <i>Central Washington State College</i> )	

19. Nuclear decays following muon capture, G.A. Beer, G.R. Mason, R.M. Pearce, C.E. Picciotto, C.S. Wu (*Univ. of Victoria*), G.A. Bartholomew, E.D. Earle, F.C. Khanna (*Chalk River Nuclear Laboratories*), D.G. Fleming (*Univ. of British Columbia*), W.C. Sperry (*Central Washington State College*)
20. Isotope effect in  $\mu$  capture, G.A. Beer, G.R. Mason, R.M. Pearce, C.E. Picciotto, C.S. Wu (*Univ. of Victoria*), D.G. Fleming (*Univ. of British Columbia*), W.C. Sperry (*Central Washington State College*)
21. Optical activity induced by polarized elementary particles, L.D. Hayward, D.C. Walker (*Univ. of British Columbia*)
22. Fragmentation of light nuclei by low-energy pions, H.B. Knowles et al. (*Washington State University*). Now known as 'Negative pion capture and absorption on carbon, nitrogen and oxygen'. [Passed to Biomedical Experiments Evaluation Committee]
- 23a. Search for the decay mode  $\pi^0 \rightarrow 3\gamma$ , P. Depommier, J-P Martin, J-M Poutissou, R. Poutissou (*Univ. de Montréal*)
- 23b. Investigation of the decay mode  $\pi^+ \rightarrow e^+ + \nu_e + \gamma$ , P. Depommier, J-P Martin, J-M Poutissou, R. Poutissou (*Univ. de Montréal*)
- 23c. A study of the decay  $\pi^+ \rightarrow \pi^0 + e^+ + \nu_e$ , P. Depommier, J-P Martin, J-M Poutissou, R. Poutissou (*Univ. de Montréal*)
24. Elastic scattering of polarized protons on  $^{12}\text{C}$ , G.A. Moss, G. Roy, D.M. Sheppard, H. Sherif (*Univ. of Alberta*) [Combined with Exp. 14]
26. Measurement of the differential cross-section for free neutron-proton scattering and for the reaction of  $\text{D}(n,p)2n$ , L.P. Robertson (*Univ. of Victoria*), E.G. Auld, D.A. Axen (*Univ. of British Columbia*), J. Va'vra (*SLAC*), C. Amsler, D.V. Bugg, J.A. Edgington (*Queen Mary College*), J.R. Richardson (*UCLA*), A.S. Clough (*Univ. of Surrey*), N.M. Stewart (*Bedford College*)
27. Measurement of the polarization in free neutron-proton scattering, E.G. Auld, D.A. Axen (*Univ. of British Columbia*), J. Va'vra (*SLAC*), L.P. Robertson (*Univ. of Victoria*), G. Roy (*Univ. of Alberta*), J.R. Richardson (*UCLA*), C. Amsler, D.V. Bugg, J.A. Edgington (*Queen Mary College*), A.S. Clough (*Univ. of Surrey*), N.M. Stewart (*Bedford College*)
28. A programme of direct pickup reactions at intermediate energies, D.G. Fleming (*Univ. of British Columbia*)
29. A study of the reactions  $\pi + p \rightarrow \pi + p$  at pion kinetic energies from 10 to 90 MeV, D.A. Axen, R.R. Johnson (*Univ. of British Columbia*), E.W. Blackmore (*TRIUMF*)
30. Scattering of pions from isotopes of hydrogen and helium, D.S. Bhakar, N. Davidson, W. Falk, W.T.H. van Oers (*Univ. of Manitoba*)
31. p-n elastic scattering with polarized protons and polarized neutrons, J.M. Daniels, P. Kirkby, R.S. Timsit (*Univ. of Toronto*), J. McAndrew (*Memorial University*)
33. Basic radiobiological experiments with pions versus 260-280 kV X-rays, M.J. Ashwood-Smith (*Univ. of Victoria*) [to Biomedical EEC]
34. Low-energy ( $\pi^+, \pi^-$ ) differential and total cross-section measurements, R.R. Johnson (*Univ. of British Columbia*)
35. A study of positive muon depolarization phenomena in chemical systems, J.H. Brewer, D.G. Fleming, L.C. Vaz, D.C. Walker, J.B. Warren (*Univ. of British Columbia*), K.M. Crowe (*Univ. of California, Berkeley*), R.M. Pearce (*Univ. of Victoria*), A.E. Pifer (*Univ. of Arizona*)
36. Neutron diffraction, J. Trotter (*Univ. of British Columbia*), M.J. Bennett (*Univ. of Alberta*), G. Bushnell (*Univ. of Victoria*), F.W. Einstein (*Simon Fraser University*)
37. Search for  $\mu^- + \text{Cu} \rightarrow e^+ + \text{Co}$ , D.A. Bryman (*TRIUMF*), G.A. Beer, J.A. Macdonald, L.P. Robertson (*Univ. of Victoria*), M. Blecher, K. Gotow (*Virginia Polytechnic Institute and State University*)



38. Neutron scattering from fluids and amorphous solids, C.A. McDowell (*Univ. of British Columbia*), P.A. Egelstaff (*Univ. of Guelph*), I.M. Thorson (*Simon Fraser University*)
39. S-wave pion-nuclear interactions, D.A. Axen, G. Jones (*Univ. of British Columbia*)
40. A proposal for neutron experiments at TRIUMF, D.A. Axen, M.K. Craddock (*Univ. of British Columbia*), J. Va'vra (*SLAC*), D.V. Bugg, J.A. Edgington (*Queen Mary College*), N.M. Stewart (*Bedford College*), A.S. Clough (*Univ. of Surrey*), I.M. Blair (*AERE*) 24
- 41a. Radiative capture of pions in light nuclei, M.K. Craddock, M.D. Hasinoff, M. Salomon (*Univ. of British Columbia*) 27
- 41b. Charge exchange of stopped negative pions, D. Berghofer, M.K. Craddock, M.D. Hasinoff, R. MacDonald, M. Salomon (*Univ. of British Columbia*), J-M Poutissou (*Univ. de Montréal*) 27
- 42a.  $\pi^- - {}^3\text{He}$ : Strong interaction shift, G.A. Beer, M.S. Dixit, S.K. Kim, J.A. Macdonald, G.R. Mason, A. Olin, R.M. Pearce, C.E. Picciotto, L.P. Robertson, C.S. Wu (*Univ. of Victoria*), M. Krell (*Univ. de Sherbrooke*), D.A. Bryman, J.S. Vincent (*TRIUMF*)
- 42b.  $\pi^- - {}^3\text{He}$ : Neutron-neutron scattering length, G.A. Beer, M.S. Dixit, J.A. Macdonald, G.R. Mason, R.M. Pearce, C.E. Picciotto, L.P. Robertson, C.S. Wu (*Univ. of Victoria*), M. Krell (*Univ. de Sherbrooke*), D.A. Bryman, J.S. Vincent (*TRIUMF*)
46. Hyperfine splitting in polarized muonic  ${}^{209}\text{Bi}$  atoms, G.T. Ewan, H.B. Mak, B.C. Robertson (*Queen's University*), G.A. Beer, G.R. Mason, A. Olin, R.M. Pearce (*Univ. of Victoria*), K. Nagamine, T. Yamazaki (*Univ. of Tokyo*), D.G. Fleming (*Univ. of British Columbia*)
47. Photon asymmetry in radiative muon capture, J.H. Brewer, M.D. Hasinoff, R. MacDonald (*Univ. of British Columbia*), K.A. Krane (*Oregon State Univ.*), J-M Poutissou (*Univ. de Montréal*)
48. Fertile-to-fissile conversion in electrical breeding (spallation) targets (FERFICON), F.M. Kiely, B.D. Pate, I.M. Thorson (*Simon Fraser University*), J.S. Fraser (*Chalk River Nuclear Laboratories*) 67
49. A comparative study of the radiation effects of pions and electrons, D.C. Walker (*Univ. of British Columbia*) [Letter of intent]
50. A measurement of the muon neutrino mass, G. Jones, P.W. Martin, M. Salomon (*Univ. of British Columbia*), D.A. Bryman (*TRIUMF*)
51. Search for transfer of  $\mu^-$  from lithium lattice to heavy impurities, G.A. Beer, A.D. Kirk, G.R. Mason, A. Olin, R.M. Pearce, L.P. Robertson (*Univ. of Victoria*), D.A. Bryman (*TRIUMF*)
52. A measurement of the  $\pi \rightarrow e\nu$  branching ratio, D.A. Bryman, J.S. Vincent (*TRIUMF*), G.A. Beer, M.S. Dixit, J.A. Macdonald, G.R. Mason, A. Olin, R.M. Pearce, C.E. Picciotto, L.P. Robertson (*Univ. of Victoria*), D. Berghofer (*Univ. of British Columbia*), J-M Poutissou (*Univ. de Montréal*)
53. Emission of heavy fragments in pion absorption, G. Jones, P.W. Martin, M. Salomon, E.W. Vogt (*Univ. of British Columbia*), D.R. Gill (*TRIUMF*), J.M. Cameron (*Univ. of Alberta*) 39
54.  $\pi^\pm$  reaction cross-section measurements on isotopes of calcium, K.L. Erdman, R.R. Johnson (*Univ. of British Columbia*), J.L. Beveridge (*TRIUMF*) 37
55.  $\mu^-$  capture in deuterium and the two-neutron interaction, J.M. Cameron, W.J. McDonald, G.C. Neilson (*Univ. of Alberta*), H. Fearing (*TRIUMF*) [Letter of intent]
56. A study of the decay of the muon, D. Berghofer, M.D. Hasinoff, R. MacDonald, D.F. Measday, M. Salomon, J.E. Spuller (*Univ. of British Columbia*), P. Depommier, J-M Poutissou (*Univ. de Montréal*)
57. Search for the  $\mu^+ \rightarrow e^+ + \gamma$  decay mode, P. Depommier, J-P Martin, J-M Poutissou, R. Poutissou (*Univ. de Montréal*)



58. Polarization effects of the spin-orbit coupling of nuclear protons, J.M. Cameron, W.K. Dawson, P. Kitching, W.J. McDonald, C.A. Miller, G.A. Moss, G.C. Neilson, W.C. Olsen, G. Roy, J.T. Sample, D.M. Sheppard, H.S. Sherif, G.M. Stinson (*Univ. of Alberta*), D.A. Hutcheon (*TRIUMF*) 44
59. Investigation of the (p,2p) reactions on  $^3\text{He}$ ,  $^3\text{H}$  and  $^4\text{He}$ , B.S. Bhakar, W.T.H. van Oers (*Univ. of Manitoba*), J.M. Cameron, G.A. Moss (*Univ. of Alberta*), J.B. Rogers (*TRIUMF*)
60. Study of muonium formation in MgO and related insulators and its diffusion into a vacuum, J.H. Brewer, D.G. Fleming, G. Jones, J.B. Warren (*Univ. of British Columbia*) 35
61. Pre-clinical research on the  $\pi^-$  beam at TRIUMF (Biomedical), C.J. Gregory, R.W. Harrison, R.M. Henkelman, B. Palcic, K.R. Shortt, L.D. Skarsgard (*B.C. Cancer Foundation*), R.O. Kornelsen, M.E.J. Young (*B.C. Cancer Control Agency*) 60
62. Measurement of the  $\pi^-$  atomic cascade time in light elements, G.A. Beer, G.R. Mason, A. Olin, R.M. Pearce, L.P. Robertson (*Univ. of Victoria*), D.A. Bryman (*TRIUMF*)
63. Measurement of the  $\pi^-$  mass, G.A. Beer, S.K. Kim, G.R. Mason, A. Olin, R.M. Pearce, C.E. Picciotto (*Univ. of Victoria*), D.A. Bryman (*TRIUMF*)
64. Total cross-section and total reaction cross-section measurements for the p- $^3\text{He}$  systems and n- $^3\text{He}$  systems, B.S. Bhakar, C.A. Goulding, M.S. de Jong, W.T.H. van Oers, A.M. Sourkes (*Univ. of Manitoba*), J.M. Cameron, G.A. Moss (*Univ. of Alberta*), R.F. Carlson, A.J. Cox (*Univ. of Redlands*)
65. Radiosensitivities of tumours in situ to  $\pi^-$ -meson irradiation, S. Okado, T. Ono, K. Sakamoto, N. Suzuki (*Univ. of Tokyo*)
66. Survey of p-p bremsstrahlung far off the energy shell, H.W. Fearing, J.G. Rogers (*TRIUMF*), J.M. Cameron, A.N. Kamal, A. Szyjewicz (*Univ. of Alberta*), A.W. Stetz (*Oregon State Univ.*), J.V. Jovanovich (*Univ. of Manitoba*), J.R. Richardson (*UCLA*) 34
67. Two-nucleon emission following reactions induced by stopped pions, J.M. Cameron, W.J. McDonald, G.C. Neilson (*Univ. of Alberta*), P.W. Martin (*Univ. of British Columbia*), G.A. Beer, G.R. Mason, A. Olin (*Univ. of Victoria*)
68. Feasibility study of use of high purity germanium detectors for detection of high-energy charged particles, J.M. Cameron (*Univ. of Alberta*), D.R. Gill (*TRIUMF*), F.S. Goulding, R.H. Pehl (*Lawrence Berkeley Laboratory*), P.W. Martin, M. Salomon (*Univ. of British Columbia*)
69. Pion double charge exchange on very light nuclei, A.W. Stetz (*Oregon State Univ.*), N.E. Davidson, B.T. Murdoch, W.T.H. van Oers (*Univ. of Manitoba*), J.M. Cameron, W.J. McDonald (*Univ. of Alberta*), V. Perez-Mendez (*Lawrence Berkeley Laboratory*)
70. Proton total cross-section and total reaction cross-section measurements for light nuclei, B.S. Bhakar, C.A. Goulding, B.T. Murdoch, W.T.H. van Oers, A.M. Sourkes (*Univ. of Manitoba*), R.F. Carlson, A.J. Cox (*Univ. of Redlands*), J.M. Cameron (*Univ. of Alberta*), H. Postma (*Univ. of Groningen*)
71. Muon spin rotation project, R. Hayano, S. Kobayashi, K. Nagamine, S. Nagamiya, N. Nishida, T. Yamazaki (*Univ. of Tokyo*), J.H. Brewer, A. Duncan, D.G. Fleming (*Univ. of British Columbia*) 51
72. Solid-state studies by muonic X-ray polarization, R. Hayano, K. Nagamine, N. Nishida, T. Yamazaki (*Univ. of Tokyo*), R.M. Pearce (*Univ. of Victoria*)
73. Artificial muon polarization, R. Hayano, K. Nagamine, N. Nishida, T. Yamazaki (*Univ. of Tokyo*), J.H. Brewer, D.G. Fleming, M.D. Hasinoff (*Univ. of British Columbia*), H.B. Mak (*Queen's University*) 58
74. Proposal to measure D, R and R' in pp scattering, 200 to 520 MeV, D.V. Bugg, J.A. Edgington, C. Oram, K. Shakarchi (*Queen Mary College*), D.A. Axen (*Univ. of British Columbia*), J. Va'vra (*SLAC*), S. Jaccard (*Univ. de Neuchâtel*), N.M. Stewart (*Bedford College*), A.S. Clough (*Univ. of Surrey*), G. Ludgate (*Univ. of Victoria*) 24

75. The  $d(p, \pi^+)t$  pion production reaction for high momentum transfer, P. Kitching, W.C. Olsen (*Univ. of Alberta*), H.W. Fearing, D.A. Hutcheon, P. Walden (*TRIUMF*), C.F. Perdrisat (*College of William and Mary*), G. Jones, T. Masterson (*Univ. of British Columbia*)
76. A proposal to study elastic scattering on  $^{16}\text{O}$  and  $^{40}\text{Ca}$ , D.P. Gurd, P. Kitching, W.J. McDonald, C.A. Miller, G.C. Neilson, W.C. Olsen, G. Roy, G.M. Stinson (*Univ. of Alberta*), D.A. Hutcheon (*TRIUMF*)
77. Evaporation-cooled metallic cesium target assembly for production of  $^{123}\text{I}$ , J.W. Blue (*NASA Cleveland*), T.A. Hodges (*Univ. of Victoria*), J.S. Vincent (*TRIUMF*), R.T. Morrison, D.M. Lyster (*Vancouver General Hospital*), J.B. Warren (*Univ. of British Columbia*), W.J. Wieseahn (*Simon Fraser University*) 65
78. Importance of defects in  $\mu^+\text{SR}$  in metals, K. Nagamine, T. Yamazaki (*Univ. of Tokyo*), A.T. Stewart (*Queen's University*), B. Bergersen, J.H. Brewer, D.G. Fleming, L.C. Vaz (*Univ. of British Columbia*)
79. Low-energy  $\pi$  production as a function of energy at 500 MeV and below, G.A. Beer, G.R. Mason, A. Olin, R.M. Pearce, L.P. Robertson (*Univ. of Victoria*), P.W. James (*AECL*), D.A. Bryman, J.S. Vincent (*TRIUMF*), J-M Poutissou (*Univ. de Montréal*), R.R. Johnson, J.B. Warren (*Univ. of British Columbia*)
80. Measurements of pionic X-ray energies, widths and intensities, G.A. Beer, M.S. Dixit, J.A. Macdonald, G.R. Mason, A. Olin, R.M. Pearce, L.P. Robertson (*Univ. of Victoria*), C. Wiegand (*Lawrence Berkeley Laboratory*), D.A. Bryman (*TRIUMF*) 39
81. Interaction of stopped negative pions with complex nuclei, J.K.P. Lee (*McGill Univ.*), G.R. Mason, A. Olin (*Univ. of Victoria*), D.A. Bryman (*TRIUMF*), M.D. Hasinoff, M. Salomon (*Univ. of British Columbia*), J-M Poutissou (*Univ. de Montréal*), G.E. Coote (*INS, DSIR, New Zealand*), W.J. Wieseahn (*Simon Fraser University*)
82. Mössbauer spectroscopic studies using short-lived sources, C.H.W. Jones (*Simon Fraser University*), J. Sams (*Univ. of British Columbia*)
83. Bound muon decay in nuclei, J.H. Brewer, F. Corriveau, M.D. Hasinoff, R. MacDonald (*Univ. of British Columbia*), J-M Poutissou (*Univ. de Montréal*), K. Nagamine (*Univ. of Tokyo*)
84. The  $(\pi^\pm, d)$  reaction on light nuclei, K.L. Erdman, R.R. Johnson, H.R. Johnston, T.G. Masterson (*Univ. of British Columbia*), J.S. Vincent (*TRIUMF*), V.G. Lind, R.E. McAdams, O.H. Otteson (*Utah State University*)
85. Single and coincidence studies of prompt gamma-rays in  $\pi$ -nuclear interactions, W. Denig, E.N. Hatch, V.G. Lind, R.E. McAdams, O.H. Otteson (*Utah State University*), H. Dollard, K.L. Erdman, R.R. Johnson, H.R. Johnston, T.G. Masterson (*Univ. of British Columbia*), R.B. Clark (*Texas A&M*), H.S. Plendl (*Florida State University*)
86. Elastic and inelastic scattering of polarized protons from calcium and lead, J.M. Cameron, J. Källne, P. Kitching, W.J. McDonald, C.A. Miller, G.C. Neilson, G. Roy, H.S. Sherif, G.M. Stinson (*Univ. of Alberta*), D.K. McDaniels (*Univ. of Oregon*), J.S. Blair (*Univ. of Washington*), W.T.H. van Oers (*Univ. of Manitoba*), D.A. Hutcheon (*TRIUMF*)
87. Proton radiography studies at TRIUMF, E.W. Blackmore, D.A. Bryman, G.H. Mackenzie (*TRIUMF*) 63
88. Systematic studies of total muon capture rates, R. Hayano, K. Nagamine, N. Nishida, T. Yamazaki (*Univ. of Tokyo*), J-M Bangoura, J.H. Brewer, M.D. Hasinoff, D.F. Measday, T. Suzuki (*Univ. of British Columbia*)
89.  $\mu$  fission, S.N. Kaplan (*Lawrence Berkeley Laboratory*), G.A. Beer, M.S. Dixit, J.A. Macdonald, G.R. Mason, A. Olin, R.M. Pearce (*Univ. of Victoria*)
90. Test of time reversal invariance, B.K.S. Koene, B.T. Murdoch, W.T.H. van Oers (*Univ. of Manitoba*), J.M. Cameron, L.G. Greeniaus, C.A. Miller, G.A. Moss, G. Roy (*Univ. of Alberta*), R.G. Beurtey, J.C. Duchazeaubeneix (*CEN, Saclay*), M. Simonius (*ETH Zürich*)

91. Muonium in semiconductors, J.H. Brewer (*Univ. of British Columbia*)
92. The effect of nuclear structure on fragmentation processes with 300 MeV protons, L.B. Church (*Reed College*), R.E.L. Green, R.G. Korteling (*Simon Fraser University*)
93. Production of radioisotopes at medium energies for pure and applied research, L. Moritz, J.S. Vincent (*TRIUMF*), B.D. Pate, C.H.W. Jones (*Simon Fraser University*), D.M. Lyster, W. Rowe (*Vancouver General Hospital*), L. Patrick (*Univ. of British Columbia*)
94. The optical transitions of pionium and muonium, A.L. Carter, D. Kessler (*Carleton University*), C.K. Hargrove, E.P. Hincks, R.J. McKee, H. Mes (*National Research Council*)



## SCIENTIFIC INAUGURATION

Friday, June 4, 1976

Erich W. Vogt, Chairman, TRIUMF Board of Management —  
*Welcome*

### Morning Session:

J. Reginald Richardson, Director of TRIUMF  
*The status of TRIUMF*

Ernest M. Henley, University of Washington, Seattle  
*Exploration of some symmetries*

Hans A. Bethe, Cornell University  
*Interaction of pions with nuclei*

### Afternoon Session:

Henry Primakoff, University of Pennsylvania  
*Muon capture by light nuclei*

Bruce Dropesky, Los Alamos Scientific Laboratory  
*Some early results of nuclear chemistry  
research at LAMPF*

Sir Denys H. Wilkinson, Oxford University  
*Measuring the charges of the quarks*











